THE REARRANGEMENT OF DIAMIDOSILYL ETHER LIGANDS TO AMIDO-AMINO-SILOXO LIGANDS AND THEIR CHROMIUM COMPLEXES

by

Farzad(Frank) Haftbaradaran
B. Sc., Simon Fraser University 2002

THESIS SUBMITTED IN PARTIAL FULFILLMENT OF
THE REQUIREMENTS FOR THE DEGREE OF

MASTER OF SCIENCE

In the

Department of Chemistry

SIMON FRASER UNIVERSITY

Fall 2006

APPROVAL

Name: Farzad(Frank) Haftbaradaran

Degree: Master of Science

Title of Thesis: The Rearrangement of Diamidosilyl Ether Ligands to Amido-Amino-Siloxo Ligands and their Chromium Complexes

Examining Committee:

Chair: Dr. George R. Agnes (Professor)

Dr. Daniel B. Leznoff (Associate Professor)
Senior Supervisor

Dr. Jason A.C. Clyburne (Associate Professor)
Committee Member

Dr. Vance E. Williams (Assistant Professor)
Committee Member

Dr. Robert A. Britton (Assistant Professor)
Internal Examiner

Date Approved: **August 8, 2006**

ABSTRACT

The synthesis and characterization of three new symmetrical diamidosilyl ether ligands {[$RNHSiMe_2]_2O$} ($H_2[^RNON]$; R = Propyl, 3,5-Me_2Ph, Ferrocenyl) are described. A retro-Brook-type silyl migration from oxygen to nitrogen of the dilithiated ligands {[$RNLiSiMe_2]_2O$} (R = Propyl, 3,5-Me_2Ph, 2,4,6-Me_3Ph, 2,6-$^iPr_2Ph$, 3,5-$(CF_3)_2Ph$) in THF resulted in new non-symmetrical mixed-donor amido-amino-siloxo ligands of the form {$RNLiSiMe_2N(R)SiMe_2OLi$}, termed $Li_2[^RNN'O]$, in one step and quantitative yield; most were structurally characterized and exhibited a range of aggregate structures including triple-stacked cubes, ladders and rings. Reaction kinetics were determined by VT ^1H NMR and show that the rate of rearrangement increases with decreasing steric hindrance, and with increasing electron-donating ability of the R substituents.

Several paramagnetic chromium complexes including {$Cr[^{Me_3Ph}NN'O]\bullet THF\}_2$, {$Cr[^{iPr_2Ph}NN'O]\}_2$, {$Cr[^{Me_3Ph}NN'O]_2Li_2\bullet THF\}$, {$(Cr_2[^{Me_3Ph}NN'O]_2)_2CrCl_2\}$, and {$Cr[^{Pr}NON]_2\}$ were synthesized. Amido- or siloxo-bridged binding motifs, a very strong η^2-(N,C_{ipso}) arylamido interaction, and a Cr(II) ate complex are featured, along with their magnetic properties and activity towards ethylene polymerization.

Keywords: Diamidosilyl ether ligands; retro-Brook rearrangement; non-symmetrical mixed-donor ligands; paramagnetic chromium complexes; amido and siloxo ligands.

DEDICATION

To my parents

ACKNOWLEDGEMENTS

I would like to express my deep and sincere gratitude to my senior supervisor Dr. Daniel B. Leznoff. His wide knowledge, guidance, and logical way of thinking have been of remarkable value for me and the work presented in this thesis. I am also deeply grateful to my committee supervisors Dr. Jason A. C. Clyburne and Dr. Vance E. Williams for their detailed and constructive comments, and for their support throughout this work.

I wish to express my sincere thanks to my former and present colleagues in the Leznoff research group who contributed to this work. Especially, a great thanks to Michael J. Katz for collecting and solving the X-ray data, Julie Lefebvre for collecting and interpreting the SQIUD data, and Angela M. Kuchison for synthesizing the $H_2[^{Me_2Ph}NON]$ ligand. I would also like to acknowledge the following X-ray crystallographers: Dr. Raymond J. Batchelor, Prof. James F. Britten (McMaster University), and Dr. Gabriele Schatte (University of Saskatchewan). Furthermore, a great thanks to the following SFU technicians: Mr. Miki K. Yang (EA), Mrs. Marcy M. Tracy (NMR), and Mr. Phil Ferreira (MS).

Finally, a special thanks to my family, who provided me the inspiration and the moral support.

TABLE OF CONTENTS

LIST OF FIGURES

LIST OF TABLES

LIST OF ABBREVIATIONS

Å	Angstrom (10^{-10} m)
Anal.	analysis
B.M.	Bohr magneton
br	broad
^{n}Bu	*n*-butyl (-$CH_2CH_2CH_2CH_3$)
^{t}Bu	*t*-butyl [-$C(CH_3)_3$]
°C	degrees Celsius
Calcd.	calculated
CI	chemical ionization
Cp	cyclopentadienyl
D	donor(s)
d	doublet
DEAC	diethylaluminium chloride
deg	degree(s)
EA	elemental analysis
E_a	activation energy
EI	electron impact
Et	ethyl (-CH_2CH_3)
Et_2O	diethyl ether
eV	electron volt
Fc	ferrocenyl
G	Gauss
g	gram(s)
GC-MS	gas chromatography-mass spectrometry
^{1}H	proton
K	Kelvin
k_b	Boltzmann's constant

M	central metal atom (or "molar" when referring to concentration)
m	multiplet
M^+	molecular ion
MAO	methylaluminoxane
Me	methyl ($-CH_3$)
Mes	mesityl
MHz	megahertz
mL	millilitre
MMAO	modified methylaluminoxane
mmol	millimoles
mp	melting point
MS	mass spectrometry
m/z	mass to charge ratio
NMR	nuclear magnetic resonance
NON	diamidosilyl ether ligand(s)
N'NO	mixed-donor amido-amino-siloxo ligand(s)
ORTEP	Oak Ridge Thermal Ellipsoid Plot
Ph	phenyl
PMDETA	pentamethyldiethylenetriamine
ppm	parts per million
Pr	propyl
^{i}Pr	isopropyl [$-CH(CH_3)_2$]
py	pyridine
S	total electron spin
s	singlet or seconds
SQUID	superconducting quantum interference device
T	temperature
t	triplet or time
THF	tetrahydrofuran
v br	very broad
vs.	versus
χ_m	molar magnetic susceptibility

δ	isomer or chemical shift
$\Delta G^{\ddagger}$	free energy of activation
$\Delta H^{\ddagger}$	activation enthalpy
$\Delta S^{\ddagger}$	activation entropy
λ	wavelength
μ_{eff}	effective magnetic moment
μ_{so}	spin-only magnetic moment
$\tau_{1/2}$	half-life
^{o}	degrees

CHAPTER 1:
INTRODUCTION

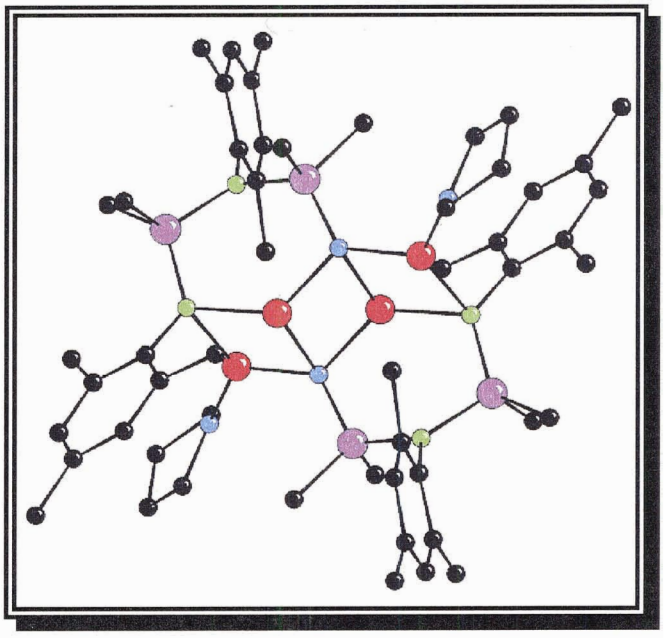

1.1 Early History of Chelating N- and O-Donor Ligands

In addition to the cyclopentadienyl (Cp) ligand, amido N-donor (R_2N^-) and alkoxo O-donor (RO^-) chelating ligands have proven to be excellent candidates for stabilizing electron-poor transition metals in medium to high oxidation states.[1-8] This is due to their hard basic nature,[9,10] chelating capability,[11] and strong π-donating ability.[12] These ligands offer a chelating mode or chelate-bridging coordination and therefore, should have different chemistry from complexes with monodentate amido and alkoxo ligands. Perhaps the most important difference is due to this chelate effect: in general, complexes

with multidentate chelate ligands are more stable than complexes with comparable monodentate ligands.[11]

Chelating O- or N-donor-based ligands are versatile because the steric and electronic profile of the ligand can be varied over a wide range by the modification of the R groups attached to the donor centres. Thus, the coordination number, coordination geometry, electron richness of the metal centre, reactivity, and stability of the complex can be significantly modified by the alteration of the substituents on the nitrogen and oxygen centres. Many interesting complexes such as transition metals with unusual low coordination numbers at the metal centres have been stabilized by the help of these ligands.[13-15] Furthermore, chelating N- and chelating O-donor complexes of transition metals have been the subject of extensive studies into non-metallocene polymerization catalysts in the last decade.[14,16-26]

The discovery of the first highly active non-metallocene catalyst of a nickel complex with diimine ligands by Brookhart *et al.* in 1995 pioneered this area of chemistry.[27] In 1996, the first highly active chelating diamido catalysts based on Ti were reported by McConville *et al.* (Figure 1.1 **A**).[28,29] Later, the reactivity of these complexes were enhanced by additional ligand-metal coordinative flexibility via the introduction of electron-pair donor groups, such as N, O, and S into the ligand system.[30-36] For instance, in 1996, Horton *et al.* showed that incorporation of the N_{amino}-donor function into the ligand frame (Figure 1.1 **B**) increases the ethene polymerization activity of the Zr diamido complexes.[30] In another example, Schrock *et al.* showed that Zr complexes bearing chelating diamido ligands with an additional neutral O-donor group (Figure 1.1 **C**) can act as catalysts for the polymerization of ethene.[34] The additional

neutral donor group in these "diamido-donor" complexes is less strongly bound to the metal center and thus can actively participate in chemical transformations via dissociation and recoordination to the metal center.[37] This means that the diamido-donor-based complexes are electronically flexible during the polymerization process; they can receive electrons from the coordinating olefin through the metal center and give electrons from the donor atom to the metal center to facilitate the olefin insertion reaction.[16] Indeed, DFT calculations by McConville *et al.* suggested that the zirconium diamido-$N_{pyridine}$-donor ligand system has a similar electronic flexibility to the Cp_2Zr fragment complexes which serve after activation with MAO as highly active catalysts for ethene polymerization.[38,39]

The generally facile synthesis of silicon-based amido ligands (i.e. Si attached to the N-donor atom in a terminal position (e.g. **B**, Figure 1.1) or within the ligand backbone (e.g. **D**, Figure 1.1)) via the reaction of lithium amides with chlorosilanes makes them readily accessible.[8,17,40] For example, Bochmann *et al.* reported a series of Zr complexes containing diamidosilyl ether ligands (Figure 1.1 **D**) that are active alkene polymerization catalysts.[40] These chelating ligands with additional donor atoms are coordinately flexible and they can attach to the metal center using two or three of their donors depending on if the O-donor moiety is involved in coordination or not.[14] In this way they form chelate complexes with *n*-membered chelate rings. In general, five- and six-membered rings are more stable since the chelate rings have relatively little ring strain, and therefore form readily.[41]

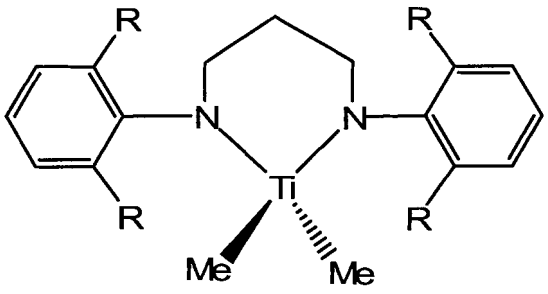

A. R = ^{i}Pr, Me

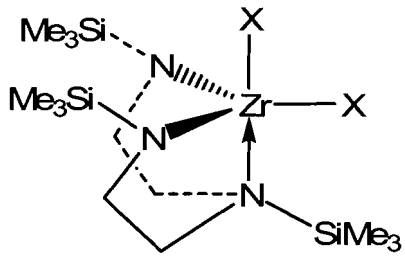

B. X = Me, CH_2Ph

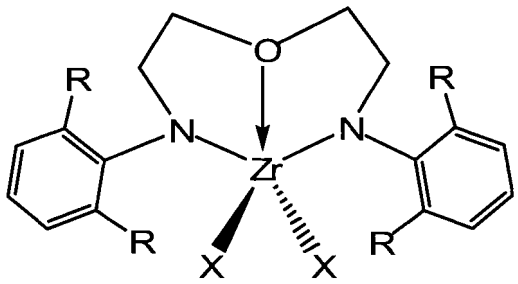

C. R = ^{i}Pr, Me X = Me, CH_2CHMe_2

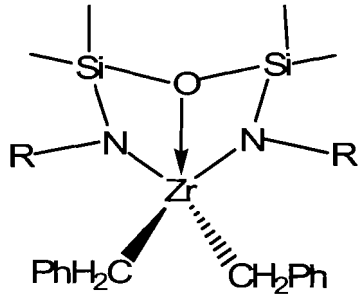

D. R = ^{t}Bu, Cyclohexyl, 8-aminoquinoline

Figure 1.1 Examples of Group 4 complexes with symmetrical chelating diamido ligands with or without additional donor substituents.

These discoveries accelerated research on non-metallocene catalysts and considerable effort is being expended on modifying the existing or designing new high-valent diamagnetic Group 4 transition metals (e.g. Ti(IV) and Zr(IV)) complexes of symmetrical chelating N-donor[16-20,42] and O-donor[24,43-46] ligands. However, chelating N- and O-donor ligands have been used to a much lesser extent with paramagnetic first-row transition metals such as chromium despite their potential application as polymerization catalysts.[17,47] These observations have prompted the Leznoff research group to explore the design, synthesis and use of new diamidosilyl ether ligands of the form

$\{[RN(SiMe_2)]_2O\}^{2-}$, termed $[^RNON]^{2-}$ (R = alkyl or aryl), for the preparation of first-row transition metal complexes with the aim of developing new and possibly more active catalysts. In addition to the symmetrical diamido-donor ligands previously reported by the Leznoff research group,[48,49] three new ligands $[^RNON]^{2-}$ with R = Pr, 3,5-Me_2Ph, and ferrocenyl were synthesized in this thesis. The details of synthesis, characterization, and chromium coordination chemistry of these new diamidosilyl ether ligands are presented in the following chapters.

1.2 Focus of the Thesis: Non-Symmetrical Donor Ligands

Most of the studies on non-metallocene catalysts have been carried out on symmetrical donor ligands and relatively less attention has been paid to design of related non-symmetrical N-donor (i.e. different amido functions) and mixed-donor (i.e. different donor functions) ligands.[16,17] However, recently a number of research groups have explored the use of non-symmetrical donor ligands as catalysts for olefin polymerization.[50-57] For instance, Lorber *et al.* reported a zirconium complex containing non-symmetrical diamido ligands (Figure 1.2 **A**), which shows relatively low activity toward ethylene polymerization.[50] In another example, Rausch and coworkers reported a titanium complex supported by a chelating mixed-amido-alkoxo-donor ligand (Figure 1.2 **B**) with high activity for the polymerization of olefin in the presence of MAO.[57] Perhaps, the most recognized non-symmetrical mixed-N_{amino}-O-donor ligand systems are the chelating Schiff-base ligands (e.g. acen, salen and their derivatives), which their application with Group 4 olefin polymerization were first investigated in 1995 by Jordan and his coworkers (Figure 1.2 **C**).[58,59] These non-symmetrical ligands are of interest due

to their potential to generate electronically and sterically non-symmetrical reaction sites, which possibly gives an alternating character to the resulting polymer.[50,52] Furthermore, these non-symmetrical ligand designs will help to better understand the influence of electronic and steric effects of the supporting ligands on the catalytic properties of these non-symmetrical complexes.

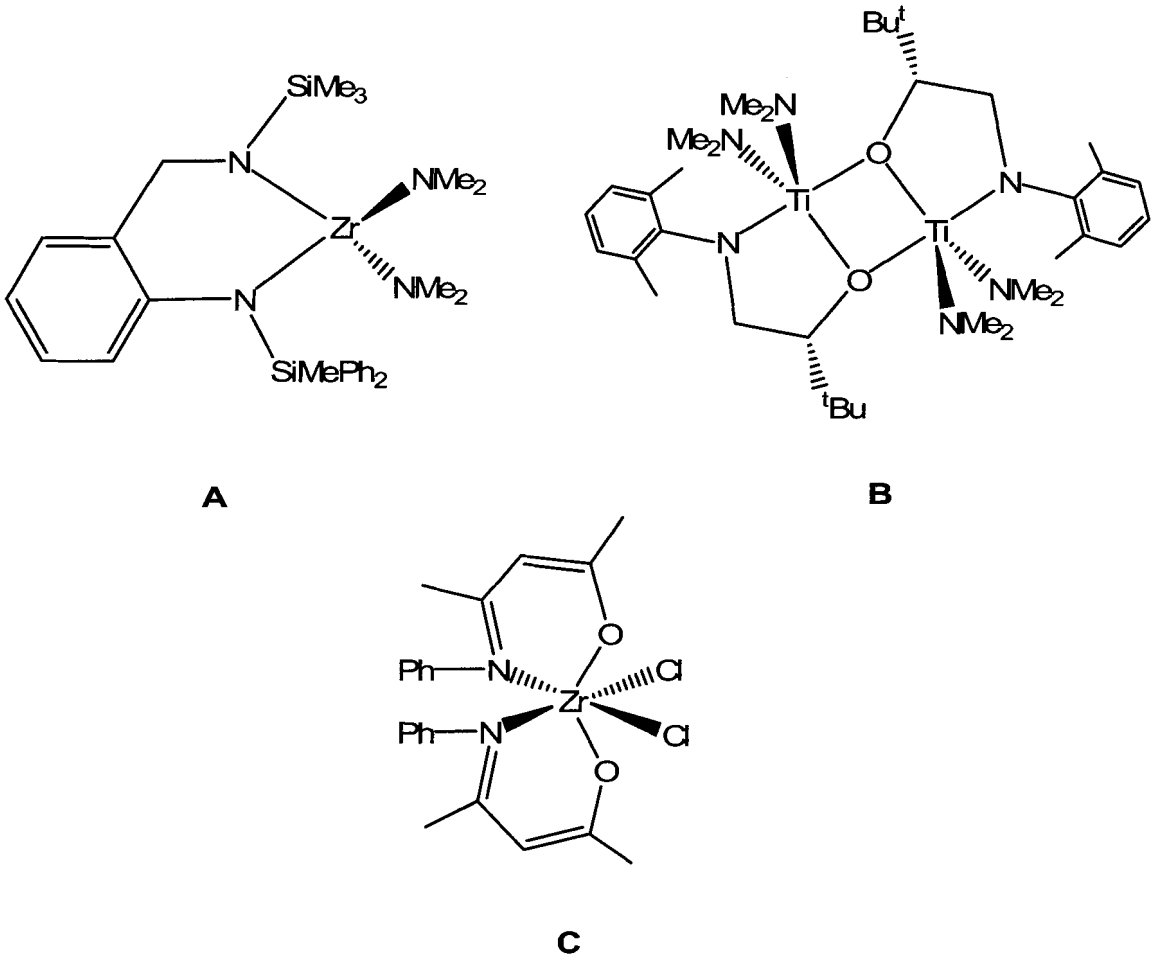

Figure 1.2 Examples of Group 4 complexes with non-symmetrical chelating diamido (**A**), mixed-donor amido-alkoxo (**B**), and mixed-donor acen-type ligands (**C**).

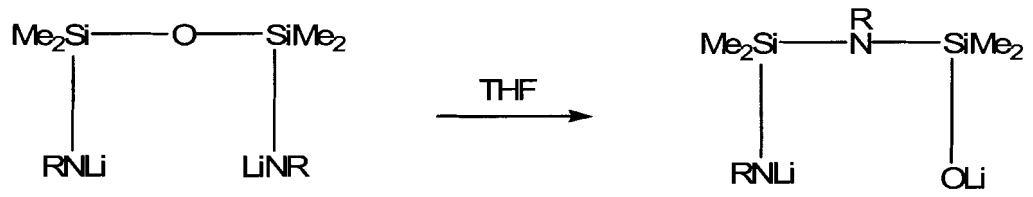

Symmetrical diamidosilyl ether ligand

Non-symmetrical mixed-donor amido-amino-siloxo ligand

R = Pr, 3,5-Me_2Ph, 2,4,6-Me_3Ph, 2,6-$^i Pr_2$Ph, 3,5-$(CF_3)_2$Ph

Figure 1.3 General reaction scheme for rearrangement of diamidosilyl ether ligands to mixed-donor amido-amino-siloxo ligands.

In general, the synthesis of non-symmetrical donor ligands requires more challenging synthetic procedures. This is because it is harder to modify the substituents of each donor group independently or assemble two or more dissimilar building blocks, each of which may also require a multi-step synthesis in its own right. However, during the course of studies in the Leznoff research group using the symmetrical diamidosilyl ether ligands, we encountered an interesting example of a silyl migration reaction. We recognized that if the lithiation reaction of synthesized diamidosilyl ether ligands $H_2[^R NON]$ (R = Propyl, 3,5-Me_2Ph, 2,4,6-Me_3Ph, 2,6-$^i Pr_2$Ph, 3,5-$(CF_3)_2$Ph) is conducted in THF, or if the isolated *N*-lithio derivatives of the ligands $Li_2[^R NON]$ are stirred in THF, they undergo an intramolecular rearrangement in which one silyl group migrates from oxygen to the amido-nitrogen (Figure 1.3). Such Brook-type silyl-migrations have been studied extensively in the past (see the following section for the details of Brook-type reactions).[60-63] However, the value of the anionic products of such reactions as new ligands has not been previously considered.[64] Thus, this retro-Brook silyl migration was

used as a facile, high-yield route to synthesize a new class of non-symmetrical mixed-donor ligands of the form $[RNSiMe_2N(R)SiMe_2O]^{2-}$,[65] termed $[^{R}NN'O]^{2-}$: the chemistry of these ligands forms the core of this thesis. Details of the synthesis, characterization, and Cr coordination chemistry of these amido-amino-siloxo ligands are presented in the following chapters, but an introduction to the extensive background on the Brook-type rearrangement will be presented first.

1.3 Brook and Retro-Brook Rearrangements

The Brook-rearrangement is a silicon-based rearrangement in which an organosilyl group migrates to neighbouring oxygen atom under the influence of a base (Figure 1.4).[60,61,66,67] The studies of this reaction have been carried out by A. G. Brook whose name is now associated with this reaction. The reaction mechanism starts with the proton abstraction from a hydroxyl site near to silicon by the base B (Figure 1.5). The generated nucleophile (oxyanion) then attacks silicon intramolecularly, giving rise to a five-coordinate transition state at silicon. The formation of the intermediate species is favoured by the availability of empty, low-energy *d* orbitals on silicon.[68] After the breaking of the Si–C bond, the electron pair is transferred from oxygen to a carbon, which can abstract a proton from a proton source such as solvent to form the final rearranged product.

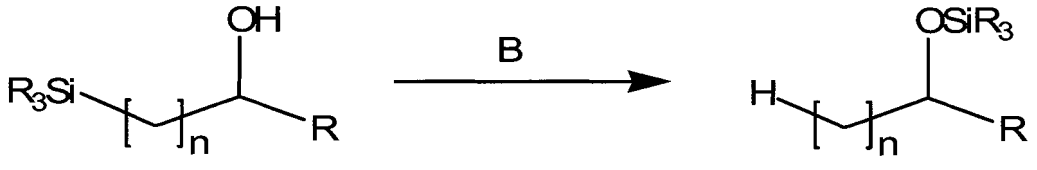

Figure 1.4 General reaction scheme of Brook rearrangement (n = 2–5, B is a base).[69]

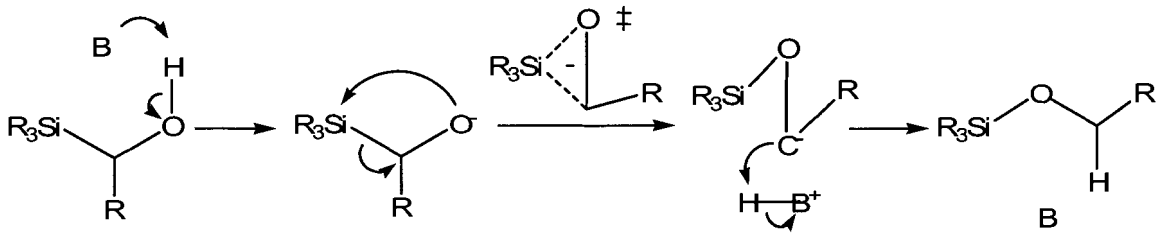

Figure 1.5 General reaction mechanism of Brook rearrangement reaction (B is a base).[69]

The general driving force for such rearrangements is the formation of the relatively high strength Si–O bond. For example, the [1,2]-silyl C→O rearrangement involves the formation of a stronger Si–O bond (bond dissociation energy of 530 kJ/mol) and dissociation of a weaker Si–C bond (bond dissociation energy of 320 kJ/mol). However, the formation of the carbanion from alkoxide is generally an endothermic process, which reduces this driving force. Thus, by stabilizing the carbanion species with the presence of conjugating group such as phenyl group, the rearrangements become synthetically more useful.[70,71] Although initially the Brook rearrangement only included the [1,2]-silyl C→O migrations,[72,73] other combinations [1,n]-silyl A→O (n = 2–5; A = C, N, O, and S) have been reported.[74] However, most of these migrations involve a 1,2 anionic rearrangement, and higher order reactions (i.e. n higher than 2) are generally considered to be less facile.[75]

The kinetic studies by Brook[60,66,68,76] and others[71,77,78] have indicated that the rate of the Brook-type rearrangement reaction significantly depends on the nucleophilicity of the anion toward the silicon and the stability of the carbanion intermediate. For instance, Brook and Duff showed that aminoalkylsilanes (R_3SiCR_2NHR') can be rearranged to the isomeric alkylaminosilanes ($R_3SiNR'CHR_2$) by traces of ^{n}BuLi.[79] The kinetic results

from their study indicated that these rearrangement reactions greatly depend on the electronic effects of the substituents on the carbon and nitrogen centres. The N-phenyl compounds (e.g. R_3SiCH_2NHPh) failed to rearrange upon addition of ^nBuLi. They suggested that the electron delocalization from nitrogen into the phenyl group (electron-withdrawing group) weakens the nucleophilicity of the N_{amide} centre toward the silicon, which restrains the intramolecular attack on silicon. On the other hand, the C-phenyl compounds (e.g. R_3SiCPh_2NHPh) readily rearranged at room temperature upon activation with ^nBuLi, now due to the stabilization of the carbanion intermediate by the electron-withdrawing ability of phenyl groups. Thus in general, changing the R groups on oxygen from aryl (electron-withdrawing) to alkyl (electron-donating) increase the rate of the rearrangement due to the increase of the nucleophilicity of the oxyanion. On the other hand, changing the R groups on carbon or silicon from electron-withdrawing groups to electron-donating groups decreases the rate of the reaction due to the destabilization of the carbanion intermediate.

In another study, Mullins and Vedejs clearly showed the importance of steric effects on the rearrangement reaction.[80] Silylation of the sulphoxide derivative [$PhCH_2S(O)(^tBu)$] resulted in a mixture of diastereomers, one of which rearranged below room temperature, whereas the other had to be heated to 70 °C for rearrangement to occur (Figure 1.6). They rationalized this observation by proposing that the isomer which rearranged at low temperature has a relatively unhindered conformation for intramolecular silyl transfer while the other isomer suffers from steric hindrance from interaction between the phenyl and ^tBu substituents during the silyl transfer.

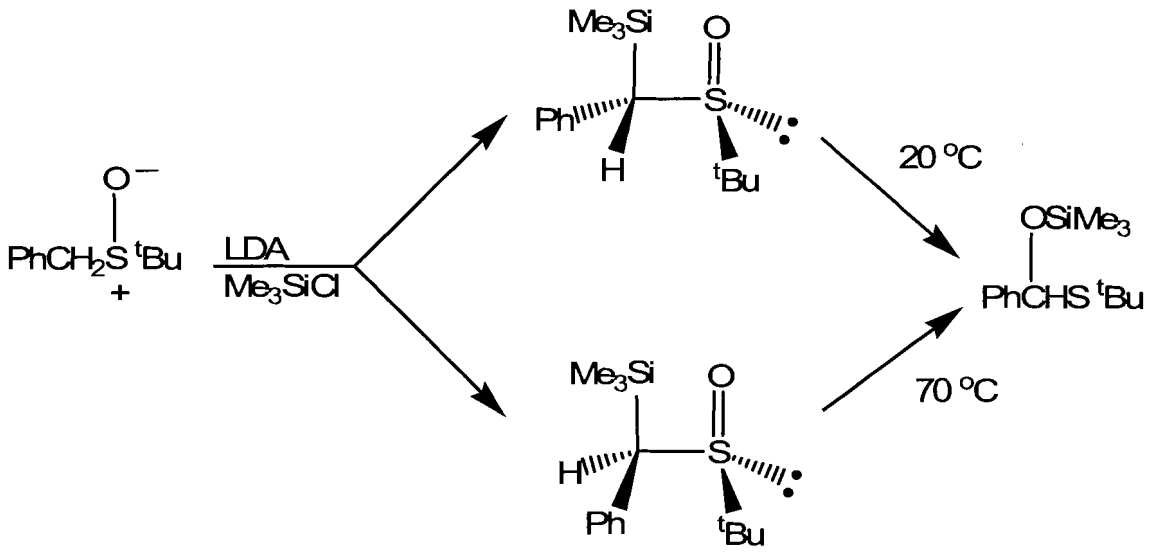

Figure 1.6 Reaction scheme for silylation of the sulphoxide derivative following by a silyl rearrangement reaction (LDA = lithium diisopropylamide).[80]

The migration of a silyl group can also occur from oxygen to a formally anionic carbon or nitrogen; this is termed a [1,n]-silyl O→A migration (A = C or N, n = 2-4).[81-85] This "reverse" Brook reaction, referred to as a retro-Brook rearrangement, is not frequently encountered.[86-89] As mentioned earlier, the migration of silicon from carbon to oxygen requires the driving force provided by the formation of a stronger Si–O bond compared to a Si–C bond. However, the reaction also depends on the balance between the stabilities of the oxyanions and carbanions. In the case when the carbanion is less stabilized compared to oxyanion, the Brook rearrangement can be reversed.[81] The factors that influence anion stability include the solvent (anion solvation), the counter ion, and the temperature at which the reaction takes place.[81] For instance, West and Boudjouk reported that, upon deprotonation, N,O-bis(silyl)hydroxylamines undergo a [1,2]-silyl O→N migration to form an equilibrium mixture of unrearranged and rearranged anions (Figure 1.7).[78] However, derivatization of the anions with MeI indicated that silyl

migration from oxygen to nitrogen had occurred due to the greater stability of the oxyanion vs. the amide ion. On the other hand, derivatization of the mixture of ions with pyrrole yielded unrearranged material, indicating that the amide ion preferentially reacted with this proton source, resulting in the reversal of the equilibrium.

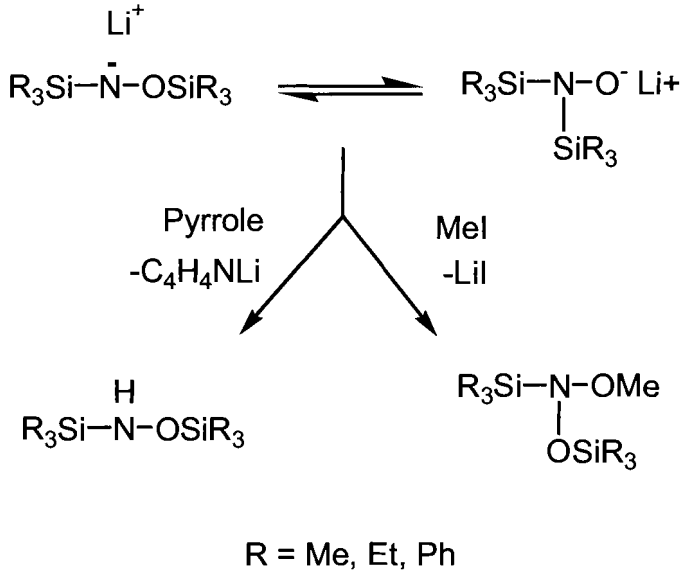

Figure 1.7 Reaction scheme for [1,2]-anionic silyl rearrangement of organosilylhydroxylamines and the derivatizations with pyrrole and MeI.[78]

In another example which has particular relevance for the ligands studied in this thesis, Pearce *et al.* reported the first case of a [1,3]-silyl O→N migration in *N*-lithiocyclosiloxazane rings (Figure 1.8).[90] They showed that the dilithiation of eight-membered siloxazane ring (**A**) in 1,2-dimethoxyethane at –60 °C results in the *N,N'*-dilithio salt **B**. However, if the solution is allowed to reach –30 °C and stirred for 1 hour, it undergoes the [1,3]-silyl retro-Brook migration to form the isomeric six-membered siloxazane ring (**C**). If the same solution is allowed to reach the room temperature and stirred for six hours, further ring-contraction is observed via yet another silyl migration to

form the isomeric four-membered cyclodisilazane (**D**). The rearrangement can also occur in THF, but it is very slow in Et_2O or hexanes. Note the similarity of the diamidodisiloxo salt **B** (Figure 1.8) with the diamidomonosilyl ether ligand $Li_2[^{R}NON]$ (Figure 1.3 left); both rearrange to give amido-siloxo moieties in THF but not in less polar solvents.

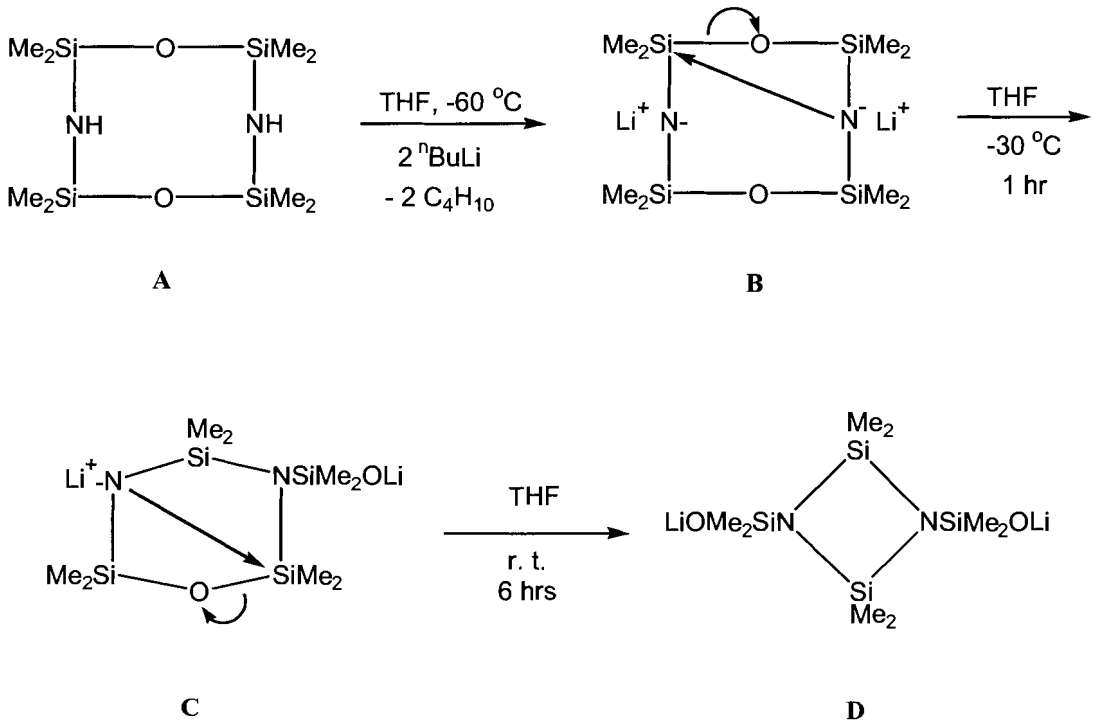

Figure 1.8 Reaction scheme for the [1,3]-silyl O→N migration in the *N*-lithiocyclosiloxazane ring.[90]

1.4 Structural Features of Lithium Organo-Amide and Alkoxide

The deprotonation of diamines or dialcohols to yield diamido- and dialkoxo-salts is the most common route to reacting these ligands with transition metal centers via transmetallation.[1,2,6] The lithium salts are, in general, particularly preferred for this purpose owing to their availability, relatively low nucleophilicity, and strong Brønsted basicity.[91] Due to their high degree of air and moisture sensitivity, lithium organo-amides

were often prepared in situ by lithiation of amines, and without isolation (assuming a 100% yield), were used for further chemical synthesis.[92,93] However, more interests emerged regarding the structural characterization of the lithium amides and alkoxides since it was determined that their structures or more specifically their degree of aggregation often translates into the reactivity level of these compounds.[94,95] Lappert *et al.* ssuggested that the lower the degree of molecular aggregation, the greater the amide reactivity and selectivity; for instance, the solvated bis(trimethylsilyl)amidolithium [$(SiMe_3)_2NLi$•PMDETA] is a monomer in the solid phase and outstandingly reactive and selective as a proton abstractor.[94] In this thesis, structures of a range of $Li_2[^RNN'O]$ ligands were collected in order to explore these reactivity and stability issues, and hence a short background description of common structural features of known lithium amides and alkoxides is worthwhile.

Lithium amides often aggregate both in solution and the solid phase due to the relatively high polarity of the Li–N bond.[96-100] The degree of aggregation in these compounds mainly depends on the steric constraints imposed by the R substituents and the degree of lithium ion solvation by donor solvents.[92,95,97,101] For instance, bis(trimethylsilyl)amidolithium, $(Me_3Si)_2NLi$, forms a dimer-tetramer equilibrium in non-polar solvents, while in polar solvents, a dimer-monomer equilibrium is observed.[102] Lithium amide compounds exist in donor-free $[R_2NLi]_n$ or solvated $[R_2NLi.L_x]_n$ (L = donor solvent) forms depending on the type of solvents they are generated in.[103] In general, the more bulky the R substituents at the nitrogen center become, the higher the steric crowding and the lower the degree of aggregation. Monomers are observed when the steric bulk of R substituents at nitrogen centre prevent aggregation or the additional

donor solvent bases saturate the coordination sphere of lithium centre. However, in the absence of donor solvent or when less bulky R groups are employed, lithium amides can form simple $(R_2NLi)_n$ rings (Figure 1.9).[92,93,103,104] These $(R_2NLi)_n$ rings can act as smaller building blocks and yet further associate either in a lateral (side-by-side) or a vertical (face-to-face) manner, which are usually referred as "ring-laddering" and "ring-stacking", respectively (Figure 1.9).[92,97] Lithium amides exhibiting ring-laddering structures are composed of (R_2NLi) rungs either in a stepped or a cyclized arrangement. On the other hand, lithium amides with ring-stacking structural arrangement can form tetramers (i.e. lateral stack of two $(R_2NLi)_2$ rings), hexamers (i.e. stack of two $(R_2NLi)_3$ rings) or polymers composed of many stacked rings.[101]

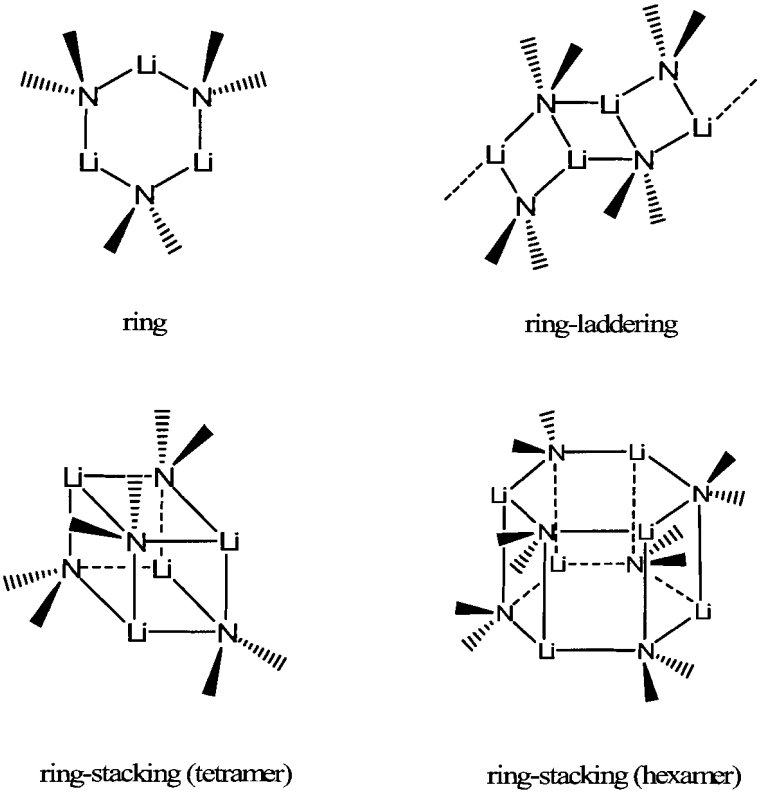

Figure 1.9 Schematic illustration of general structural types in aggregated lithium amides.

Like amidolithium compounds, ring-laddering and ring-stacking is the norm for lithium alkoxides, and ring dimers, tetrameric cubanes and hexameric stacks are also found.[104,105] However, in general, anionic oxygen donors display a stronger attraction for Li^+ ions and thus in contrast to lithium amides, only few monomeric lithium alkoxide are known.[105] Furthermore, ROLi complexes are usually less bulky than the corresponding R_2NLi since the oxygen centre carries only one organic group, which results in a higher degree of aggregation in these compounds compared to lithium amides.[101]

1.5 Magnetism

In chapter three, the magnetic behaviour of some of the synthesized chromium complexes will be discussed. Thus, a brief discussion of basic magnetochemistry is worthwhile. However, a detailed discussion of magnetism is beyond the scope of this thesis and can be pursued through other sources.[106-108]

Electrons are negatively-charged species in motion inside the atom and can be regarded as miniature bar magnets. Thus, when a compound is placed in a magnetic field, the magnetic field inside the material will be the sum of the external magnetic field and the magnetic field generated by the material itself. In general, two primary types of magnetism exist: diamagnetism and paramagnetism. In diamagnetic compounds, each orbital is filled with two electrons (paired electrons) and the magnetic moment generated by the electrons in that orbital cancel each other out. Diamagnetic behaviour is characterized by the slight repulsion of a substance out of an applied magnetic field, with a negative value of magnetic susceptibility (χ_m). The diamagnetic behaviour is

temperature independent, and is roughly proportional to the molecular weight of the material.

On the other hand, paramagnetic materials have one or more unpaired electrons. This paramagnetic behaviour is characterized by the attraction of a substance into the magnetic field and therefore they possess a positive magnetic susceptibility (χ_m). The strength of paramagnetic interactions is temperature-dependant. However, some substances exhibit temperature independent paramagnetism due to a coupling between the magnetic ground state and a non-thermally populated excited state. The magnitude of the magnetic susceptibility for the paramagnetic material depends on the number of unpaired electrons in their molecules. The volume magnetic susceptibility χ_v is defined as:

$$\chi_v = M / H$$

where M is the magnetization (a property of material), and H is the external magnetic field. The volume magnetic susceptibility can also be expressed as gram magnetic susceptibility χ_g (χ_v divided by density of the sample) or molar magnetic susceptibility χ_m (χ_g multiplied by molecular weigh of the sample). The magnetic susceptibility of compounds in the solid state can be measured by using devices like Gouy or Faraday balances, SQUID, and in solution by an NMR method (the Evans method).[108]

The measure of magnetic interaction is often expressed as effective magnetic moment μ_{eff} and is calculated as:

$$\mu_{eff} = 2.828 (\chi_m T)^{1/2}$$

where μ_{eff} is the effective magnetic moment in Bohr magneton (B.M.), and T is the temperature in Kelvin. For a paramagnetic material, perhaps the most important

electronic property for interpreting the paramagnetic behaviour is determining the number of unpaired electrons. The spin-only value of the magnetic moment (μ_{so}) of a paramagnetic compound can be calculated as:

$$\mu_{so} = g \{ S (S + 1) \}^{1/2}$$

where g is a constant (2.0023), and S is the total electron spin. However, paramagnetic effects originate from two sources: the spin angular momentum and orbital angular momentum of the electrons. Thus, when both spin and orbital motion of the electrons are taken into account then the equation can be written as:

$$\mu_{eff} = \{ 4 S (S + 1) + L (L + 1) \}^{1/2}$$

where L is the total orbital angular momentum. This equation is derived for compounds which are magnetically dilute (compounds without significant interactions between spins) and have partially occupied symmetric and degenerate orbitals with unequal electronic populations. However, for paramagnetic first-row transition metal compounds the spin-only formula is often used as a first rough approximation and is often a good estimation for determining the number of unpaired electrons since the orbital contribution L is mostly quenched.

The magnetic susceptibility of diamagnetic materials shows no variation with temperature. However, in the case of paramagnetic materials, as temperature increases, the magnetic susceptibility (χ_m) decreases. The source of this temperature dependency is the disruption of the alignment of molecular magnetic moments due to the thermal motion of the atoms. In some paramagnetic compounds, the magnetic susceptibility is inversely proportional to the temperature. This is referred to as the Curie Law which is:

$$\chi_m = C / T$$

where χ_m is molar magnetic susceptibility, C is the Curie constant, and T is temperature (Figure 1.10).

However, in many paramagnetic compounds, although this inverse relationship is observed, the extrapolation to zero temperature does not obey the Curie Law. These compounds obey the Curie-Weiss Law which is:

$$\chi_m = C / (T - \theta)$$

where θ is the Weiss constant. Plots of $1/\chi_m$ vs. T for such compounds are linear with a slope of 1/C and an X intercept of θ (Figure 1.10).

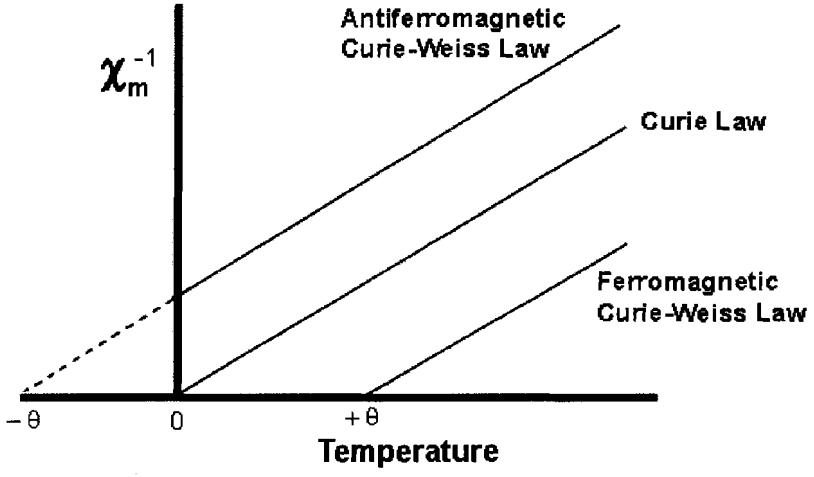

Figure 1.10 Plot of inverse molar magnetic susceptibility as a function of temperature for paramagnetic compounds that obey Curie or Curie-Weiss Laws.

In the case of chromium complexes, both high-spin and low-spin states are observed.[109-111] For instance, in the presence of weak-field ligands (e.g. water, ammonia, amido, and alkoxo ligands) octahedral Cr(II) complexes are generally high-spin with $t_{2g}^3 e_g^1$ configuration (four unpaired electrons; μ_{so} = 4.90 B.M.) (Figure 1.11 **a**). A Jahn-

Teller effect is expected for this electron configuration and may result in a tetragonally-distorted octahedral arrangement or even in extreme cases a square-planar geometry. However, this does not influence the spin-state; a high-spin state is still expected for a square-planar Cr(II) system (Figure 1.11 **c**). In the presence of strong-field ligands (e.g. CO and cyanide), a low-spin t_{2g}^4 configuration is generally adopted (two unpaired electrons; μ_{so} = 2.83 B.M.) (Figure 1.11 **b**). Polynuclear Cr(II) complexes with short Cr–Cr distances (2.0 - 2.5 Å) exhibit weak to medium antiferromagnetic coupling which results in magnetic moments lower than the expected μ_{so} value. Strong antiferromagnetic interactions are observed for dinuclear Cr complexes with Cr–Cr distances less than 2.0 Å. These Cr(II) compounds which contain strong quadruple metal-metal bonds are generally diamagnetic.[112]

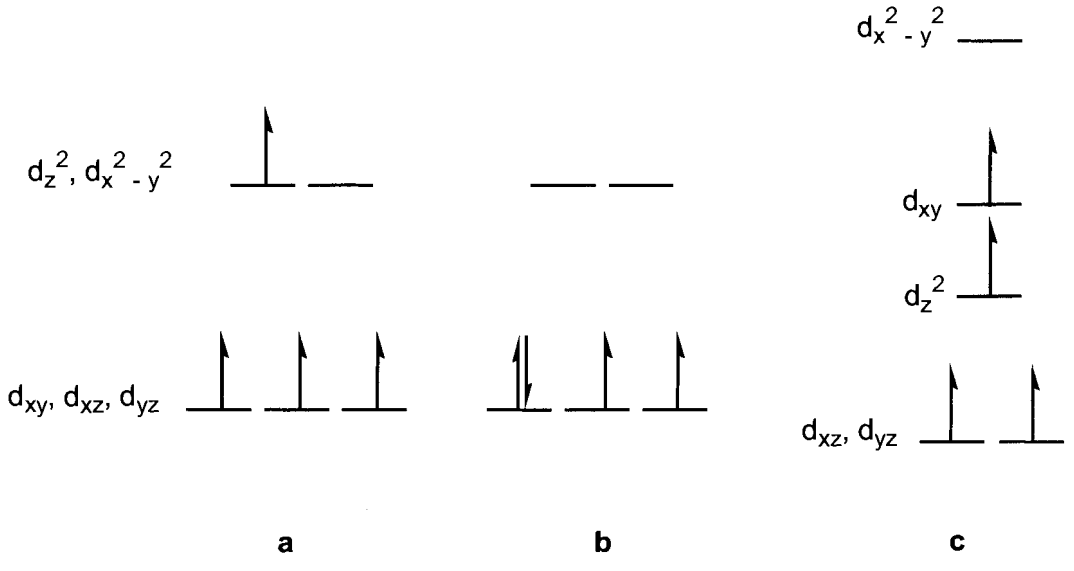

Figure 1.11 Occupancy of *d* orbitals in chromium(II) complexes (d^4): (**a**) high-spin octahedral, (**b**) low-spin octahedral, and (**c**) square-planar.

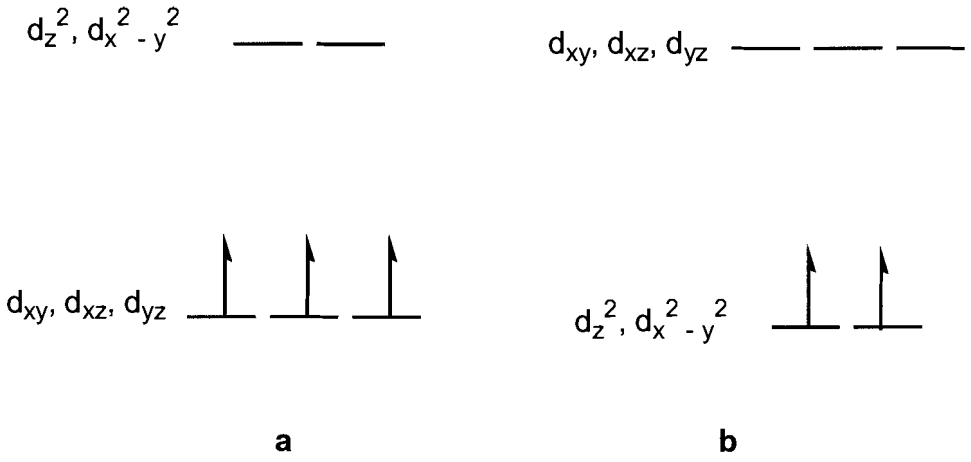

Figure 1.12 Occupancy of *d* orbitals in (**a**) octahedral chromium(III) and (**b**) tetrahedral chromium(IV) complexes.

Mononuclear, octahedral Cr(III) complexes have a t_{2g}^3 electron configuration and display temperature-independent magnetic moments close to the spin-only μ_{so} of 3.87 B.M. due to the presence of three unpaired *d* electrons (Figure 1.12 **a**). The magnetic moments of polynuclear Cr(III) complexes are temperature-dependent and are usually lower than the value of μ_{so} due to antiferromagnetic interaction between the Cr(III) centers.[110] Tetrahedral Cr(IV) complexes have an e^2 electron configuration and show magnetic moments close to the spin-only μ_{so} value expected for d^2 systems (two unpaired electrons; μ_{so} = 2.83 B.M.) (Figure 1.12 **b**).

For paramagnetic compounds that are not magnetically dilute, the spin coupling of adjacent metal centres may result in ferromagnetic or antiferromagnetic interactions. If this coupling occurs in a way in which the magnetic fields all tend to align in the same direction, ferromagnetic coupling results and the effective magnetic moment is expected to be higher than the spin-only value. Antiferromagnetic coupling results when the magnetic fields are coupled in opposite directions and the effective magnetic moment is expected to be lower than the spin-only value.

In case of ideal paramagnetic compounds (spin-only with no coupling), the magnetic moment does not vary with temperature (Figure 1.13). However, variations of magnetic moment with temperature are observed for ferromagnetic and antiferromagnetic materials (Figure 1.13). Ferromagnetic materials display an upward curve from the line for an ideal paramagnet as the ferromagnetic interaction energy overcomes thermal energy. This is because at lower temperatures, the spin-randomness of electrons decrease and the local magnetic exchange interactions become more favourable. On the other hand, antiferromagnetic interactions display downward curve with decreasing temperature as the magnetic moment for the sample goes to zero. The high-T values of μ_{eff} and the speed and extent to which the curves change with decreasing T gives an indication as to the strength of the magnetic interaction between the metals. This can be modelled using an interaction parameter J, but the details are beyond the scope of this thesis.

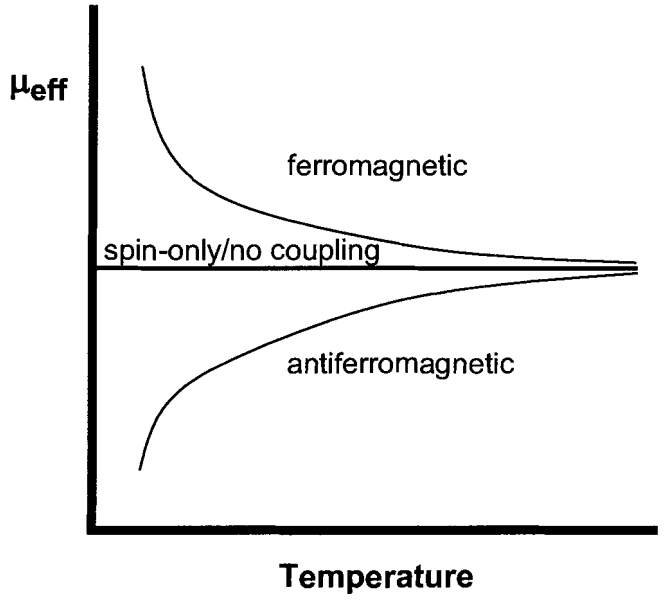

Figure 1.13 A typical plot for the μ_{eff} as a function of temperature for pure paramagnetic (spin-only with no coupling), ferromagnetic, and antiferromagnetic materials.[108]

CHAPTER 2:
LITHIUM SALTS OF CHELATING DIAMIDOSILYL ETHER AND AMIDO-AMINO-SILOXO LIGANDS

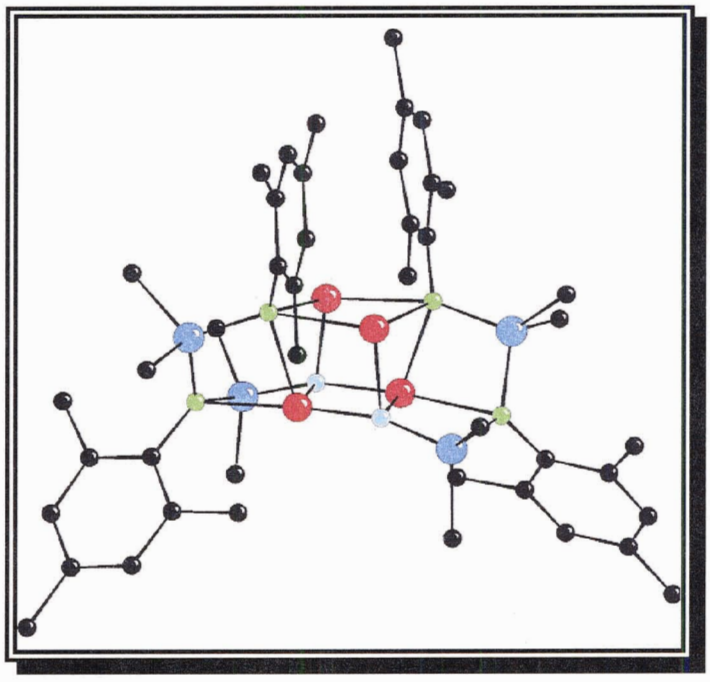

2.1 Introduction

Diamidosilyl ether ligands of the form $\{[RN(SiMe_2)]_2O\}^{2-}$, termed $[^{R}NON]^{2-}$, can be easily modified via the nitrogen substituent to achieve a range of steric and electronic profiles.[40,113-115] For example, bulky aryl moieties such as 3,5-$(CF_3)_2$Ph can be used to tune the amido ligand to be moderately sterically encumbered and strongly electron-withdrawing. On the other hand, less steric alkyl groups such as propyl can be used to make the amido ligands more sterically unencumbered and electron-donating. Indeed,

this versatility is the case for diamido and diamido-donor ligands in general and thus a wide range of symmetrical chelating such ligands with a selection of backbones have been reported in the past.[2,8,15,19,29,40,116-126] However, due to more challenging synthetic procedures, the related non-symmetrical N-donor (i.e. two different amido groups) and mixed-donor (i.e. different donor atoms) ligands are less accessible.[127]

The first part of this chapter will discuss the synthesis and characterization of new symmetrical alkyl- and aryl-substituted diamidosilyl ether ligands via two different routes: the excess amine route and the lithiated amide route. In addition to the $[^{R}NON]^{2-}$ ligands previously reported in the Leznoff research group[48,49] and elsewhere,[40,116] the range of substituents on the nitrogen atom has been further extended to include non-steric propyl, moderately steric 3,5-Me_2Ph, and redox-active ferrocenyl groups in order to explore the electronic and steric impact of the amido-R-groups on the reactivity of the metal complexes to be prepared.

The second part of this chapter is focused on the synthesis and characterization of new non-symmetrical mixed-donor ligands. As mentioned in chapter one, the *N*-lithio derivatives of the symmetrical diamidosilyl ether ligands $Li_2[^{R}NON]$ (R = Pr, 3,5-Me_2Ph, 2,4,6-Me_3Ph, 2,6-$^{i}Pr_2$Ph, 3,5-$(CF_3)_2$Ph) undergo an anionic intramolecular retro-Brook rearrangement in which one silyl group migrates from the oxygen to the amido-nitrogen atom. Thus, this retro-Brook silyl migration was used to synthesize the non-symmetrical mixed-donor amido-amino-siloxo ligands $[^{R}NN'O]^{2-}$. Finally, kinetic studies of this retro-Brook rearrangement will be discussed at the end.

2.2 Synthesis and Characterization of New Diamidosilyl Ether Ligands $H_2[^RNON]$

Most previously reported diamidosilyl ether ligands $\{[RNH(SiMe_2)]_2O\}$[40,48,49] were prepared via the lithium amide route, which involves the reaction of 1,3-dichloro-1,1,3,3-tetramethyldisiloxane with the appropriate lithium amide (Figure 2.1).

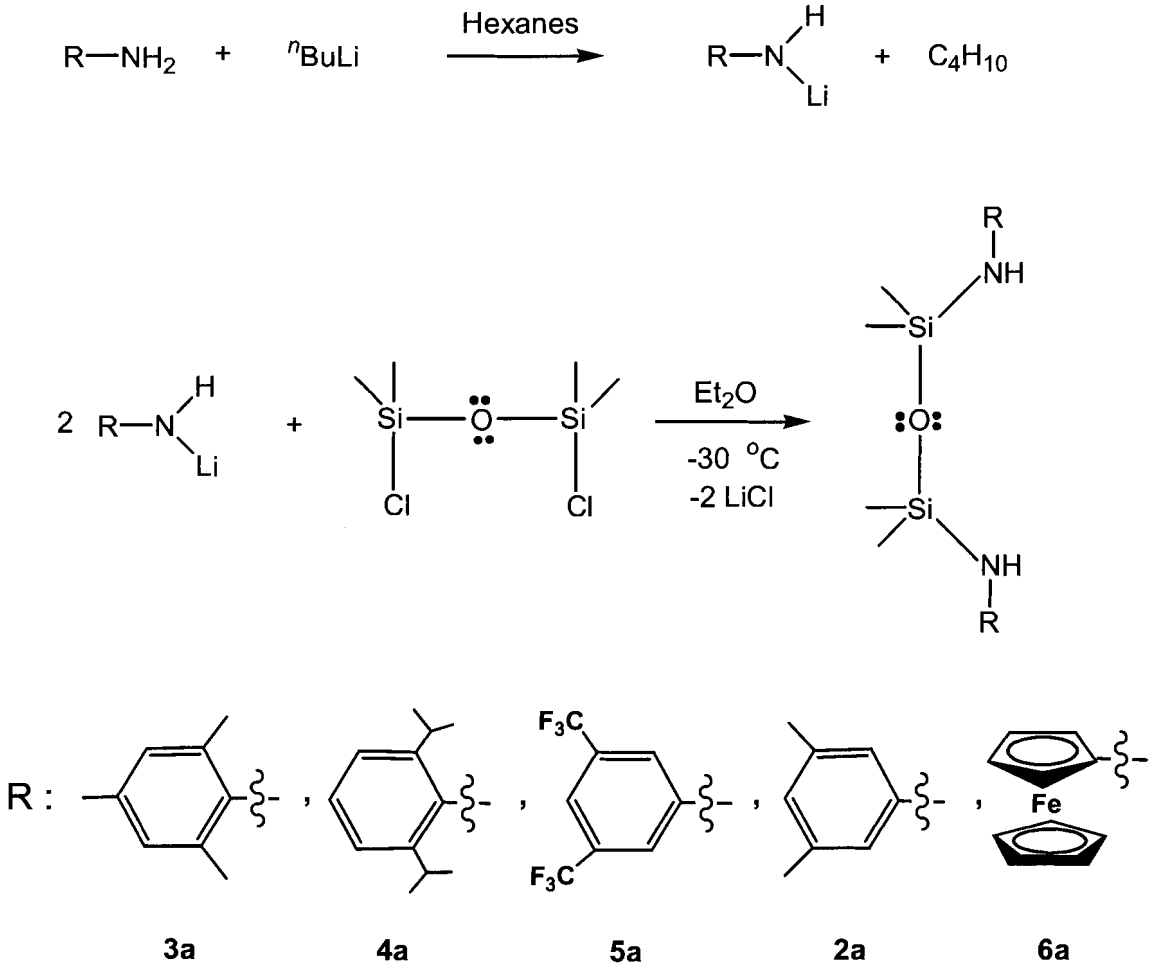

Figure 2.1 General synthesis of the symmetrical diamidosilyl ether ligands $H_2[^RNON]$ (R = 2,4,6-Me_3Ph (**3a**), 2,6-$^iPr_2Ph$ (**4a**), and 3,5-$(CF_3)_2Ph$ (**5a**)),[48,49] $H_2[^{Me_2Ph}NON]$ (**2a**), and $H_2[^{Fc}NON]$ (**6a**) via the two-step amide route.

However, attempts to prepare the analogous R = propyl {[PrNH($SiMe_2$)]$_2$O} ligand via a similar procedure failed and instead resulted in a mixture of products, the majority of which were identified as cyclosiloxazane compounds. These can form by intramolecular and intermolecular HCl elimination (Figure 2.2). MS analysis of the reaction of LiNHPr with 1,3-dichloro-1,1,3,3-tetramethyldisiloxane indicated that the dominant products are four- and eight-membered silicon-containing rings (the mass spectrum of the product mixture shows two major molecular ion peaks at *m/z* 190 and *m/z* 379, corresponding to $C_7H_{19}NOSi_2$ and $C_{14}H_{38}N_2O_2Si_4$ respectively, as shown in Figure 2.2). This side reaction presumably is facile in this case due to the relatively small steric profile and good electron donating ability of the propyl group, permitting inter- and intramolecular attack of the mono-substituted $RNHSiMe_2OSiMe_2Cl$ intermediate. Similar reactions of cyclosiloxazane compounds are known.[128-130] For instance, treating the 1,3-dichloro-1,1,3,3-tetramethyldisiloxane ethereal solution with gaseous ammonia following by distillation results in the formation of the eight-membered ring cyclosiloxazane compound $[HNSiMe_2OSiMe_2]_2$.[129] However, when methylamine reacts under the same conditions with dichlorotetramethyldisiloxane, a mixture of products of linear {[MeNH($SiMe_2$)]$_2$O} and incompletely silylated methylamines result.[129]

Thus, a different method, the "excess amine route" was employed to access the desired R = Pr derivative. In this synthesis, direct addition of 1,3-dichloro-1,1,3,3-tetramethyldisiloxane to an excess of neat anhydrous propylamine afforded a colorless oil $H_2[^{Pr}NON]$ (**1a**) in high yield. The addition of $(ClSiMe_2)_2O$ to this highest concentration of propylamine results in rapid replacement of both Cl^- groups with external $PrNH^-$, which competes effectively with the inter- and intramolecular reactions, thereby

completely inhibiting ring formation (Figure 2.2). The propylamine solvent also serves to mop up the HCl produced, generating a white precipitate of $[PrNH_3]Cl$. The previously prepared R = ^{t}Bu and Ph analogues[40,116] use a similar amine-addition route, but excess amine is not required in those cases.

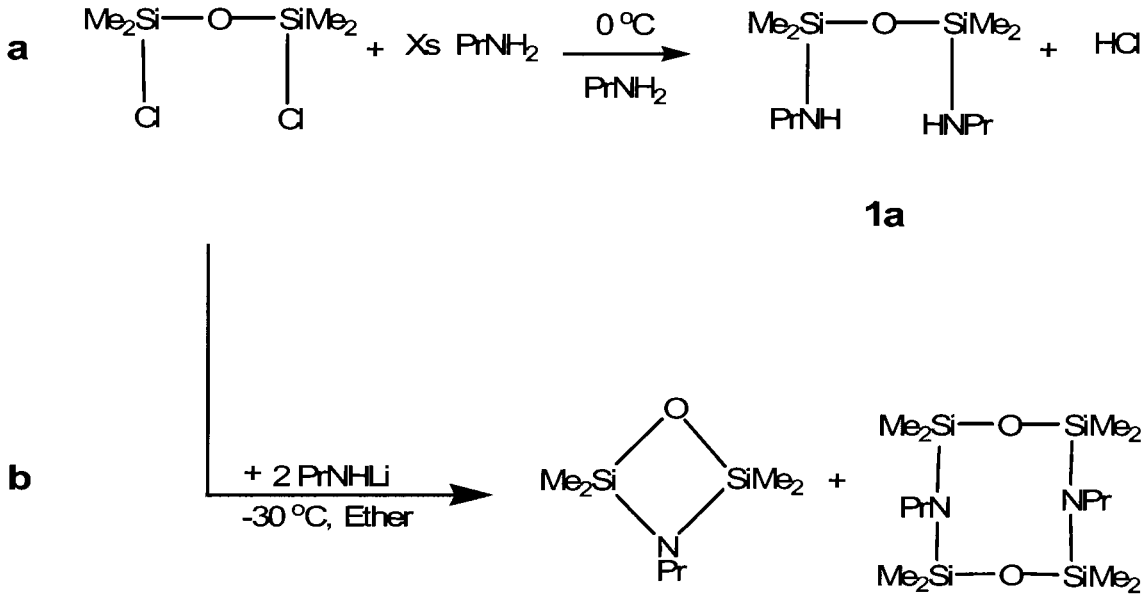

Figure 2.2 (**a**) Synthesis of the diamidosilyl ether ligand precursor $\{[PrNHSiMe_2]_2O\}$ (**1a**) via the excess amine route, (**b**) formation of closed rings when the lithium amide route was utilized.

In the case of the more steric arylamido R-groups 3,5-Me_2Ph and Fc, the two-step lithium amide route was used without difficulty to synthesize the respective diamidosilyl ether ligands. Thus, 3,5-dimethylaniline was treated with one equivalent of ^{n}BuLi at –78 °C, resulting in a quantitative yield of a green powder of 3,5-Me_2PhNHLi. Addition of 1,3-dichloro-1,1,3,3-tetramethyldisiloxane at –30 °C resulted in the isolation of the dark orange oil $H_2[^{Me_2Ph}NON]$ (**2a**) (Figure 2.1). In the same manner, *N*-ferrocenyl amine $\{Fe(\eta^5\text{-}C_5H_5)(\eta^5\text{-}C_5H_4\text{-}NH_2)\}$, $FcNH_2$[131,132] was reacted with one equivalent of ^{n}BuLi at

−78 °C, resulting in a high yield of the dark orange powder FcNHLi. Addition of 1,3-dichloro-1,1,3,3-tetramethyldisiloxane at −30 °C resulted in the isolation of the dark orange powder $H_2[^{Fc}NON]$ (**6a**) (Figure 2.1).

Compounds **1a**, **2a**, and **6a** were characterized by ^1H NMR, mass spectroscopy, and elemental analysis. As a representative example, the ^1H NMR of **1a** in benzene-d_6 consists of five peaks assigned to the silyl-methyl (δ 0.18, s, 12H), amine (δ 0.67, br s, 2H), γ-methyl (δ 0.84, t, 6H, $-CH_2CH_2\boldsymbol{CH_3}$), β-methylene (δ 1.35, m, 4H, $-CH_2\boldsymbol{CH_2}CH_3$), and α-methylene (δ 2.72, m, 4H, $-\boldsymbol{CH_2}CH_2CH_3$) protons. The mass spectrum of **1a** consists of a major molecular ion peak at *m/z* 249 (M^+) as well as molecular fragment ion peaks at *m/z* 234 (M^+ − Me) and at *m/z* 190 (M^+ − Me − Pr) (Figure 2.3).

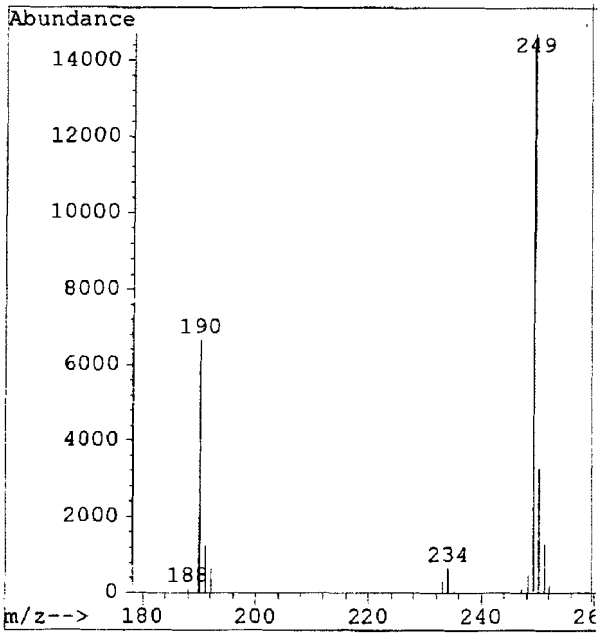

Figure 2.3 Electron impact mass spectrum of $\{[PrNH(SiMe_2)]_2O\}$ (**1a**).

The related diamidosilyl ether ligand precursors {[RNH($SiMe_2$)]$_2$O} (R = 2,4,6-Me_3Ph, H_2[^{Me_3Ph}NON] (**3a**); 2,6-^{i}Pr_2Ph, H_2[^{iPr_2Ph}NON] (**4a**); 3,5-$(CF_3)_2$Ph, H_2[^{CF_3Ph}NON] (**5a**)) have been previously reported by Leznoff *et al.*,[48,49] but no solid-state structures were described. As a representative example and to compare with the solid-state structures of the *N*-lithio derivatives of the ligands (see the following section), the solid state structure of the previously reported (but not crystallized) diaminosilyl ether H_2[^{Me_3Ph}NON] **3a** was obtained. Suitable single crystals of ligand **3a** were obtained from cooling a saturated hexanes solution. The single crystal X-ray structure of **3a** reveals a monomeric structure (Figure 2.4); selected interatomic distances and bond angles are detailed in Table 2.1. The silyl ether backbone forms a twisted zigzag chain with a tetrahedral geometry around the silicon centres and a trigonal planar geometry around the sp^2 nitrogen atoms. The Si–N bond lengths are relatively short (1.707(5) and 1.712(5) Å). A Si–N single bond (from covalent radii) has been estimated as 1.80–1.87 Å,[133] while in fact a typical Si–N bond length falls in the range of 1.65-1.75 Å (e.g. Si–N in $HN(SiMe_3)_2$ is 1.735(12) Å).[134] This is presumably due to significant π bonding by delocalization of the electrons of the nitrogen *p* orbitals into the vacant Si *d* orbitals.[134] The relatively short Si–O bonds (1.604(4) and 1.635(4) Å) are comparable to those in $Me_3SiOSiMe_3$ (1.630(5) and 1.632(5) Å).[135]

In general, Si–O bonds are shorter than Si–N bonds, due to the better π-bonding overlap between oxygen and silicon.[60] The Si–O–Si bond angle of 148.9(3)° is close to that of $Me_3SiOSiMe_3$ (142.2(3)°),[135] smaller than that of $Ph_3SiOSiPh_3$ (180°)[136] and moderately large when compared with that in other siloxanes.[137-139] This obtuse angle has been attributed to delocalization of the oxygen lone pair electrons from the filled valance

shell of oxygen into the vacant *3d* orbitals of silicon, forming substantial Si–O π-bonding.[140] Furthermore, the Si–O bonds of 1.604(4) and 1.635(4) Å are considerably shorter than the sum of the single bond covalent radii (1.91 – 1.93 Å), which is also consistent with the Si–O double bond character.[141]

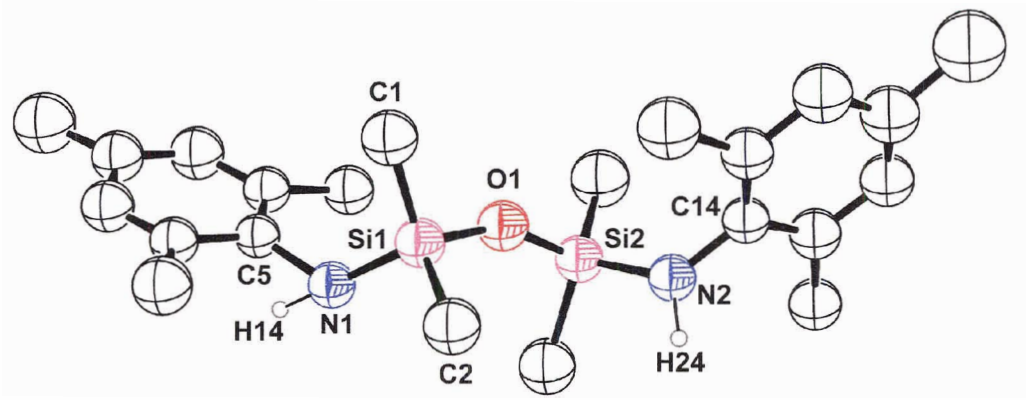

Figure 2.4 Molecular structure of $H_2[^{Me_3Ph}NON]$ (**3a**) (ORTEP view with 33% probability ellipsoids; Non-amino hydrogen atoms are removed for clarity).

Table 2.1 Selected interatomic distances (Å) and bond angles (deg) for $H_2[^{Me_3Ph}NON]$ (**3a**).

Si(1)–O(1)	1.604(4)	Si(1)–N(1)	1.707(5)
Si(1)–C(1)	1.841(7)	Si(1)–C(2)	1.865(7)
Si(2)–O(1)	1.635(4)	Si(2)–N(2)	1.712(5)
N(1)–C(5)	1.438(7)	N(2)–C(14)	1.437(7)
O(1)–Si(1)–N(1)	113.8(2)	Si(1)–N(1)–C(5)	126.7(4)
C(1)–Si(1)–C(2)	114.4(4)	Si(2)–N(2)–C(14)	128.8(4)
O(1)–Si(2)–N(2)	113.3(2)	Si(1)–O(1)–Si(2)	148.9(3)

2.3 Synthesis and Characterization of New Mixed-Donor Amido-Amino-Siloxo Ligands $Li_2[^RNN'O]$

Deprotonation of **1a** – **5a** with two equivalents of ^{n}BuLi in non-polar solvents such as Et_2O or toluene yielded the *N*-lithio derivatives $\{[RNLi(SiMe_2)]_2O\}$ (R = Pr, $Li_2[^{Pr}NON]$ (**1b**); 3,5-Me_2Ph, $Li_2[^{Me_2Ph}NON]$ (**2b**); 2,4,6-Me_3Ph, $Li_2[^{Me_3Ph}NON]$ (**3b**); 2,6-$^i Pr_2$Ph, $Li_2[^{iPr_2Ph}NON]$ (**4b**); 3,5-$(CF_3)_2$Ph, $Li_2[^{CF_3Ph}NON]$ (**5b**)) as shown in Figure 2.5. Ligands **1b** – **5b** were characterized by ^{1}H NMR and elemental analysis. The most distinguishing feature in the ^{1}H NMR spectrum is the disappearance of the amine proton peaks upon *N*-lithio derivative $\{[RNLi(SiMe_2)]_2O\}$ formation when compared to that of the non-lithiated ligands.

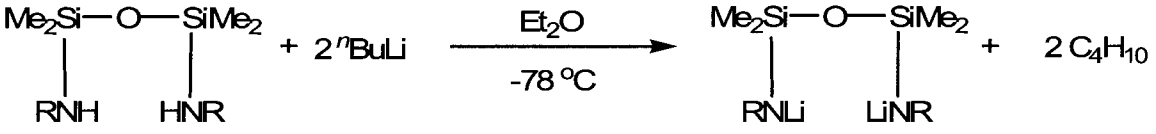

R = Pr, **1a**
3,5-Me_2Ph, **2a**
2,4,6-Me_3Ph, **3a**
2,6-$^i Pr_2$Ph, **4a**
3,5-$(CF_3)_2$Ph, **5a**

R = Pr, **1b**
3,5-Me_2Ph, **2b**
2,4,6-Me_3Ph, **3b**
2,6-$^i Pr_2$Ph, **4b**
3,5-$(CF_3)_2$Ph, **5b**

Figure 2.5 Deprotonation in Et_2O of diamidosilyl ether ligand precursors **1a** – **5a** via addition of two equivalents of ^{n}BuLi.

However, if the lithiation reaction of compounds **1a** – **5a** is conducted in THF, or if the isolated *N*-lithio derivatives of the ligands **1b** – **5b** are stirred in THF, they undergo the anionic intramolecular [1,3]-O→N silyl retro-Brook rearrangement in which one silyl

group migrates from oxygen to the amido-nitrogen (Figure 2.6). Thus, this reaction yields compounds of the form {RNLiSiMe$_2$N(R)SiMe$_2$OLi} (R= Pr, Li$_2$[^{Pr}NN'O] (**1c**); 3,5-Me$_2$Ph, Li$_2$[^{Me_2Ph}NN'O] (**2c**); 2,4,6-Me$_3$Ph, Li$_2$[^{Me_3Ph}NN'O] (**3c**); 2,6-^{i}Pr$_2$Ph, Li$_2$[^{iPr_2Ph}NN'O] (**4c**); 3,5-(CF$_3$)$_2$Ph, Li$_2$[^{CF_3Ph}NN'O] (**5c**)); these can be viewed as new mixed-donor amido-amino-siloxo ligands prepared in one-step and high-yield.

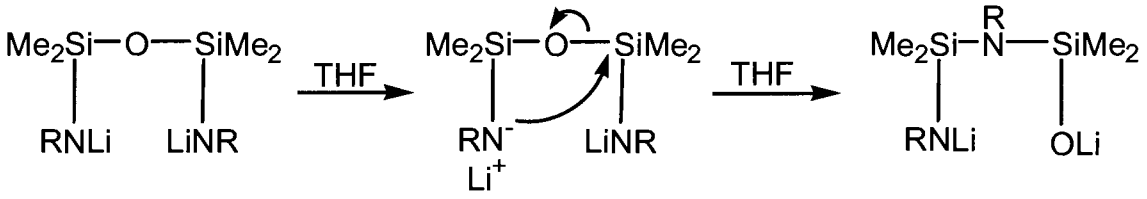

R (conditions) =

Pr, **1b** (70 °C, 72 hrs)
3,5-Me$_2$Ph, **2b** (25 °C, 15 min)
2,4,6-Me$_3$Ph, **3b** (25 °C, 2 hrs)
2,6-^{i}Pr$_2$Ph, **4b** (25 °C, 48 hrs)
3,5-(CF$_3$)$_2$Ph, **5b** (70 °C, 10 days)

R (yield)=

Pr, **1c** (92%)
3,5-Me$_2$Ph, **2c** (98%)
2,4,6-Me$_3$Ph, **3c** (94%)
2,6-^{i}Pr$_2$Ph, **4c** (78%)
3,5-(CF$_3$)$_2$Ph, **5c** (76%)

Figure 2.6 Synthesis of mixed-donor amido-amino-siloxo ligands from symmetrical diamidosilyl ether ligands via the retro-Brook rearrangement.

The rearrangement reaction was confirmed by ^{1}H NMR spectroscopy. In the unrearranged form, the structure has mirror symmetry and thus a single resonance is observed for each set of symmetrical protons. However, in the rearranged form, the protons are not equivalent anymore, and therefore two different peaks of equal intensity are observed for each set of protons; representative data for R = Pr (**1b** and **1c**) are shown in Figure 2.7.

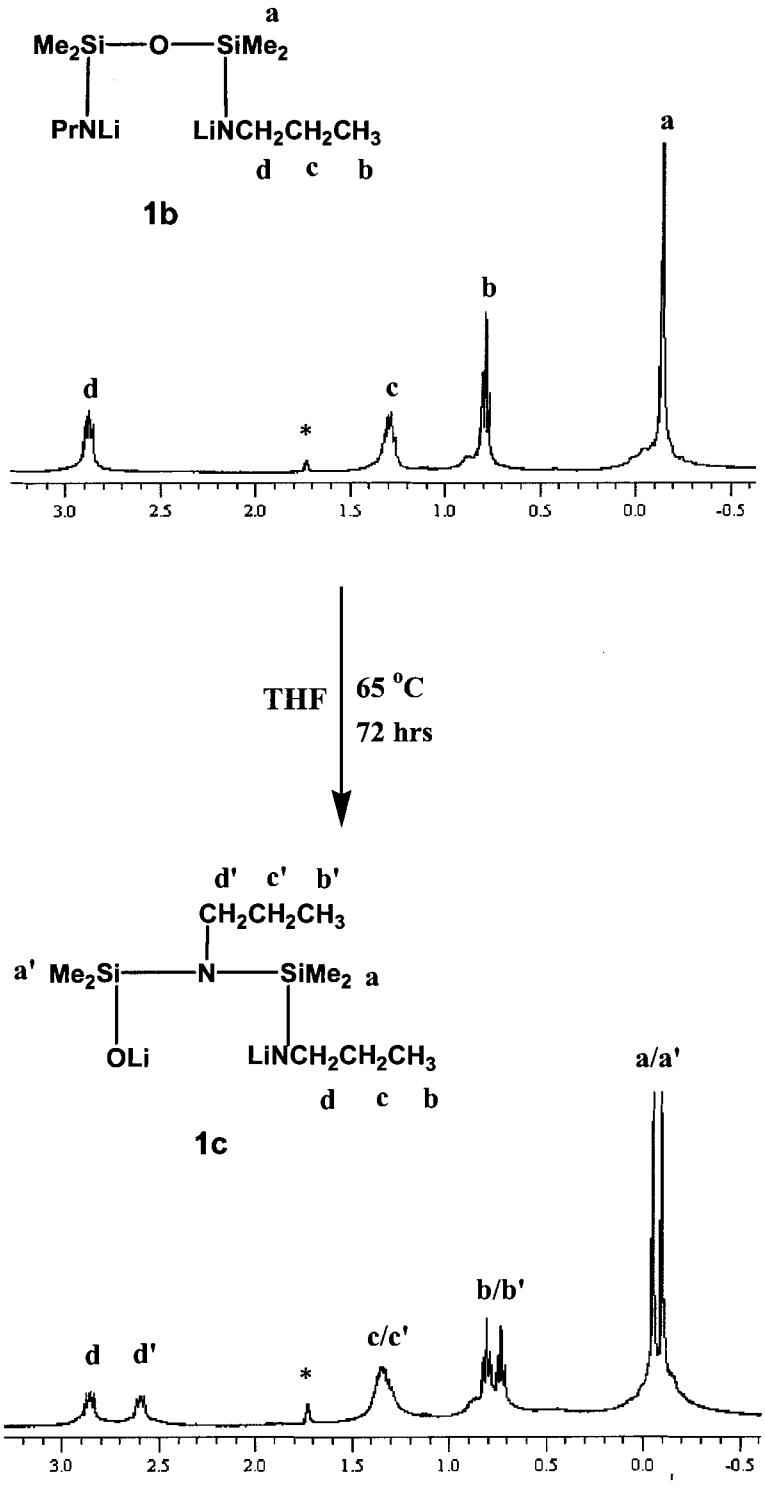

Figure 2.7 400 MHz ^{1}H NMR spectra of **1b** (top) and **1c** (bottom) in THF-d_8*.

Single crystals of compounds **1c**, **3c**, and **4c** suitable for X-ray diffraction were obtained from the slow evaporation of pentane/toluene (**1c**), THF/toluene (**3c**), and Et_2O/toluene (**4c**) solutions at room temperature. In the solid state, $Li_2[^{Pr}NN'O]$ (**1c**) is a tetrameric cluster with a rare triple-stack of fused twisted cubes of lithium surrounded by four ligands (Figure 2.8). Owing to the high coordination number of the Li atoms (four-coordinate), the Li–O and Li–N bonds are fairly long with distance ranges of 1.984(17)–2.104(17) Å and 2.024(18)–2.248(18) Å respectively (Table 2.2).

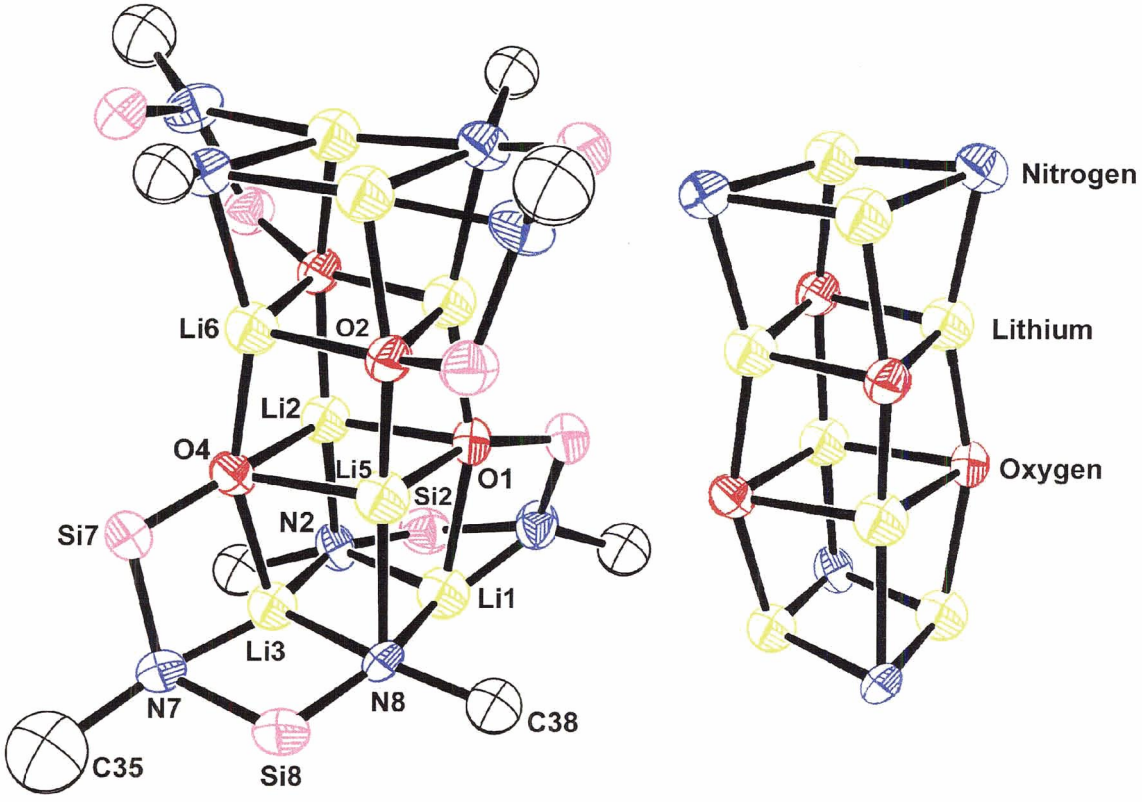

Figure 2.8 Left: Molecular structure of the tetrameric cluster of $Li_2[^{Pr}NN'O]$ (**1c**) (ORTEP view with 33% probability ellipsoids; alkyl groups are simplified for clarity). Right: Simplified triple-stacked lithium cubane in the structure's core.

Table 2.2 Selected interatomic distances (Å) and bond angles (deg) for $Li_2[^{Pr}NN'O]$ (**1c**).

N(2)–Li(1)	2.066(17)	O(1)–Li(5)	2.026(17)
N(2)–Li(3)	2.032(17)	O(2)–Li(5)	1.984(17)
N(7)–Li(3)	2.179(17)	O(4)–Li(2)	2.017(16)
N(8)–Li(1)	2.033(18)	Si(7)–N(7)	1.751(7)
N(8)–Li(5)	2.124(17)	Si(7)–O(4)	1.614(5)
N(8)–C(38)	1.497(9)	Si(8)–N(7)	1.769(7)
N(8)–Li(3)	2.061(16)	Si(8)–N(8)	1.699(7)
O(1)–Li(1)	2.104(17)		
N(7)–Si(8)–N(8)	104.5(4)	Li(2)–O(4)–Li(5)	78.4(6)
Li(3)–O(4)–Li(6)	157.2(7)	Si(8)–N(7)–Si(7)	124.4(5)
Li(1)–N(8)–Li(3)	66.5(7)	N(8)–Li(3)–N(2)	113.6(8)
N(8)–Li(1)–N(2)	113.4(8)	Li(3)–N(2)–Li(1)	66.4(7)
N(2)–Li(1)–O(1)	92.4(7)	O(1)–Li(2)–N(2)	92.6(6)
O(1)–Li(5)–O(4)	101.7(7)	N(2)–Li(1)–O(1)	92.4(7)

The four central Li atoms are coordinated by one amide nitrogen and three siloxide oxygen atoms. The four outer lithium atoms are coordinated by one siloxide oxygen, two amide nitrogens and one amine nitrogen atom. The $Li(3)–N(7)_{amine}$ bond of 2.179(17) Å is significantly longer than the $Li(3)–N(8)_{amido}$ bonds of 2.061(16) Å. The structure can also be regarded as an alternating stack of four Li_2N_2 and Li_2O_2 rings. Thus, each siloxo group is quadruply bonding, each amido group is triply bonding and the amine groups only bind to one lithium centre.

A similar triple-stacking structure is observed in the alkoxolithium mixed-anion compound $\{[LiO(^tBu)][Li(^nBu)]\}_4$.[142] In this compound, the four central Li atoms are coordinated by an α-C atom of ^nBu (av. Li–C, 2.22 Å) and three oxygens of the tert-butoxy anions (av. Li–O, 1.89 Å). The four outer lithiums are coordinated by one oxygen (av. Li–O, 1.84 Å), two α-C atoms (av. Li–C, 2.19 Å), and a β-CH_2 group of one of two

n-butyl anions (av. Li–C, 2.35 Å; Li–H, 2.34 Å). The bond lengths of the $Li_4O_2N_2$ cubane core in **1c** are comparable to those in $[Li_4(C_5H_3NMeNHSiMe_2O)_4]$,[143] which has an isolated pseudo-cubane Li-O core (Li-O distances of 1.91(1)-2.009(8) Å) and $[Li_2(\mu\text{-}C_6H_4(NSiMe_3)_2)]_2$,[144] which has an isolated pseudo-cubane Li-N core (Li-N distances of 2.028(3)-2.082(4) Å). The largest oligomeric organolithium cubane-type stack is $[(^tBuC{\equiv}CLi)_{12}{\bullet}THF_4]$, which exhibits a six-fold stacking of $(CLi)_2$ rings terminated by THF molecules.[145]

Compound **3c** is a solvent adduct of formula $\{Li_2[^{Me_3Ph}NN'O]{\bullet}THF\}_2$ in the solid state. The higher steric bulk of the 2,4,6-Me_3Ph substituents and the complexation of THF molecules inhibit stacking or higher aggregation and as a result **3c** crystallizes as a dimer (Figure 2.9). The structure consists of a dimeric ladder made up of a lateral attachment of two Li–N–Li–O rings or, alternatively, four Li–N and Li–O rungs. The degree of stacking in lithium salts of amides and alkoxides are often limited by the presence of the bulky R substituents and many cases of isolated ladder-type structures have been observed for those with bulky substituents.[1,92,97,99,101] The central ring of the ladder, Li(1)–O(1)–Li(1)*–O(1)*, is planar, with the outer rings straddling this plane on opposite sides in a chair fashion. Thus, two six-membered rings are fused to opposite sides of the central ladder, forming an overall puckered ladder or stair-shaped structure. The O–Si–N–Si–N backbone acts as a dianionic chelate; in other words, the central silylamine does not bind to any lithium, unlike in **1c**.

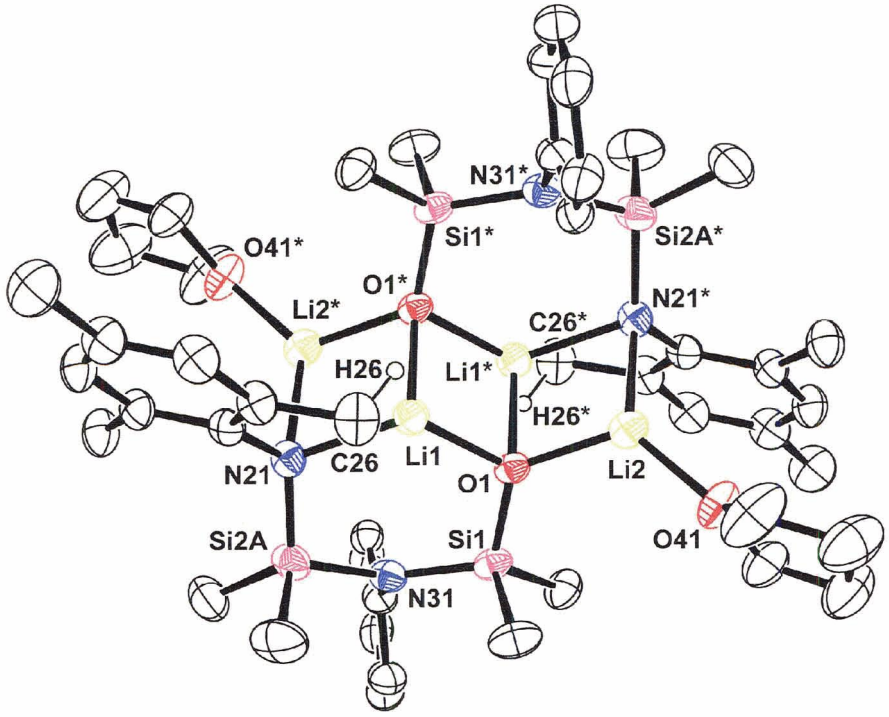

Figure 2.9 Molecular structure of $\{Li_2[^{Me_3Ph}NN'O]\bullet THF\}_2$ (**3c**) (ORTEP view with 33% probability ellipsoids; aryl groups simplified for clarity).

Table 2.3 Selected interatomic distances (Å) and bond angles (deg) for $\{Li_2[^{Me_3Ph}NN'O]\bullet THF\}_2$ (**3c**).

Si(1)–O(1)	1.621(3)	N(31)–Si(2A)	1.786(4)
Si(1)–N(31)	1.770(4)	O(1)–Li(1)	1.886(7)
N(21)–C(20)	1.427(5)	O(1)–Li(1)*	1.911(7)
N(21)–Li(1)	2.004(8)	O(1)–Li(2)	1.859(5)
N(21)–Li(2)*	2.046(8)	O(1)*–Li(1)	1.911(7)
N(21)–Si(2A)	1.760(5)	O(41)–Li(2)	1.872(14)
O(1)–Si(1)–N(31)	111.49(15)	Si(2A)–N(21)–Li(2)*	128.1(3)
N(21)–Si(2A)–N(31)	105.3(3)	C(20)–N(21)–Si(2A)	123.0(3)
Si(1)–O(1)–Li(1)	110.9(3)	O(1)–Li(1)–O(1)*	101.2(3)
Si(1)–O(1)–Li(2)	121.1(3)	O(1)–Li(1)–N(21)	126.9(4)
Si(1)–O(1)–Li(1)*	136.5(3)	O(1)*–Li(1)–N(21)	104.8(4)
Li(1)–O(1)–Li(1)*	78.8(3)	Li(1)–O(1)–Li(2)	123.7(3)
Si(1)–N(31)–Si(2A)	132.7(3)	Si(2A)–N(21)–Li(1)	112.7(3)

*Symmetry transformations used to generate equivalent atoms: -x + 1, -y + 1, -z + 1

The non-bonding Li(1)–N(31) distance is 3.078(15) Å, which is much longer than the Li–N_{amine} bond lengths observed in **1c** (e.g. Li(3)–N(7) is 2.179(17) Å). In **1c**, the distorted tetrahedral geometry around the N_{amine} is such that one of the N_{amine} sp^3 lobes points directly to the Li atom, facilitating a Li–N_{amine} interaction and generating a trigonal *fac* geometry of the N_{amido}, N_{amino}, and O centres with respect to Li centre. However, in **3c**, the steric bulk of the 2,4,6-Me_3Ph substituents prevents such an arrangement and the non-bonding *p* lobe of the N_{amine} is positioned away from the Li centre (*mer* geometry). Thus, each inner Li centre is coordinated by one amide nitrogen and two siloxide oxygen atoms and each terminal Li centre is coordinated by only one siloxide oxygen and one amide nitrogen atom. The low coordination number of the terminal lithium centres is alleviated by the formation of a dative bond from a THF donor. The Li–N distances of the outer rings are 2.004(8) and 2.046(8) Å for Li(1)–N(21) and Li(2)–N(21)* respectively (Table 2.3).

The Li–O distances are relatively shorter than those of **1c** and range from 1.859(5) and 1.911(7) Å due to the lower coordination of Li atoms (three-coordinate). Similar limited-ladder structures have been previously observed.[93,146-148] For example, $[Li(py)OSiPh_2OSiPh_2OLi(py)]_2$[146] has a ladder-shaped structure with a central four-membered $(Li–O)_2$ ring with an average Li–O distance of 2.00 Å. The outer Li are three-coordinate and have an average Li–O distance of 1.84 Å. Similarly, $[\{Li(Mes)N\}_2SiMe_2]_2$ has a ladder-shaped structure with an average Li-N bond length of 1.96 Å.[147] In **3c**, the inner lithium centres (Li(1) and Li(1)*) are additionally stabilized by an agostic interaction to hydrogen atom of methyl groups (C(26)H(26)···Li(1) and C(26)*H(26)*···Li(1)*) with a relatively short distance of 2.151(9) Å. Agostic

interactions with lithium amides with similar distances have previously been found[147,149,150] and for instance in $[Li^{i}Pr_2PhNCH_2CH_2N^{i}Pr_2PhLi]_2$[147], agostic Li···H distances of 2.24 Å to the protons of the diisopropyl groups were reported.

In the solid state, **4c** is a solvated monomer, $\{Li_2[^{iPr_2Ph}NN'O]\bullet(Et_2O)_3\}$ as shown in Figure 2.10; selected interatomic distances and bond angles are detailed in Table 2.4. The highly sterically encumbering 2,6-$^{i}Pr_2$ groups on the aromatic ring and higher degree of solvation compared to that of **1c** and **3c** prevent any aggregation of the molecules in the solid state. Both Li(1) and Li(2) are three-coordinate with distorted trigonal planar geometries. Li(1) is chelated by the ligand, which results in the formation of a puckered six-membered ring. The structure is further stabilized by complexation of three Et_2O molecules: one is attached to Li(1) and two are attached to Li(2). The N(11)–Li(1) distance is 1.915(13) Å.

In **4c**, the O(11)–Li(1) and O(11)–Li(2) distances (1.860(12) and 1.793(14) Å respectively) are relatively shorter when compared to the Li–O distances in **1c** (1.984(17) – 2.104(17) Å) presumably due to the lower coordination of Li centres (three-coordinate). Here again, the steric bulk of $^{i}Pr_2Ph$ results in a *mer* geometry of N_{amido}, N_{amino}, and O centres with respect to the Li(1) centre. The non-bonding *p* lobe of the N_{amine} is positioned out of the ring plane away from the Li(1) centre and as a result precludes any Li–N_{amino} interaction (Li(1)–N(31) distance of 3.082 Å). Similarly, a shorter Li–N_{amido} bond length (1.915(13) Å) is observed in **4c** when compared to those of **1c** (2.032(17) – 2.124(17) Å) and **3c** (2.004(8) and 2.046(8) Å).

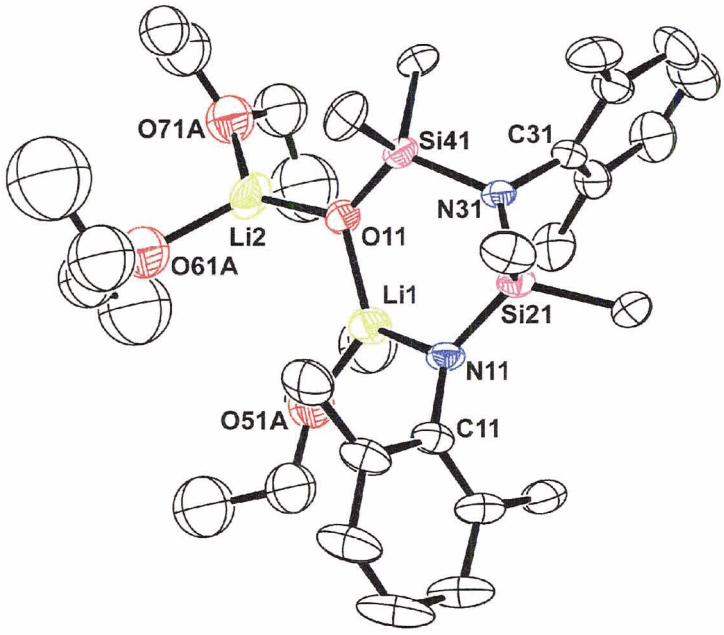

Figure 2.10 Molecular structure of $\{Li_2[^{iPr_2Ph}NN'O]\bullet(Et_2O)_3\}$ (**4c**) (ORTEP view with 33% probability ellipsoids; diisopropyl groups are simplified for clarity).

Table 2.4 Selected interatomic distances (Å) and bond angles (deg) for $\{Li_2[^{iPr_2Ph}NN'O]\bullet(Et_2O)_3\}$ (**4c**).

Si(21)–N(11)	1.677(5)	N(11)–Li(1)	1.915(13)
Si(21)–N(31)	1.756(5)	O(11)–Li(1)	1.860(12)
Si(21)–C(22)	1.867(8)	O(11)–Li(2)	1.793(14)
Si(41)–N(31)	1.751(5)	Li(1)–O(51A)	1.893(19)
Si(41)–O(11)	1.604(5)	Li(2)–O(61A)	2.00(2)
N(11)–C(11)	1.395(7)		
N(11)–Si(21)–N(31)	107.2(2)	Si(21)–N(11)–Li(1)	117.6(4)
O(11)–Si(41)–N(31)	112.9(2)	Si(41)–N(31)–Si(21)	124.0(3)
O(71A)–Li(2)–O(61A)	102.6(10)	Si(41)–O(11)–Li(2)	127.4(6)
C(11)–N(11)–Si(21)	126.2(4)	Si(41)–O(11)–Li(1)	112.5(5)
C(11)–N(11)–Li(1)	115.9(6)	Li(2)–O(11)–Li(1)	118.7(7)

2.4 Kinetic Study of the Retro-Brook Rearrangement of $Li_2[^RNON]$ to $Li_2[^RNN'O]$

The kinetic parameters of the retro-Brook rearrangement reactions for *N*-lithio derivatives of the ligands $Li_2[^RNON]$ (R= Pr (**1c**); 3,5-Me_2Ph (**2c**); 2,4,6-Me_3Ph (**3c**); 2,6-$^iPr_2$Ph (**4c**); 3,5-$(CF_3)_2$Ph (**5c**)) were determined by peak integration analysis of the ^1H NMR spectra in THF-d_8 taken during the course of the reactions. Time-dependent NMR spectra were obtained at three different temperatures for each ligand. For instance, in the case of **1c**, the NMR spectra were obtained at 32, 50, and 65 °C during the course of the reaction (at one day intervals) in THF-d_8. The integrated peak areas for peaks of the $-CH_2N-$ protons were used to calculate the concentration of the unrearranged *N*-lithio derivative of the ligand (Figure 2.11).

Plots of ln $[^RNON]$ vs. time (where ln $[^RNON]$ is the natural logarithm of the concentration of unrearranged *N*-lithio derivative) were made for each temperature (Figure 2.12). Nearly linear plots were obtained in all cases, indicating that the rearrangement reaction follows a first-order process. For first-order kinetics, the rate law is:

$$\ln [^RNON] = \ln [^RNON]_o - kt$$

where $[^RNON]_o$ is the initial concentration of the unrearranged ligand, and t is time. Thus the observed rate constants k_{obs} for each temperature set can be calculated from the –slope of the line and the half-life $\tau_{1/2}$ can be calculated from ln $2/k_{obs}$.[151]

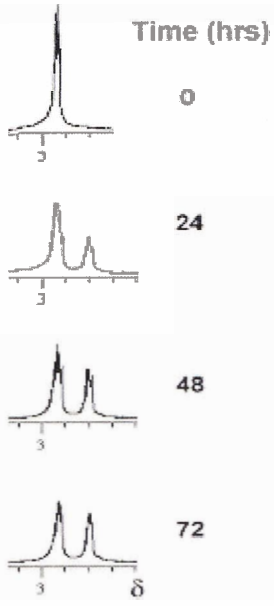

Figure 2.11 400 MHz ^{1}H NMR spectrum of {(PrNLiSiMe$_2$)$_2$O} (**1b**) as function of time (hours) for the –CH$_2$N– protons (20 mg/mL of THF-d_8 at 65 °C).

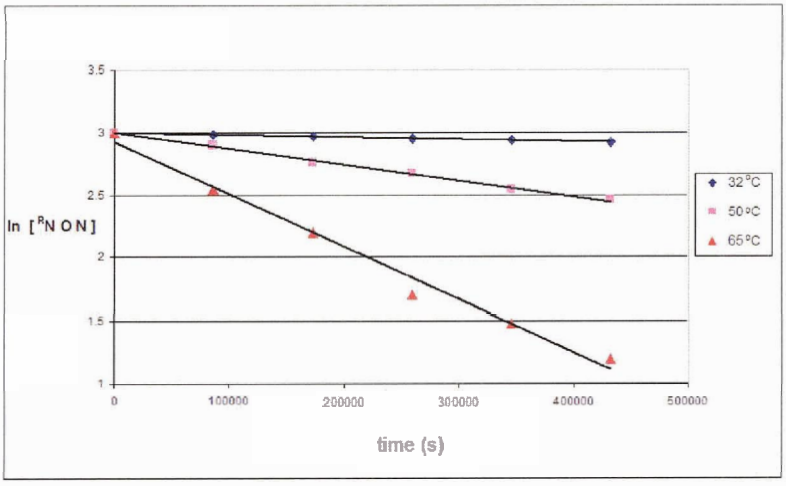

Figure 2.12 Analysis of kinetic data for the retro-Brook rearrangement reaction of **1b** to **1c**. The plots of ln[^{Pr}NON] vs. t at 32, 50, and 65 °C are nearly linear, indicating a first-order reaction.

The activation energy E_a can be calculated using the Arrhenius activation energy equation:

$$\ln k_{obs} = \ln A - E_a/RT$$

where A is frequency factor, T is temperature, and R is the universal gas constant. The plots of ln k_{obs} vs. $1/T$ for the reaction of $Li_2[^RNON]$ to $Li_2[^RNN'O]$ are very close to linear and the activation energy E_a is calculated from $-R$ times the slope of the line. Furthermore, the kinetic parameters were determined from the Eyring plot (graph of $\ln(k_{obs}/T)$ vs. $1/T$) and the Eyring equation:[151]

$$\ln (k_{obs}/T) = [\ \ln(k_b/h) + (\Delta S^{\ddagger}/R)\ ] - (\Delta H^{\ddagger}/RT)$$

where k_b is Boltzmann's constant and h is Planck's constant.

Thus, the activation enthalpy $\Delta H^{\ddagger}$ is the –slope of the Eyring line times R (universal gas constant) and the activation entropy $\Delta S^{\ddagger}$ is R times [intercept – $\ln(k_b/h)$] (Figure 2.13). Finally, the value of the free energy of activation $\Delta G^{\ddagger}$ can be calculated from:

$$\Delta G^{\ddagger} = \Delta H^{\ddagger} - T\ \Delta S^{\ddagger}$$

Using this procedure, the values of $\Delta H^{\ddagger}$, $\Delta S^{\ddagger}$, $\Delta G^{\ddagger}$, E_a, and $\tau_{1/2}$ for the rearrangement reaction of the $Li_2[^RNON]$ ligands are summarized in Table 2.5. The straight-line plots show that the rearrangement reaction is an intramolecular and a first-order process. It is also apparent that the rate of the rearrangement reaction is governed largely by electronic and to a lesser extent to steric effects of the substituent R-group on the nitrogen atoms as will be detailed below.

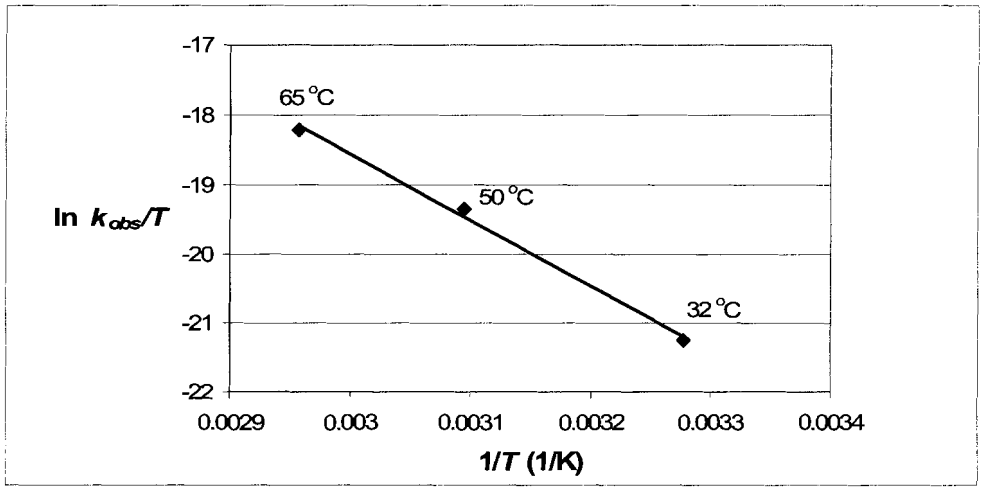

Figure 2.13 Analysis of kinetic data for the retro-Brook rearrangement reaction of **1b** to **1c**. The graph shows the Eyring plot (graph of $\ln(k_{obs}/T)$ vs. $1/T$) at 32, 50, and 65 °C.

Table 2.5 Summary of the kinetic parameters for rearrangement reactions of compounds **1b – 5b** to **1c – 5c**.

R-group	$\Delta H^{\ddagger}$ *(kJ mol^{-1})*	$\Delta S^{\ddagger}$ *(J K^{-1} mol^{-1})*	$\Delta G^{\ddagger}$ *(kJ mol^{-1}) at 300 K*	E_a *(kJ mol^{-1})*	$\tau_{1/2}$ *(s) at 298 K*
Pr (1)	79.3	-79.8	103.3	82.0	3.83×10^{6}
Me_2Ph (2)	50.9	-110.8	84.2	53.2	5.68×10^{1}
Me_3Ph (3)	66.7	-71.7	88.3	69.1	3.05×10^{2}
$^{i}Pr_2Ph$ (4)	78.0	-62.4	96.7	78.6	9.31×10^{3}
$(CF_3)_2Ph$ (5)	117.1	-11.5	120.5	119.9	1.45×10^{8}

Prior studies on the mechanism of the Brook-type rearrangement reactions (see section 1.3) are consistent with these observations; in general, increasing the nucleophilicity of the amido-nitrogen would decrease the activation energy for intramolecular attack on silicon and thus increase the rate of the rearrangement. Changing

the concentration of the NMR sample has no effect on the rate of the rearrangement; comparable kinetic data was obtained using 10, 20, and 30 mg/mL ($Li_2[^{Pr}NON]$/THF-d_8) concentrations. Furthermore, no other products were detected in the ^1H NMR spectra. Both of these points indicate that the rearrangement is predominantly an intramolecular process.

The half-life ($\tau_{1/2}$) values at room temperature (298 K) fall in the broad range of seconds to days, expressing the significance of steric and electronic effects of the amido-R substituent on the rearrangement reaction. Activation energies are relatively low (53-120 kJ/mol) which suggests that the transition state is of relatively low energy. This is presumably due to the availability of vacant *d* orbitals on silicon which facilitate the formation of the pentacoordinated bridged structure between oxygen and nitrogen.[68] The greater ionic stability of the lithium siloxide compared to the starting lithium amide presumably offsets the energy required to break a Si–O and form a weaker Si–N bond (443 and 318 kJ, respectively).[78] Furthermore, the $\Delta S^{\ddagger}$ values are relatively large and negative, approximately −12 to −111 J/K.mol depending on the system, suggesting considerable reduction of freedom in the transition state.[61]

Compound **5b** has the slowest rearrangement rate. The relatively high electron withdrawing ability of the CF_3 groups in $Li_2[^{CF_3Ph}NON]$ results in electron delocalization from nitrogen into the phenyl group, weakening the nucleophilicity of the amido-nitrogen. This low nucleophilicity of the amide inhibits the attack on silicon such that **5b** has the largest $\Delta G^{\ddagger}$ and $\tau_{1/2}$ values (120.5 kJ/mol and 1.45×10^8 s, respectively). As a comparison, both **5b** and **2b** have substituents with similar steric profiles at the meta positions of the aromatic ring; these ligands have the least steric hindrance at the N-donor

of any aniline-based ligands presented here. The Me-group is electron-donating, which significantly increases the nucleophilicity of the amide in $Li_2[^{Me_2Ph}NON]$ compared to that in $Li_2[^{CF_3Ph}NON]$. Therefore the electron rich, sterically unencumbered N-donor readily attacks Si in **2b**, yielding smallest observed $\Delta G^{\ddagger}$ and $\tau_{1/2}$; indeed, the $\tau_{1/2}$ for electron-rich **2b** is nearly 2.5×10^6 faster than the electron-poor **5b**.

Compounds $Li_2[^{Me_3Ph}NON]$ (**3b**) and $Li_2[^{Me_2Ph}NON]$ (**2b**) only have Me substituents on the aromatic rings and therefore have relatively similar electronic profiles. However, the methyl groups in the ortho positions of **3b** sterically hinder the amide from attacking the Si, which lowers the reaction rate and slightly increases the $\Delta G^{\ddagger}$ value from 84.2 to 88.3 kJ/mol. The further additional steric bulk from the 2,6-^{i}Pr groups in $Li_2[^{iPr_2Ph}NON]$ (**4c**) compared to the 2,4,6-Me groups significantly hinders the nucleophilic amide attack on the silicon centre. Thus, the values of $\tau_{1/2}$ and $\Delta G^{\ddagger}$ increase from **2c** to **3c** to **4c** as the steric hindrance increases. However, despite the large steric impediment generated by 2,6-^{i}Pr$_2$Ph groups, the $\tau_{1/2}$ value only increases by a factor of about 160 from the less bulky 3,5-Me$_2$Ph group and is still about 10^4 faster than the less bulky 3,5-(CF$_3$)$_2$Ph. Thus, electronic effects appear to be more important than steric hindrance in influencing the kinetics of the retro-Brook rearrangement in this case.

The propyl substituent in $Li_2[^{Pr}NON]$ (**1b**) yields the most nucleophilic amide among the ligands studied and it also exerts the least steric hindrance of any R group presented here. Thus, it could be expected that **1b** should have the fastest rearrangement, yet the rearrangement of $Li_2[^{Pr}NON]$ occurs with a greater $\Delta G^{\ddagger}$ and $\tau_{1/2}$ (103.3 kJ/mol and 3.83×10^6 s respectively) than the non-fluorinated ligands. In the solid state, $Li_2[^{Pr}NN'O]$ has a tetrameric structure with three fused Li cubes and presumably, this aggregation may

exist in some degree in solution for the non-rearranged form as well. Thus, the energy barrier required to break the aggregated clusters of Li–N bonds prior to intramolecular attack on silicon may inhibit the rearrangement process. At room temperature, a broad peak in the ^{6}Li NMR spectrum of **1b** was observed which indicates that the complex is fluctional in solution. This broadness may also be a result of the quadrupolar interaction between ^{7}Li and ^{14}N. It is also possible that the relatively high nucleophilicity of the amido nitrogen in **1b** may increase the Li–N ionic bond strength and prevent dissociation of Li^{+} from the amide in THF, also inhibiting rearrangement.

The rearrangement of $Li_2[^{tBu}NON]$ was attempted in THF-d_8 for 32 days at 55 °C, but the peaks in the ^{1}H NMR spectrum remained the same. Despite the high nucleophilicity of the N-donor, presumably the steric bulk of the ^{t}Bu completely inhibits the intramolecular nucleophilic attack of Si, or equally likely, the putative final product, containing a $Me_2Si–N(^{t}Bu)–SiMe_2$ backbone is simply too sterically encumbered to form at all.

These kinetic observations are comparable to the kinetic studies previously reported by Brook *et al.*[68] They reported that, in general, the activation energies for anionic Brook-type rearrangement are low, but entropies of activation are large and negative.[68] For instance, the rates of rearrangement of $[R_3SiCR'_2O]^{-}$ (R and R' = H, Me, Phenyl) showed that the energies of activation E_a were of the order of 33 to 46 kJ/mol and the $\Delta S^{\ddagger}$ were of the order of -146 to -167 J/K.mol depending on the R groups.[62] Changing R groups on silicon from phenyl to methyl decreases the rate by a factor of about 6 per substitution. On the other hand, changing the R' groups on carbon from hydrogen or methyl to phenyl increases the rate by a factor of about 10^3 per substitution.

This is strongly indicative of sensitivity of the rearrangement to the substituents and specifically to the negative charge that develops on the benzylic carbon during formation of the transition state, which is stabilized by electron-withdrawing and destabilized by electron-donating groups. Furthermore, they also reported the Hammett ρ-σ relationship for several series of R' = para-substituted phenyls with relatively large positive ρ values from 3.4 to 4.6. This indicates that the transition state has considerable negative charge dispersed into the phenyl ring and therefore there is considerable negative charge at the benzyl carbon atom, which shows the sensitivity of Brook-type rearrangement to the electronic effects of the substituents.

2.5 Summary

New symmetrical alkyl- and aryl-substituted diamidosilyl ether ligands were synthesized by two distinct routes: the excess amine route and the lithiated amide route. In the case of the moderately steric arylamido R-groups 3,5-Me_2Ph and Fc, the two-step lithium amide route was used to synthesize the respective diamidosilyl ether ligands **2a** and **6a**. However, in the case of R = Pr, employing a similar procedure failed and instead resulted in a mixture of cyclosiloxazane compounds. Therefore, the excess amine route was employed to synthesize ligand **1a**.

Deprotonation of ligands **1a – 5a** with two equivalents of ^{n}BuLi in non-polar solvents such as ether or hexanes yielded the *N*-lithio derivatives $\{[RNLi(SiMe_2)]_2O\}$. However, if the deprotonation is conducted in THF, or if the isolated $Li_2[^RNON]$ ligands are stirred in THF, they undergo an anionic 1,3-silyl retro-Brook rearrangement which can be employed to synthesize new mixed-donor amido-amino-siloxo ligands

$Li_2[^RNN'O]$ in one facile step and in high yield. The kinetic parameters of the retro-Brook rearrangement reactions for *N*-lithio derivatives of the ligands $Li_2[^RNON]$ (R= Pr (**1c**); 3,5-Me_2Ph (**2c**); 2,4,6-Me_3Ph (**3c**); 2,6-$^iPr_2$Ph (**4c**); 3,5-$(CF_3)_2$Ph (**5c**)) were determined and showed that the rate of rearrangement increases with decreasing steric hindrance of the R substituent and increases with increasing electron-donating ability of the R substituent. The abnormally slow rate for propyl ligand suggests that the putative high nuclearity cluster structure of $Li_2[^{Pr}NON]$ system may impede the reaction.

The X-ray crystallographic study of the mixed-donor amido-amino-siloxo ligands **1c**, **3c**, and **4c** indicated that these ligands can adopt a wide range of structural and bonding patterns from a single-ring monomer to a tetrameric cluster. The degree of aggregation in the above complexes appears to be largely dictated by the steric constraints imposed by the R groups, the degree of solvation, and the type of the donor solvent. The structural studies also revealed that the chelating amido-amino-siloxo ligands are able to bind to lithium centres in both bidentate as well as tridentate modes making N_{amido}–, N_{amino}–, and O_{siloxo}–Li bonds. Due to their mixed-donor nature and flexible binding abilities, these ligands should have an extensive and unique coordination chemistry.

2.6 Experimental Section

2.6.1 General procedures, materials and instrumentation

All reactions were carried out under an inert atmosphere of dry nitrogen gas using standard Schlenk and vacuum line or glovebox (mBraun Labmaster 130) techniques. Hexanes and toluene (Fisher) were passed through an mBraun solvent purification system

connected to a glovebox. The tetrahydrofuran, THF (Fisher), was distilled from a potassium/benzophenone mixture under a nitrogen atmosphere. The diethyl ether, Et_2O (Caledon), was distilled from a sodium/benzophenone mixture under a nitrogen atmosphere. All glassware including the NMR test tubes were dried overnight prior to use. Benzene-d_6 (Aldrich), and THF-d_8 (Cambridge Isotope Laboratories) were dried over activated 4 Å molecular sieves (Acros)/sodium and stored under a nitrogen atmosphere. Anhydrous pentane (Aldrich) was dried with KH (Aldrich) and filtered over dried neutral alumina (Fisher) and stored under a nitrogen atmosphere. Amines were passed through a column of dried neutral alumina (Fisher) prior to use. All other reagents were used as received. $H_2[^{tBu}NON]$,[40,116] $H_2[^{Me_3Ph}NON]$,[48] $H_2[^{iPr_2Ph}NON]$,[48,113] $H_2[^{CF_3Ph}NON]$,[48,113] $Li_2[^{tBu}NON]$,[152,153] and $FcNH_2$[131,132] were prepared from published procedures.

NMR spectra were recorded at 294 K, unless otherwise stated, in benzene-d_6, or THF-d_8 employing a 500 MHz Varian Unity spectrometer or a 400 MHz Bruker AMX spectrometer. All ^1H chemical shifts are reported in ppm relative to the ^1H impurity of the internal solvent specifically, benzene-d_6, δ 7.16 (^1H), and THF-d_8, δ 3.58 (^1H). All ^6Li chemical shifts are reported in ppm relative to an external aqueous solution of LiCl. NMR data were processed with MESTREC® NMR data processing software (MESTRECLAB research). Elemental analyses (C, H, and N) were performed at Simon Fraser University by Mr. Miki Yang (SFU) employing a Carlo Erba EA 1110 CHN Elemental Analyzer. Mass spectra were measured using a HP-5985 GC-MS CI instrument operating at 70 eV by Mr. Phil Ferreira (SFU). X-ray crystallographic experimental details can be found in the Appendix.

2.6.2 Synthesis of {[PrNH(SiMe$_2$)]$_2$O}, H$_2$[^{Pr}NON] (1a)

1,3-dichloro-1,1,3,3-tetramethyldisiloxane (3.0 mL, 15.3 mmol) was added dropwise to an excess of neat anhydrous propylamine (9.066 g, 153 mmol) at 0 °C while stirring. The resulting white mixture was stirred overnight, and then the excess propylamine was removed *in vacuo*. The product was extracted with hexanes and filtered through Celite. The removal of hexanes *in vacuo* resulted in a clear colorless oil of **1a**. Yield: 3.324 g (87 %). Anal. Calcd. for $C_{10}H_{28}N_2OSi_2$: C, 48.33; H, 11.36; N, 11.27. Found: C, 48.20; H, 11.26; N, 11.16. ^{1}H NMR (benzene-d_6): δ 0.18 (s, 12H, Si(C*H*$_3$)$_2$), 0.67 (br s, 2H, N-*H*), 0.84 (t, 6H, CH$_2$CH$_2$C*H*$_3$), 1.35 (m, 4H, CH$_2$C*H*$_2$CH$_3$), 2.72 (m, 4H, C*H*$_2$CH$_2$CH$_3$). MS (CI): *m/z* 249 (M$^+$), 234 (M$^+$ – Me), 190 (M$^+$ – Me – Pr). The mass spectrum of the product mixture (form the lithium amide route) shows two major molecular ion peaks at *m/z* 190 (M$^+$) and *m/z* 379 (M$^+$), corresponding to $C_7H_{19}NOSi_2$ and $C_{14}H_{38}N_2O_2Si_4$ respectively.

2.6.3 Synthesis of {[3,5-Me$_2$PhNH(SiMe$_2$)]$_2$O}, H$_2$[^{Me_2Ph}NON] (2a)

A red/brown solution of anhydrous 3,5-dimethylaniline (5.0 g, 41.3 mmol) in 75 mL of Et$_2$O was cooled to −78 °C and one equivalent of 1.6 M ^{n}BuLi in hexanes (25.8 mL, 41.3 mmol) was added dropwise. The reaction was stirred for 5 hours at room temperature, yielding a light green mixture. The solvent was removed *in vacuo* and the product was washed with a minimum amount of cold pentane and dried to obtain a quantitative yield of monolithiated 3,5-dimethylaniline. Then a green solution of 3,5-Me$_2$PhNHLi (5.227 g, 41 mmol) in 150 mL of Et$_2$O was cooled to −30 °C and 1,3-dichloro-1,1,3,3-tetramethyldisiloxane (4.0 mL, 20 mmol) in 15 mL of Et$_2$O was added dropwise. Gradually, the reaction became cloudy orange. The reaction was warmed to

room temperature and stirred overnight. The solvent was removed *in vacuo*, the residue was extracted with hexanes and filtered through Celite. The hexanes were removed *in vacuo* to obtain a dark orange oil of **2a**. Yield: 6.907 g (90%). Anal. Calcd. for $C_{20}H_{32}N_2OSi_2$: C, 64.46; H, 8.66; N, 7.52. Found: C, 64.68; H, 8.54; N, 7.45. ^{1}H NMR (benzene-d_6): δ 0.25 (s, 12H, Si(CH_3)$_2$), 2.17 (s, 12H, *m*-CH_3), 3.39 (br s, 2H, N-*H*), 6.38 (s, 4H, *o*-*H*), 6.43 (s, 2H, *p*-*H*). MS (CI): *m/z* 372 (M^+– H).

2.6.4 Synthesis of {[PrNLi(SiMe$_2$)]$_2$O}, Li$_2$[^{Pr}NON] (1b)

A clear colorless oil of **1a** (5.0 g, 20.2 mmol) was dissolved in 30 mL of Et_2O and two equivalents of 1.6 M ^{n}BuLi in hexanes (25.15 mL, 40.3 mmol) were added dropwise at −78 °C, yielding a white mixture. After being stirred for 2 hours at room temperature, the solvent was removed *in vacuo* and the resulting white residue was brought into the glovebox. Hexanes (20 mL) were added and the resulting suspension was filtered on a frit filter and dried *in vacuo* to obtain a white powder of **1b**. Yield: 5.074 g (93 %). Anal. Calcd. for $C_{10}H_{26}N_2Li_2OSi_2$: C, 46.13; H, 10.06; N, 10.76. Found: C, 46.41; H, 10.09; N, 10.48. ^{1}H NMR (THF-d_8): δ -0.15 (s, 12H, Si(CH_3)$_2$), 0.78 (t, 6H, $CH_2CH_2CH_3$), 1.29 (m, 4H, $CH_2CH_2CH_3$), 2.87 (m, 4H, $CH_2CH_2CH_3$).

2.6.5 Synthesis of {[3,5-Me$_2$PhNLi(SiMe$_2$)]$_2$O}, Li$_2$[^{Me_2Ph}NON] (2b)

A dark orange oil of **2a** (3.0 g, 8.05 mmol) was dissolved in 60 mL of Et_2O and two equivalents of 1.6 M ^{n}BuLi in hexanes (10.1 mL, 16.1 mmol) were added dropwise at −78 °C, yielding a light yellow mixture. After being stirred for 30 minutes at room temperature, the solvent was removed *in vacuo* and the resulting residue was brought into the glovebox. Hexanes (30 mL) were added and the resulting suspension was filtered on a

frit filter and dried *in vacuo* to obtain a white powder of **2b**. Yield: 2.793 g (90%). Anal. Calcd. for $C_{20}H_{30}N_2Li_2OSi_2$: C, 62.47; H, 7.86; N, 7.28. Found: C, 62.16; H, 8.05; N, 6.96. ^{1}H NMR (THF-d_8): δ 0.12 (s, 12H, Si(C*H*$_3$)$_2$), 2.08 (s, 12H, *m*-C*H*$_3$), 5.94 (s, 2H, *p*-*H*), 6.18 (s, 4H, *o*-*H*).

2.6.6 Synthesis of {[2,4,6-Me$_3$PhNLi(SiMe$_2$)]$_2$O}, Li$_2$[^{Me_3Ph}NON] (3b)

A colorless solid of **3a** (4.23 g, 10.6 mmol) was dissolved in 50 mL of Et_2O and two equivalents of 1.6 M ^{n}BuLi in hexanes (13.2 mL, 21.1mmol) were added dropwise at –78 °C, yielding a white mixture. The reaction was warmed to room temperature and stirred overnight. The solvent was removed *in vacuo* and the resulting residue was brought into the glovebox. Hexanes (30 mL) were added and the resulting suspension was filtered on a frit filter and dried *in vacuo* to obtain a white powder of **3b**. Yield: 4.005 g (92%). Anal. Calcd. for $C_{22}H_{34}N_2Li_2OSi_2$: C, 64.05; H, 8.31; N, 6.79. Found: C, 63.79; H, 8.24; N, 6.69. ^{1}H NMR (THF-d_8): δ -0.12 (s, 12H, Si(C*H*$_3$)$_2$), 2.04 (s, 6H, *p*-C*H*$_3$), 2.17 (s, 12H, *o*-C*H*$_3$), 6.51 (s, 4H, aromatic *H*).

2.6.7 Synthesis of {[2,6-^{i}Pr$_2$PhNLi(SiMe$_2$)]$_2$O}, Li$_2$[^{iPr_2Ph}NON] (4b)

A clear colorless oil of **4a** (5.27 g, 10.9 mmol) was diluted in 50 mL of ether, cooled to –78 °C and two equivalents of 1.6 M ^{n}BuLi in hexanes (13.6 mL, 21.7 mmol) were added dropwise. Immediately a white solid formed. The reaction was warmed to room temperature and stirred for 18 hours. The solvent was removed *in vacuo*, and the remaining residue was brought into the glovebox. Hexanes (30 mL) were added and the resulting suspension was filtered on a frit filter and dried *in vacuo* to obtain a white powder of **4b**. Yield: 4.18 g (77%). Anal. Calcd. for $C_{28}H_{46}N_2Li_2OSi_2$: C, 67.70; H, 9.33;

N, 5.64. Found: C, 67.89; H, 9.22; N, 5.53. ^{1}H NMR (THF-d_8): δ -0.07 (s, 12H, Si(CH_3)$_2$), 1.05 (d, 24H, CH(CH_3)$_2$), 4.18 (m, 4H, CH(CH$_3$)$_2$), 6.18 (t, 2H, *p-H*), 6.65 (d, 4H, *m-H*).

2.6.8 Synthesis of {[3,5-(CF$_3$)$_2$PhNLi(SiMe$_2$)]$_2$O}, Li$_2$[^{CF_3Ph}NON] (5b)

A dark brown oil **5a** (5.03 g, 8.6 mmol) was diluted in 50 mL of hexanes, cooled to –30 °C, and two equivalents of 1.6 M ^{n}BuLi in hexanes (10.6 mL, 17 mmol) were added dropwise, yielding a cloudy brown mixture. The reaction was warmed to room temperature and stirred overnight. The solvent was removed *in vacuo*, and the remaining residue was brought into the glovebox. Hexanes (30 mL) were added and the resulting suspension was filtered on a frit filter and dried *in vacuo* to obtain a light brown powder of **5b**. Yield: 3.85 g (76%). Anal. Calcd. for $C_{20}H_{18}N_2F_{12}Li_2OSi_2$: C, 40.01; H, 3.02; N, 4.67. Found: C, 40.39; H, 3.40; N, 4.67. ^{1}H NMR (THF-d_8): δ 0.07 (s, 12H, Si(CH_3)$_2$), 6.23 (s, 2H, *p-H*), 6.73 (s, 4H, *o-H*).

2.6.9 Synthesis of {[PrNLiSiMe$_2$N(Pr)SiMe$_2$OLi}, Li$_2$[^{Pr}NN'O] (1c)

A white solid of **1b** (1.5 g, 5.76 mmol) was dissolved in 20 mL of THF and stirred at 70 °C for 72 hours. The solvent was then removed *in vacuo,* the resulting powder washed with a minimum amount of hexanes and dried to obtain the white powder of **1c**. Yield: 1.381 g (92%). Anal. Calcd. for $C_{10}H_{26}N_2Li_2OSi_2$: C, 46.13; H, 10.06; N, 10.76. Found: C, 46.50; H, 9.94; N, 10.40. ^{1}H NMR (THF-d_8): δ -0.10 (s, 6H, Si(CH_3)$_2$), -0.06 (s, 6H, Si(CH_3)$_2$), 0.73 (t, 3H, CH$_2$CH$_2$CH_3), 0.80 (t, 3H, CH$_2$CH$_2$CH_3), 1.35 (m, 4H, CH$_2$CH_2CH$_3$), 2.59 (m, 2H, CH_2CH$_2$CH$_3$), 2.85 (m, 2H, CH_2CH$_2$CH$_3$). ^{6}Li NMR (THF-d_8): δ 0.10 (v br). Single crystals were obtained from the slow evaporation of a saturated

toluene/pentane solution. The product **1c** can also be obtained by a one-pot reaction of diamine **1a** and two equivalents of ^{n}BuLi in THF at –78 °C followed by stirring at 70 °C for 72 hours.

2.6.10 Synthesis of {3,5-Me_2PhNLiSiMe_2N(3,5-Me_2Ph)SiMe_2OLi}, $Li_2[^{Me_2Ph}NN'O]$ (2c)

A white solid of **2b** (300 mg, 0.78 mmol) was dissolved in 60 mL of THF and stirred at room temperature for 15 minutes. The THF was then removed *in vacuo*, the resulting powder was washed with a minimum amount of pentane and dried to obtain the white powder of **2c**. Yield: 294 mg (98%). Anal. Calcd. for $C_{20}H_{30}N_2Li_2OSi_2$: C, 62.47; H, 7.86; N, 7.28. Found: C, 62.34; H, 8.17; N, 6.98. ^{1}H NMR (THF-d_8): δ 0.02 (s, 6H, Si(CH_3)$_2$), 0.40 (s, 6H, Si(CH_3)$_2$), 2.09 (s, 6H, *m*-CH_3), 2.23 (s, 6H, *m*-CH_3), 5.94 (s, 1H, *p-H*), 6.36 (s, 2H, *o-H*), 6.63 (s, 1H, *p-H*), 6.69 (s, 2H, *o-H*). The product **2c** can also be obtained by a one-pot reaction of diamine **2a** and two equivalents of ^{n}BuLi in THF at –78 °C followed by stirring at room temperature for 15 minutes.

2.6.11 Synthesis of {[2,4,6-Me_3PhNLiSiMe_2N(2,4,6-Me_3Ph)SiMe_2OLi}, $Li_2[^{Me_3Ph}NN'O]$ (3c)

A white solid of **3b** (950 mg, 2.30 mmol) was dissolved in 15 mL of THF and stirred at room temperature for two hours. The THF was removed *in vacuo,* the resulting yellow residue was washed with a minimum amount of hexanes and dried to obtain the white powder of **3c**. Yield: 891 mg (94%). Anal. Calcd. for $C_{22}H_{34}N_2Li_2OSi_2$: C, 64.05; H, 8.31; N, 6.79. Found: C, 64.27; H, 8.59; N, 6.71. ^{1}H NMR (THF-d_8): δ -0.33 (s, 6H, Si(CH_3)$_2$), -0.12 (s, 6H, Si(CH_3)$_2$), 2.05 (s, 3H, *p*-CH_3), 2.15 (s, 3H, *p*-CH_3), 2.20 (s, 6H,

o-CH_3), 2.41 (s, 6H, *o*-CH_3), 6.55 (s, 2H, aromatic *H*), 6.67 (s, 2H, aromatic *H*). Single crystals were obtained from the slow evaporation of a concentrated THF/toluene solution. The product **3c** can also be obtained by a one-pot reaction of diamine **3a** and two equivalents of ^{n}BuLi in THF at −78 °C followed by stirring at room temperature for two hours.

2.6.12 Synthesis of {[2,6-^{i}Pr$_2$PhNLiSiMe$_2$N(2,6-^{i}Pr$_2$Ph)SiMe$_2$OLi}, Li$_2$[^{iPr_2Ph}NN'O] (4c)

A white solid of **4b** (1.47 g, 2.96 mmol) was dissolved in 50 mL of THF and stirred at room temperature for 48 hours. The solvent was removed *in vacuo,* the resulting white powder was washed with a minimum amount of cold hexanes and dried to obtain the white powder of **4c**. Yield: 1.152 g (78%). Anal. Calcd. for $C_{28}H_{46}N_2Li_2OSi_2$: C, 67.70; H, 9.33; N, 5.64. Found: C, 67.80; H, 9.45; N, 5.39. ^{1}H NMR (THF-d_8): δ -0.25 (s, *6H*, Si(CH_3)$_2$), -0.07 (s, *6H*, Si(CH_3)$_2$), 1.07 (d, 12H, CH(CH_3)$_2$), 1.24 (d, 12H, CH(CH_3)$_2$), 4.14 (m, 2H, C*H*(CH$_3$)$_2$), 4.26 (m, 2H, C*H*(CH$_3$)$_2$), 6.32 (t, 1H, *p-H*), 6.75 (d, 2H, *m-H*), 6.85 (t, 1H, *p-H*), 6.94 (d, 2H, *m-H*). Single crystals were obtained from the slow evaporation of a saturated Et$_2$O/toluene solution. The product **4c** can also be obtained by a one-pot reaction of diamine **4a** and two equivalents of ^{n}BuLi in THF at −78 °C followed by stirring at room temperature for 48 hours.

2.6.13 Synthesis of {[3,5-(CF$_3$)$_2$PhNLiSiMe$_2$N(3,5-(CF$_3$)$_2$Ph)SiMe$_2$OLi}, Li$_2$[^{CF_3Ph}NN'O] (5c)

A light brown powder of **5b** (5.07 g, 8.44 mmol) was dissolved in 50 mL of THF and stirred for 10 days at 70 °C. The solvent was removed *in vacuo,* the resulting light brown powder was washed with a minimum amount of cold hexanes and dried to obtain

the light brown powder of **5c**. Yield: 3.853 g (76%). Anal. Calcd. for $C_{20}H_{18}N_2F_{12}Li_2OSi_2$: C, 40.01; H, 3.02; N, 4.67. Found: C, 40.28; H, 2.87.; N, 4.93. ^{1}H NMR (THF-d_8): δ 0.07 (s, 6H, Si(CH_3)$_2$), δ 0.09 (s, 6H, Si(CH_3)$_2$), 6.23 (s, 1H, *p-H*), 6.35 (s, 1H, *p-H*), 6.83 (s, 2H, *o-H*), 6.73 (s, 2H, *o-H*). The product **5c** can also be obtained by a one-pot reaction of diamine **5a** and two equivalents of ^{n}BuLi in THF at –78 °C followed by stirring at 70 °C for 10 days.

2.6.14 Synthesis of {[FcNH(SiMe$_2$)]$_2$O}, H$_2$[^{Fc}NON] (6a)

An orange solid of $FcNH_2$ (200 mg, 0.99 mmol) was dissolved in 25 mL of ether, cooled to –78 °C, and one equivalent of 1.6 M ^{n}BuLi in hexanes (0.62 mL, 0.99 mmol) was added dropwise. The reaction was warmed to room temperature, stirred for two hours, and the solvent was removed *in vacuo*. The remaining dark orange solid was washed with a minimum amount of pentane to obtain a quantitative yield of FcNHLi. Then a dark orange mixture of FcNHLi (170 mg, 0.82 mmol) in 25 mL of ether was cooled to –30 °C and 1,3-dichloro-1,1,3,3-tetramethyldisiloxane (83.45 mg, 0.41 mmol) in 15 mL of Et_2O was added dropwise using a syringe. Gradually, the reaction became cloudy orange. The reaction was warmed to room temperature and stirred for 24 hours. The solvent was removed *in vacuo*, the residue was extracted with hexanes and filtered through Celite. The hexanes were removed to obtain an orange powder of **6a**. Yield: 138 mg (63%). Anal. Calcd. for $C_{24}H_{32}N_2Fe_2OSi_2$: C, 54.14; H, 6.06; N, 5.26. Found: C, 54.37.; H, 6.26.; N, 5.44. ^{1}H NMR (benzene-d_6): δ 0.21 (s, 12H, Si(CH_3)$_2$), δ 2.38 (br s, 2H, N-*H*), 3.78 (m, 4H, Cp$_{subst}$-*H*(2,5)), 3.85 (m, 4H, Cp$_{subst}$-*H*(3,4)), 4.15 (s, 10H, Cp$_{unsubst}$-*H*).

2.6.15 Kinetic measurements

The rearrangement reactions were carried out in an NMR test tube equipped with a Teflon J. Young valve. The *N*-lithio derivative of the ligands, THF-d_8, and NMR test tubes were cooled down to –30 °C to inhibit the start of the rearrangement reaction prior to the first NMR run (except for the **1b** and **5b**, which relatively exhibit much slower reaction rates). The NMR samples were prepared by adding 1 mL of the THF-d_8 to 20 mg of the *N*-lithio derivative of the ligand and transferring the solution into the NMR sample tube. Then, the NMR tube was sealed and placed in the NMR probe and the first spectra were obtained as soon as possible. More spectra were obtained during the course of the reaction until the reaction was nearly completed. The variable-temperature ^{1}H NMR spectra were recorded employing a 500 MHz Varian Unity spectrometer. The NMR samples of **1c** and **5c** were heated in a temperature-controlled oil bath during the course of the reactions.

CHAPTER 3:
CHROMIUM COORDINATION CHEMISTRY OF $[^{R}NON]^{2-}$ AND $[^{R}NN'O]^{2-}$ LIGANDS

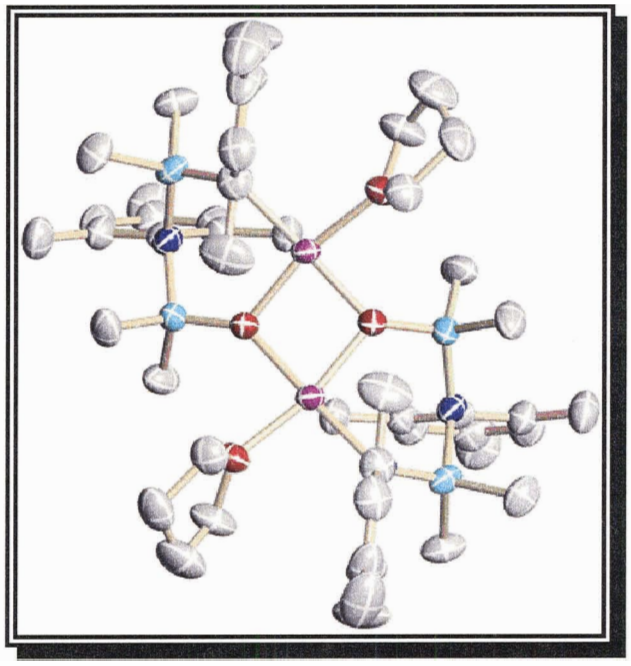

3.1 Introduction

Transition metal complexes with O- and N-donor ligands have shown interesting and useful reactivity.[14,21-23,26] For instance, mid- and high-valent chromium complexes containing O- and N-donor-based chelates have proven to be highly active catalysts for olefin polymerizations.[16,17,47] Despite their important application in polymer industry,[154] chromium catalysts have inspired less modelling activity mostly due to their

paramagnetic properties.[47] The Cr-based heterogeneous Phillips catalyst (impregnation of Cr oxides on silica followed by reduction) is used in large-scale production of polyolefins, however, the structure of the active site is still unclear.[155] Recently, a number of non-metallocene chromium complexes with hard N- and O-donor ligands have been reported.[156-160] These hard-donor chelating systems mimic the proposed binding motif of chromium to the silica surface via the oxygen linkages and thus can serve as homogenous models for the heterogeneous Phillips catalyst.[156,161,162]

In this chapter, the synthesis and characterization of new paramagnetic Cr complexes bearing chelating $[^{R}NON]^{2-}$ and $[^{R}NN'O]^{2-}$ donor ligands is presented. The immediate objective is to demonstrate how changes within the ligand system (changing the R group or changing from $[^{R}NON]^{2-}$ to $[^{R}NN'O]^{2-}$) affect their coordination chemistry toward the chromium centre. The mixed-donor amido-amino-siloxo ligands $[^{R}NN'O]^{2-}$ can offer a chelating ligand environment via the amido/siloxo and possibly also the amino centres (i.e. act in a bidentate or possibly tridentate fashion) or metal-bridging coordination via siloxo or amido units and therefore, would have different chemistry from the related diamido ether $[^{R}NON]^{2-}$ ligands. Thus, in order to investigate the fundamental coordination chemistry of the potentially tridentate $[^{R}NON]^{2-}$ and $[^{R}NN'O]^{2-}$ ligands, a series of chromium complexes were prepared and pursued for comparison. Preliminary results of the reactivity of some of these chromium complexes in the catalytic polymerization of ethylene are presented at the end.

3.2 Synthesis, Structure and Characterization of a New Cr(II) Siloxo-Bridged Dimer: {Cr[2,4,6-Me_3PhNSiMe_2N(2,4,6-Me_3Ph) SiMe_2O]• THF}$_2$*

The addition of the rearranged amido-amino-siloxo ligand $Li_2[^{Me_3Ph}NN'O]$ (**3c**) to $CrCl_2$ in THF at −30 °C in a 1:1 stoichiometry resulted in a dark green powder of $\{Cr[^{Me_3Ph}NN'O]\}_2$ in high yield. Despite numerous attempts, this green product could not be crystallized. However, recrystallization from THF solution gave single crystals of the purple THF-adduct $\{Cr[^{Me_3Ph}NN'O]\bullet THF\}_2$ (**7**). The single crystal X-ray structure of **7** is shown in Figure 3.1 with selected interatomic distances and bond angles detailed in Table 3.1.

The X-ray crystallography reveals a dinuclear structure which has two bridging siloxo ligands with Cr–O bond lengths of 2.0151(16) and 2.0244(15) Å. The more basic amido-donors remain terminally bound with a Cr–N distance of 2.0498(18) Å. The square-planar geometry around each chromium centre is satisfied not by the central amino ligand, which remains unbound (Cr–N distance of 3.341 Å) but by one THF molecule with a Cr–O distance of 2.0993(17) Å. The square planar coordination geometry for Cr(II) has previously been observed in bulky mixed-donor Cr(II) complexes in the past. For instance, $\{Cr[OSi(O^tBu)_3]_2(NHEt_2)_2\}$[163] has a square planar geometry at the chromium centre with Cr–O and Cr–N bond distances of 1.959(6) and 2.147(7) Å, respectively, which are comparable to those of compound **7**. The weak donor THF molecules of **7** can be reversibly removed *in vacuo*, effecting a colour change from purple to dark green.

---

* Haftbaradaran, F.; Mund, G.; Batchelor, R. J.; Britten, J. F.; Leznoff, D. B. *J. Chem. Soc. Dalton Trans.* **2005**, 2343. Reproduced in part by permission of The Royal Society of Chemistry. X-ray structures were completed by R.J.B. and J.F.B. $\{Cr[^{Me3Ph}NON]\}_2$ was prepared and characterized by G.M. All other work is by F.H.

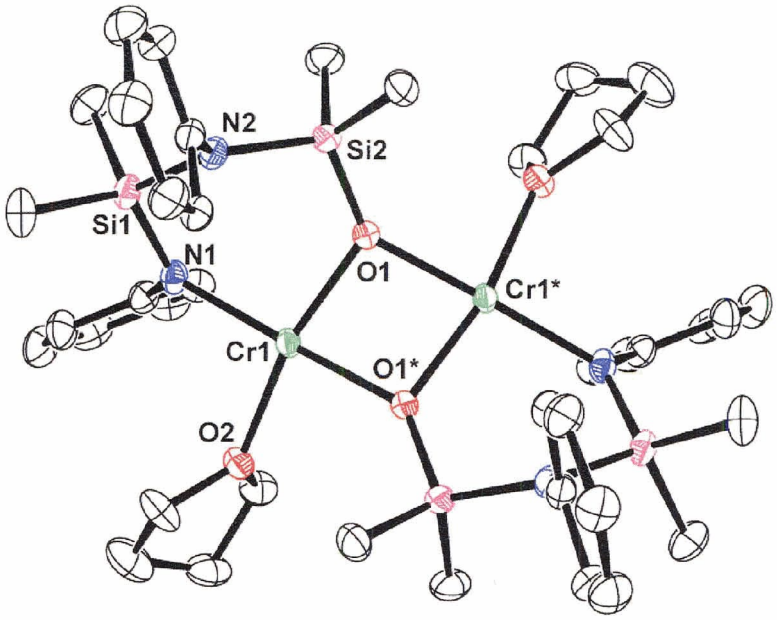

Figure 3.1 Molecular structure of $\{Cr[^{Me_3Ph}NN'O]\bullet THF\}_2$ (**7**) (ORTEP view with 33% probability ellipsoids; aryl groups are simplified for clarity).

Table 3.1 Selected interatomic distances (Å) and bond angles (deg) for $\{Cr[^{Me_3Ph}NN'O]\bullet THF\}_2$ (7).

Cr(1)–Cr(1)*	3.019	Si(1)–N(1)	1.713(2)
Cr(1)–N(1)	2.0498(18)	Si(1)–N(2)	1.757(2)
Cr(1)–O(1)	2.0151(16)	Si(2)–O(1)	1.6351(16)
Cr(1)–O(1)*	2.0244(15)	Si(2)–N(2)	1.7415(19)
Cr(1)–O(2)	2.0993(17)		
O(1)–Cr(1)–O(1)*	79.54(7)	N(1)–Cr(1)–O(2)	92.80(7)
O(1)–Cr(1)–N(1)	98.23(7)	Si(1)–N(2)–Si(2)	121.95(11)
O(1)*–Cr(1)–N(1)	177.15(7)	Cr(1)–O(1)–Cr(1)*	96.73(6)
O(1)–Cr(1)–O(2)	165.10(6)	N(1)–Si(1)–N(2)	106.37(9)
O(1)*–Cr(1)–O(2)	89.71(6)	O(1)–Si(2)–N(2)	109.44(9)

* Symmetry transformations used to generate equivalent atoms: -x+1, y, -z+1/2

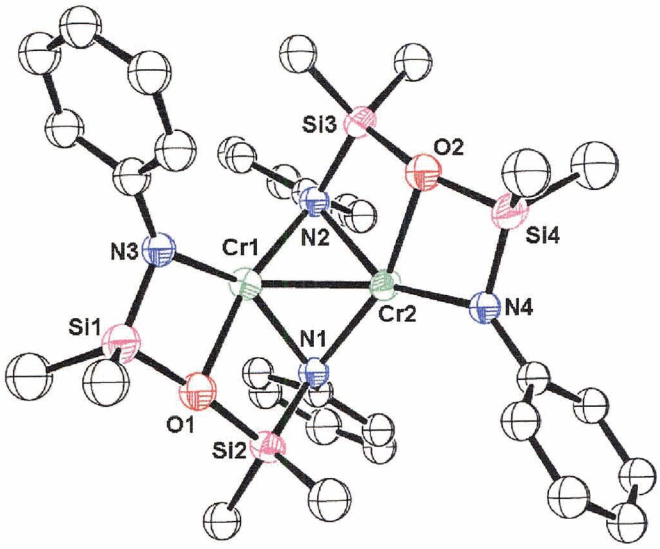

Figure 3.2 Molecular structure of $\{Cr[^{Me_3Ph}NON]\}_2$ (ORTEP view with 33% probability ellipsoids; aryl groups are simplified for clarity).

The structure of the analogous compound with the symmetrical diamidosilyl ether ligand $[^{Me_3Ph}NON]^{2-}$ has been reported in the past (Figure 3.2) by the Leznoff research group.[65,164] The dinuclear structure of $\{Cr[^{Me_3Ph}NON]\}_2$ has two terminal and two bridging amido ligands with average Cr–N distances of 2.018(6) and 2.096(6) Å, respectively. Completing the distorted square-planar geometry, each central silylether donor is also bound to a metal, with an average Cr–O distance of 2.126(6) Å. The Cr–Cr distance is 2.384(2) Å, with potential metal–metal bonding character.[165] However, compound **7** has a Cr–Cr distance of 3.019 Å, which is much longer than that observed in $\{Cr[^{Me_3Ph}NON]\}_2$, perhaps due to the less basic nature of the bridging siloxo-ligand in **7** vs. the silylamido group. Note that the potentially tridentate ligand $[^{Me_3Ph}NN'O]$ acts as a bidentate amido-siloxo donor with Cr(II) as compared with the tridentate $[^{Me_3Ph}NON]$ chromium(II) complex. Thus, differences in coordination chemistry can readily be observed between the two related donor ligands.

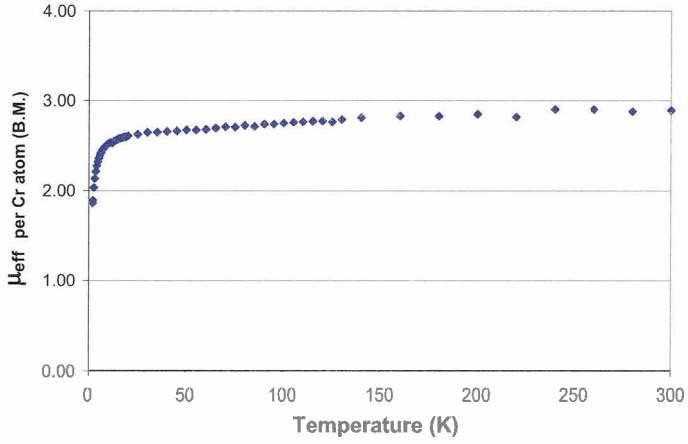

Figure 3.3 Plot of the magnetic moment vs. temperature for $\{Cr[^{Me_3Ph}NN'O]\cdot THF\}_2$ (**7**).

The temperature dependence of the magnetic susceptibility χ_m of **7** was measured from 2 to 300 K. The plot of μ_{eff} versus T per chromium atom for **7** is shown in Figure 3.3. The μ_{eff} value of 2.88 B.M. for **7** at 298 K is much lower than the expected spin-only value for a high spin Cr(II) S = 2 center (μ_{so} = 4.90 B.M.; 4 unpaired electrons). The lower than expected value in the μ_{eff} of **7** is indicative of weak antiferromagnetic coupling between the chromium centres of the dimer. Differences in the Cr(II)-coordination chemistry of the $[NON]^{2-}$ and $[NN'O]^{2-}$ ligands are also reflected in their magnetic moments. The analogous amido-bridged compound $\{Cr[^{Me_3Ph}NON]\}_2$ has a μ_{eff} of 2.38 B.M at 298 K. This is consistent with more significant antiferromagnetic coupling through the bridging amido ligands, metal–metal bonding or both.[49,166] Thus, the μ_{eff} of 2.88 B. M. at 298 K for **7** is larger than the observed 2.38 B.M. for $\{Cr[^{Me_3Ph}NON]\}_2$ and is presumably due to either the longer Cr–Cr distances in the [NN'O] system or the possibility that alkoxo ligands are poorer mediators of magnetic exchange relative to the amido bridges.[167,168]

3.3 Synthesis, Structure and Characterization of a New Cr(II) Siloxo-Bridged Dimer: {Cr[2,6-^{i}Pr$_2$PhNSiMe$_2$N(2,6-^{i}Pr$_2$Ph)SiMe$_2$O]}$_2$

When the more sterically congested ligand **4c** is reacted with $CrCl_2$, the THF-free siloxo-bridged dimer {Cr[^{iPr_2Ph}NN'O]}$_2$ (**8**) is obtained in high yield. Note that previous attempts to prepare a chromium(II) complex with the symmetrical [^{iPr_2Ph}NON]$^{2-}$ ligand did not lead to clean and tractable products. The single crystal X-ray structure of **8** is shown in Figure 3.4 with selected interatomic distances and bond angles detailed in Table 3.2. The dinuclear structure has two bridging siloxo ligands with Cr–O bond lengths of 1.962(3) and 1.990(3) Å and two terminal amido-donors with Cr–N distances of 1.963(3) Å. The geometry around the Cr centre is distorted square planar with no significant metal–metal bonding (Cr–Cr distance of 2.9298(16) Å).

In comparison to the THF-adduct {Cr[^{Me_3Ph}NN'O]•THF}$_2$ (**7**), the large steric profile of the [^{iPr_2Ph}NN'O]$^{2-}$ ligand yields a highly coordinately unsaturated, formally 10-electron Cr(II) centre in **8**,[169] which is presumably too hindered to bind the THF solvent. Instead, the ancillary [NN'O]$^{2-}$ ligand itself is activated by the electron-deficient chromium(II) centre to generate a Cr–C(11) ipso bond of 2.287(4) Å. The aromaticity in the activated ring is thereby partially disrupted, as observed by the pattern of a long C(11)–C(12) bond length of 1.425(6) Å and shorter, essentially equivalent C(12)–C(13) and C(13)–C(14) bond lengths of 1.369(6) and 1.389(6) Å, respectively. The extremely acute Cr(1)–N(1)–C(11) angle of 84.2(2)° is further evidence of this interaction and can be compared with related η^2-benzyl chromium(II) structures,[170,171] one of which shows a Cr–C_{ipso} bond length of 2.576(3) Å and a Cr–C–C_{ipso} bond angle of 89.7(2)°.

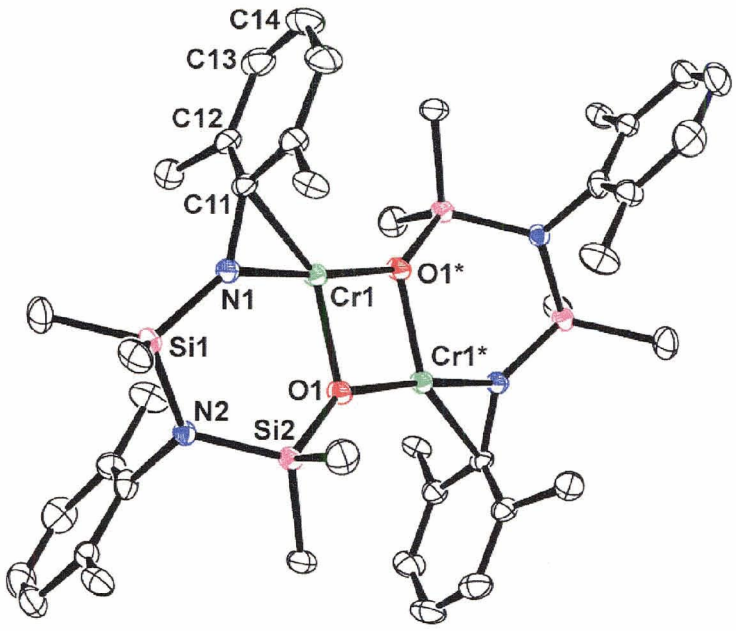

Figure 3.4 Molecular structure of $\{Cr[^{iPr_2Ph}NN'O]\}_2$ (**8**) (ORTEP view with 33% probability ellipsoids; isopropyl groups are simplified for clarity).

Table 3.2 Selected interatomic distances (Å) and bond angles (deg) for $\{Cr[^{iPr_2Ph}NN'O]\}_2$ (**8**).

Cr(1)–C(11)	2.287(4)	Si(1)–N(1)	1.695(3)
Cr(1)–Cr(1)*	2.9298(16)	Si(1)–N(2)	1.741(3)
Cr(1)–N(1)	1.963(3)	Si(2)–N(2)	1.732(3)
Cr(1)–O(1)	1.962(3)	C(11)–C(12)	1.425(6)
Cr(1)–O(1)*	1.990(3)	C(12)–C(13)	1.369(6)
Si(2)–O(1)	1.644(3)	C(13)–C(14)	1.389(6)
O(1)–Cr(1)–N(1)	100.69(12)	C(11)–N(1)–Cr(1)	84.2(2)
O(1)–Cr(1)–O(1)*	84.32(11)	Si(1)–N(2)–Si(2)	120.68(17)
N(1)–Cr(1)–O(1)*	174.85(12)	N(1)–Si(1)–N(2)	103.16(15)
Cr(1)–O(1)–Cr(1)*	95.68(11)	O(1)–Si(2)–N(2)	110.41(15)
Si(1)–N(1)–Cr(1)	131.90(19)		

*Symmetry transformations used to generate equivalent atoms: -x+1, -y, -z+2

This activation of an arylamido group has been previously observed to a lesser extent in electron-deficient f-element and group 3 – 5 to transition-metal complexes.[172-178] Related V(III) and Ti(III) η^3-amido complexes[179,180] have been reported but the metrical

parameters for the η^2-(N,C_{ipso}) arylamido bonding in compound **8** are by far the shortest and most acute in the literature. Such interactions may help to stabilize the resting state of amido-supported metal complexes that are active in alkene polymerization.[2,14]

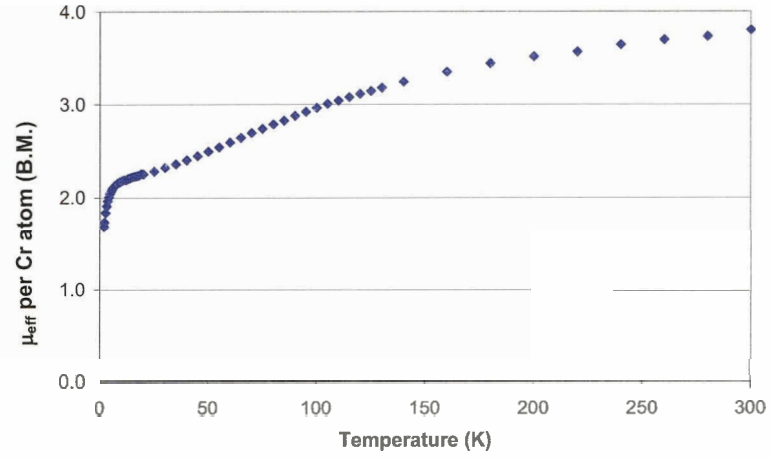

Figure 3.5 Plot of the magnetic moment vs. temperature for {Cr[^{iPr_2Ph}NN'O]}$_2$ (**8**).

The temperature dependence of the magnetic susceptibility χ_m of **8** was measured from 2 to 300 K. The plot of μ_{eff} vs. T per chromium atom for **8** is shown in Figure 3.5. As found for **7**, the μ_{eff} values of 3.80 B.M. for **8** at 298 K is lower than the expected spin-only value for a pure S = 2 high spin state (μ_{so} = 4.90 B.M.; 4 unpaired electrons). However, the μ_{eff} for compound **8** is larger than that of the 2.88 B. M. found for compound **7**. This is indicative of even weaker antiferromagnetic coupling between the chromium centres of the compound **8** despite the fact that the Cr–Cr distances (3.019 and 2.9298(16) Å for **7** and **8**, respectively) and the nature of the bridging siloxo groups

(Cr–O–Cr angle of 96.73(6) and 95.68(11)°; av. Cr–O distance of 2.02 and 1.98 Å for **7** and **8**, respectively) are similar in both.

3.4 Synthesis, Structure and Characterization of a New Cr(II) Spirocyclic Lithium-Bridged Ate Complex: {Cr([2,4,6-$Me_3PhNSiMe_2N(2,4,6\text{-}Me_3Ph)SiMe_2O$]–μ–$Li)_2$•THF}

During the course of these studies, it became obvious that the coordination chemistry of the mixed-donor ligands and chromium(II) are remarkably sensitive to the stoichiometry of the reaction and changing the stoichiometry significantly influences the product. For instance, when *two* equivalents of the lithiated amido-amino-siloxo ligand $Li_2[^{Me_3Ph}NN'O]$ (**3c**) is reacted with $CrCl_2$ in THF at –30 °C, a dark green powder of $\{Cr[^{Me_3Ph}NN'O]_2Li_2\bullet THF\}$ (**9**) can be obtained in high yield. Single crystals for X-ray crystallography were obtained from the slow evaporation of a concentrated THF solution. The structure of **9** is shown in Figure 3.6 along with selected bond lengths and angles detailed in Table 3.3.

The structure reveals that compound **9** is an "ate" complex, which refers to compounds with extra coordinated salt. Most ate complexes contain lanthanides,[120,181-183] and actinides[182] presumably due to the tendency of these large and electropositive (soft) Lewis acids to acquire high coordination numbers (higher than three) by binding alkali-metal-ion-bearing solvent molecules or bridging halide anions.[184] However, ate complexes of early transition metals such as Sc, Ti, and Fe have also been reported.[115,185,186] These ate complexes may exhibit interesting chemical and structural properties.[115,187]

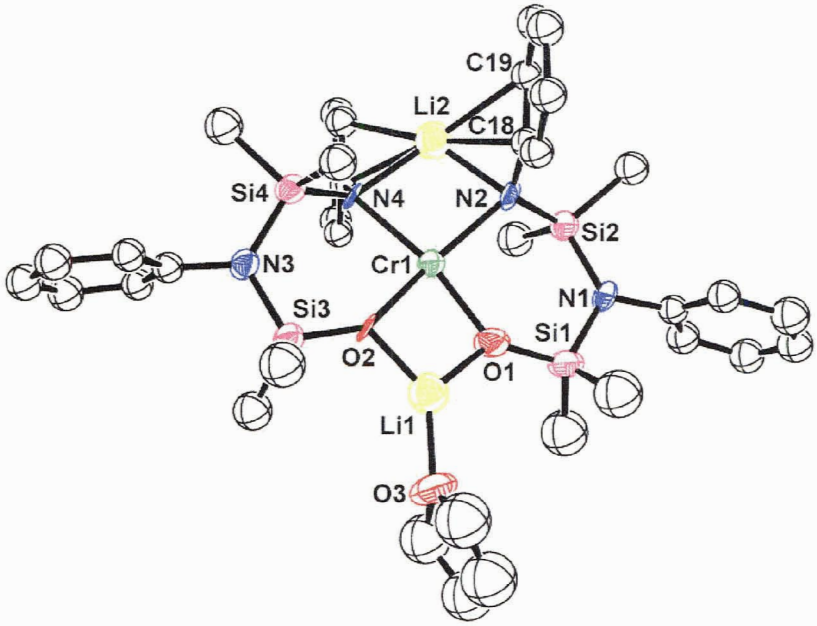

Figure 3.6 Molecular structure of ate complex {Cr[^{Me_3Ph}NN'O]$_2$Li$_2$•THF} (**9**) (ORTEP view with 33% probability ellipsoids; aryl groups are simplified for clarity).

Table 3.3 Selected interatomic distances (Å) and bond angles (deg) for {Cr[^{Me_3Ph}NN'O]$_2$Li$_2$•THF} (**9**).

Cr(1)–Li(1)	2.64(4)	Cr(1)–Li(2)	2.61(3)
Cr(1)–N(2)	2.139(12)	Cr(1)–N(4)	2.124(12)
Cr(1)–O(1)	2.001(12)	Cr(1)–O(2)	2.017(10)
Si(1)–N(1)	1.738(12)	Si(1)–O(1)	1.579(11)
Si(2)–N(1)	1.748(12)	Si(2)–N(2)	1.701(12)
O(1)–Li(1)	1.79(4)	O(2)–Li(1)	1.71(4)
O(3)–Li(1)	1.99(4)	N(2)–Li(2)	1.90(3)
N(4)–Li(2)	1.98(3)	Li(2)–C(18)	2.18(4)
Li(2)–C(19)	2.40(4)		
N(2)–Cr(1)–N(4)	94.0(4)	N(2)–Cr(1)–O(1)	93.7(4)
N(2)–Cr(1)–O(2)	163.4(5)	N(4)–Cr(1)–O(2)	93.7(4)
O(1)–Cr(1)–O(2)	83.1(4)	Cr(1)–O(1)–Li(1)	88.1(14)
Cr(1)–N(2)–Li(2)	80.2(10)	Si(1)–N(1)–Si(2)	123.1(7)

In the solid state, compound **9** is a dilithium-bridged spirocyclic monomer. The Cr(II) centre is coordinated to two amido groups and two siloxo groups. The six-

membered amido-amino-siloxo rings are nearly coplanar with a distorted square planar geometry around the Cr site with the average Cr–N and Cr–O distances of 2.132 and 2.009 Å, respectively. Despite the steric profile of the Me_3Ph substituent on the amido-nitrogen group, in the solid state, the N_{amido}-donors adopt a sterically demanding cis-coordinated configuration. This unexpected position of the aryl rings is presumably stabilized by Li–C interactions via the aryl rings on the amido groups. The Li(2) centre has close contacts with two carbon centres of each aryl ring with an average distance of 2.36 Å. These Li–C distances are relatively short compare to similar Li–C interactions to aromatic rings in other ate complexes.[103,147,188-191] For instance, $\{FeBr_2Li[Me_3PhN(SiMe_2)]_2O\}_2$[115] forms an ate complex in the solid state. The structure contains two lithium atoms that form Li–π interactions via the aryl rings on the amido groups with Li-C distances ranging from 2.481(9) to 2.532(11) Å.

The Cr–N distances of 2.139(12) and 2.124(12) Å are slightly longer than the 1.963(3) Å found in the siloxo-bridged dimer $\{Cr[2,6\text{-}^{i}Pr_2PhNSiMe_2N(2,6\text{-}^{i}Pr_2Ph)SiMe_2O]\}_2$ (**8**). This is presumably due the steric repulsion of the 2,4,6-trimethylphenyl (Me_3Ph) groups and presence of Li–N interactions which weakens the π-donating ability of amido groups. The low coordination of the Li(1) centre is further compensated by the formation of a dative bond from a donor molecule of THF. Similar spirocyclic alkali metal ion-bridged Cr(II) compounds have been previously observed.[192-197] For instance, $[Cr\{O(Ph_2SiO)_2\}_2\text{–}\mu\text{–}(Li(py)_2)_2]$[193] is a lithium-bridged spirocyclic structure which has a square planar geometry at the chromium(II) atom with two coplanar six-membered chromiasiloxane rings and average Cr–O distances of 2.00 Å.

3.5 Synthesis, Structure and Characterization of a New Pentanuclear Cr(II) Cluster: {(Cr_2[2,4,6-$Me_3PhNSiMe_2N$(2,4,6-Me_3Ph)$SiMe_2O$]$_2$)$_2$ –μ– $CrCl_2$}

Once again, the importance of the stoichiometry of the reaction on the outcome of the product is expressed in the following reaction. Addition of *four* equivalents of the lithiated amido-amino-siloxo ligand $Li_2[^{Me_3Ph}NN'O]$ (**3c**) to *five* equivalents of anhydrous $CrCl_2$ in Et_2O at 0 °C afforded a grey/green powder of {($Cr_2[^{Me_3Ph}NN'O]_2$)$_2$–μ–$CrCl_2$} (**10**) in high yield. Single crystals for X-ray crystallography were obtained from the slow evaporation of a concentrated pentane/toluene solution. The structure of **10** is shown in Figure 3.7 along with selected bond lengths and angles detailed in Table 3.4.

Single-crystal X-ray structural analysis shows that **10** is a chain made of five Cr(II) atoms fused by four six-membered rings of $[^{Me_3Ph}NN'O]^{2-}$ ligands. The geometry around each Cr(II) centre is distorted square planar, however, the formation of a Cr–C_{ipso} bond results in larger distortions from pure square planar geometry for the terminal Cr centres. The structure which has a centre of symmetry, contains relatively long Cr–Cr distances, with the outer Cr(2)–Cr(3) distances (2.892 Å) slightly shorter than the inner Cr(1)–Cr(2) ones (3.167 Å). The central Cr(1) atom bridges to two Cr(2) centers via two siloxo and two chloro groups with Cr–Cl and Cr–O distances of 2.3476(7) and 1.977(2) Å, respectively. The Cr(2) centres are coordinated by one chloro, one amido and two siloxo groups (all binding to adjacent Cr centres) with bond lengths ranging from 1.9796(19) to 2.4224(9) Å. The terminal Cr centres are coordinated with one bridging siloxo, one bridging amido, and one terminal amido groups with Cr–O, Cr–$N_{bridged}$ and Cr–$N_{terminal}$ distances of 1.954(2), 2.120(2) and 1.984(2) Å, respectively.

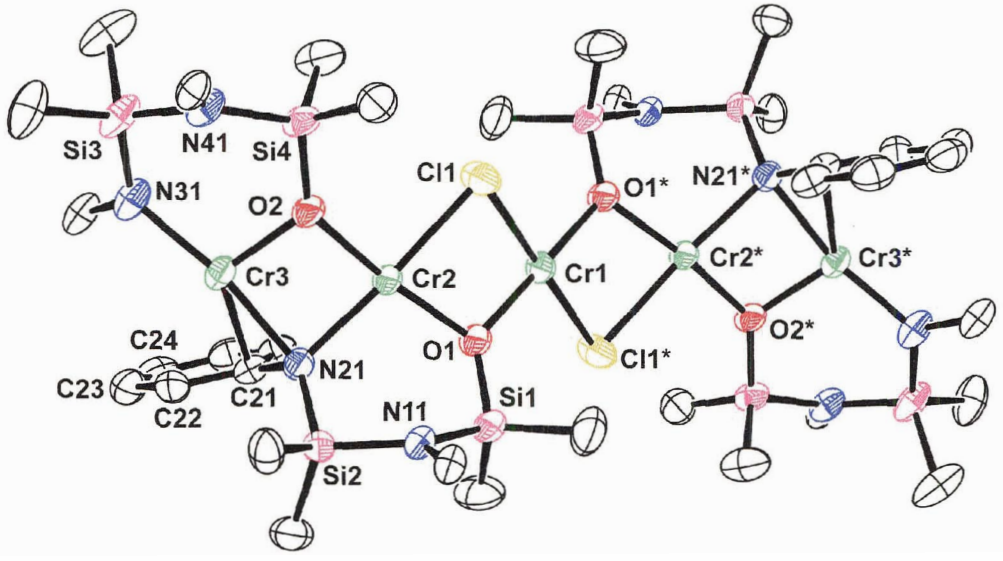

Figure 3.7 Molecular structure of $\{(Cr_2[^{Me_3Ph}NN'O]_2)_2CrCl_2\}$ (**10**) (ORTEP view with 50% probability ellipsoids; aryl groups are simplified for clarity).

Table 3.4 Selected interatomic distances (Å) and bond angles (deg) for $\{(Cr_2[^{Me_3Ph}NN'O]_2)_2CrCl_2\}$ (**10**).

Cr(1)–Cr(2)	3.167	Cr(3)–N(31)	1.984(2)
Cr(1)–O(1)	1.977(2)	Cr(3)–C(21)	2.340(3)
Cr(1)–Cl(1)	2.3476(7)	Si(1)–O(1)	1.639(2)
Cr(2)–O(1)	2.0041(19)	Si(1)–N(11)	1.753(3)
Cr(2)–O(2)	1.9796(19)	Si(2)–N(11)	1.757(2)
Cr(2)–N(21)	2.139(2)	Si(2)–N(21)	1.759(3)
Cr(2)–Cl(1)	2.4224(9)	C(21)–C(22)	1.421(4)
Cr(2)–Cr(3)	2.892	C(22)–C(23)	1.402(5)
Cr(3)–O(2)	1.954(2)	C(23)–C(24)	1.366(5)
Cr(3)–N(21)	2.120(2)		
O(1)–Cr(1)–O(1)*	180.00(13)	N(21)–Cr(2)–Cl(1)	170.39(8)
O(1)–Cr(1)–Cl(1)	83.53(6)	O(2)–Cr(3)–N(21)	88.25(9)
O(1)–Cr(1)–Cl(1)*	96.47(6)	O(2)–Cr(3)–C(21)	116.57(9)
O(2)–Cr(2)–O(1)	171.68(9)	Cr(1)–Cl(1)–Cr(2)	83.20(3)
O(2)–Cr(2)–N(21)	87.08(9)	Cr(1)–O(1)–Cr(2)	105.41(9)
O(1)–Cr(2)–N(21)	99.54(9)	Cr(3)–O(2)–Cr(2)	94.63(9)
O(2)–Cr(2)–Cl(1)	93.28(6)	C(21)–N(21)–Cr(3)	79.69(15)

*Symmetry transformations used to generate equivalent atoms: -x + 1, -y + 1, -z

Similar to compound **8**, the ancillary [NN'O] ligand is activated by the electron-deficient terminal chromium centres to generate a Cr–$C(21)_{ipso}$ bond of 2.340(3) Å and an extremely acute Cr(3)–N(21)–C(21) angle of 79.69(15)°. This angle is even more acute compared to the 84.2(2)° Cr–N–C_{ipso} angle in compound **8** (although the bond length is longer). Likewise, the aromaticity in the activated rings are partially disrupted, as observed by the pattern of a long C(21)–C(22) bond length of 1.421(4) Å and shorter C(22)–C(23) and C(23)–C(24) bond lengths of 1.402(5) and 1.366(5) Å, respectively. The central N_{amine} donors remain unbound, as in the other Cr(II) complexes.

Similar pentanuclear Cr structures with stronger metal-metal interactions have been reported.[198-202] For example, Cotton *et al.* reported the compound $\{[Cr_5(tpda)_4FCl]PF_6\}$ (tpda = tripyridyldiamide) which has an alternating short-long Cr–Cr distances, 2.032(3), 2.560(6), 1.873(5), and 2.509(4) Å. It may be that the steric bulk of the Me_3Ph substituents in $[NN'O]^{2-}$ and the shorter length of the ligand backbone vs. tpda results in longer Cr–Cr distances that suggest an insignificant metal–metal bonding interaction in **10**.[203]

3.6 Synthesis and Characterization of New Cr(IV) Complexes Containing $[^{R}NON]^{2-}$ and $[^{R}NN'O]^{2-}$ Ligands

High valent chromium(IV) compounds were once encountered only as the oxides and halides and as unstable intermediates in solution.[204] However, chromium(IV) compounds are now known to be isolable by using bulky ligands.[205] The steric bulk of the ligands presumably offer protections to the Cr centre against disproportionation, or oxidation/reduction by the ligand to Cr(III) or Cr(V) complexes as in other cases.[206] Perhaps the major challenge in synthesizing Cr(IV) complexes is the lack of appropriate

chromium(IV) halide starting materials since they are either unstable or don't exist at all.[207] For instance, chromium(IV) chloride is unstable and can only be trapped in an argon matrix. Chromium(IV) fluoride is a gas and is highly reactive; it is a powerful fluorinating agent.[109] Thus, the synthesis of high-valent Cr(IV) complexes usually engages in more demanding routes: oxidation reactions of Cr(II/III) complexes or disproportionation reactions of mid-valent Cr(III) complexes. An example of the first route is the reaction of $CrCl_3$•3THF with lithium alkyls, amides, alkoxides, or Grignard reagents to make the Cr(IV) alkyls, amides, or alkoxides CrL_4 (L = Me, ^{i}Pr, ^{t}Bu, CH_2CMe_3, OR, NR_2), which all are monomeric complexes with a tetrahedral coordination geometry at Cr centre.[109,208-210] An example of the second route is the reaction of $CrCl_3$ with $LiNEt_2$ followed by high-vacuum disproportionation to give the volatile Cr(IV) amide $Cr(NEt_2)_4$; a chromium(II) biproduct is also generated.[211] In the following sections the synthesis of new Cr(IV) complexes stabilized by $[^RNON]^{2-}$ and $[^RNN'O]^{2-}$ ligands via the above procedures will be presented.

3.6.1 Synthesis, structure and characterization of the new tetrahedral Cr(IV) complex {Cr[(PrNSiMe$_2$)$_2$O]$_2$}

Reaction of two equivalents of the dilithiodiamidosilyl ether ligand $Li_2[^{Pr}NON]$ (**1b**) with one equivalent of $CrCl_3$•3THF at –30 °C following by sublimation under vacuum resulted in the isolation of two different Cr compounds in high yield: the volatile dark green powder of $\{Cr^{IV}[(PrNSiMe_2)_2O]_2\}$ (**11**) and the non-sublimable dark green residue of $\{Cr^{II}[(PrNSiMe_2)_2O]_2Li_2\}$ (**12**). The initial ligand addition to $CrCl_3$•3THF likely generated the intermediate ate complex $\{Cr^{III}[(PrNSiMe_2)_2O]_2Li\}$, but attempts to isolate this complex failed since the Cr(III) ate complex readily undergoes a

disproportionation reaction upon standing, or more rapidly upon sublimation under vacuum at 70 °C to afford compounds **11** and **12** (Figure 3.8).

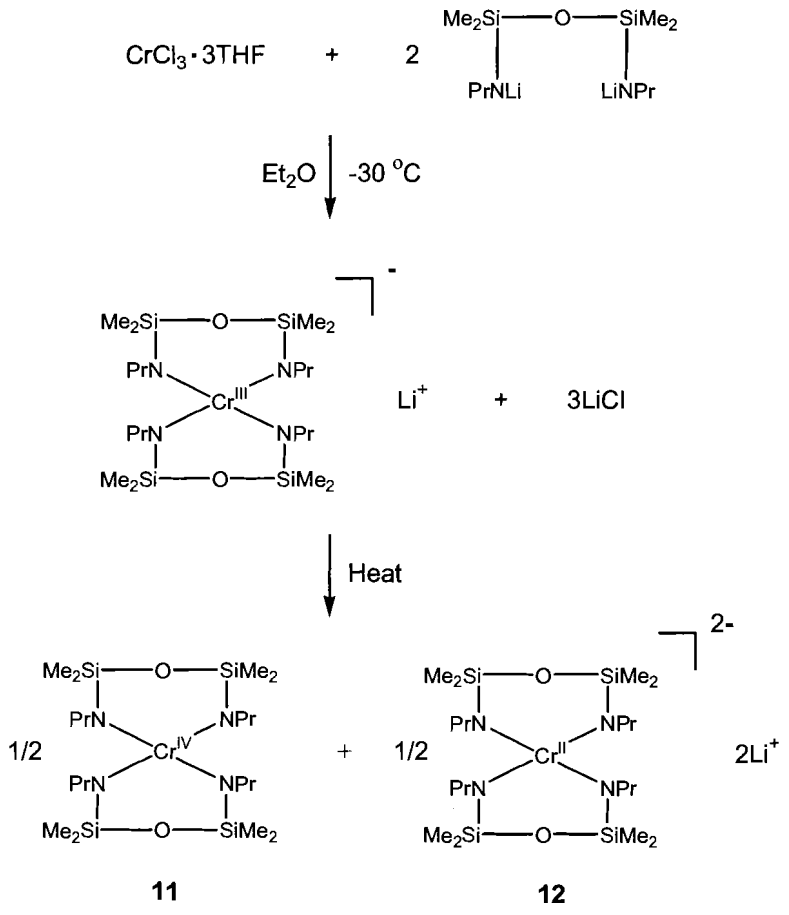

Figure 3.8 Synthesis of $\{Cr^{IV}[(PrNSiMe_2)_2O]_2\}$ (**11**) and $\{Cr^{II}[(PrNSiMe_2)_2O]_2Li_2\}$ (**12**) via a disproportionation reaction of $\{Cr^{III}[(PrNSiMe_2)_2O]_2Li\}$.

Suitable single crystals of compound **11** were obtained from the slow evaporation of a pentane/toluene solution. However, attempts to obtain single crystals of **12** failed. The single crystal X-ray structure of **11** is shown in Figure 3.9 with selected interatomic distances and bond angles detailed in Table 3.5. The structure reveals a monomeric Cr(IV) complex in the solid state. The nearly perfect tetrahedral Cr centre is coordinated to four amido donors of two bidentate ligands with an average Cr–N distance of 1.851 Å

and N–Cr–N bond angles ranging from 108.1(4)° to 110.7(4)°. The Cr–N distances are shorter than those in the Cr(II) complexes **7 – 10** due to the presence of the high valent Cr(IV) in **11**. The two six-membered Cr–diamidosilyl ether rings are nearly planar and orthogonal to each other. The average Cr–O distance of 3.243 Å precludes any bonding interaction between the metal centre and the siloxo donor in the ligand backbone.

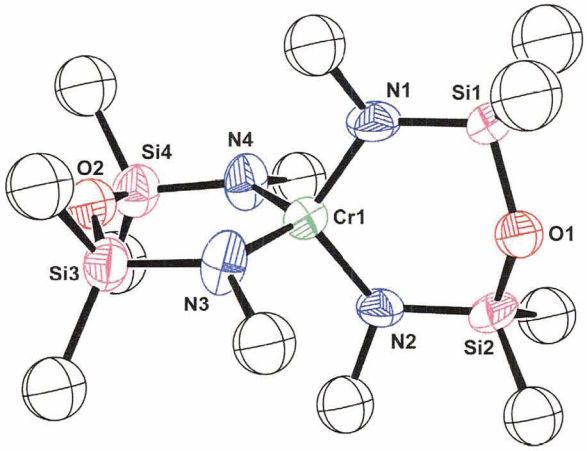

Figure 3.9 Molecular structure of $\{Cr[(PrNSiMe_2)_2O]_2\}$ (**11**) (ORTEP view with 33% probability ellipsoids; propyl groups are simplified for clarity).

Table 3.5 Selected interatomic distances (Å) and bond angles (deg) for $\{Cr[(PrNSiMe_2)_2O]_2\}$ (**11**).

Cr(1)–N(1)	1.860(8)	Cr(1)–N(2)	1.841(8)
Cr(1)–N(3)	1.852(8)	Cr(1)–N(4)	1.851(8)
Si(1)–O(1)	1.621(16)	Si(1)–N(1)	1.688(8)
Si(2)–O(1)	1.628(16)	Si(2)–N(2)	1.692(9)
Si(3)–O(2)	1.626(16)	Si(3)–N(3)	1.679(8)
Si(4)–O(2)	1.615(16)	Si(4)–N(4)	1.713(8)
N(1)–Cr(1)–N(2)	108.1(4)	N(1)–Cr(1)–N(3)	109.4(4)
N(1)–Cr(1)–N(4)	110.7(4)	N(2)–Cr(1)–N(3)	110.6(4)
N(2)–Cr(1)–N(4)	108.5(4)	N(3)–Cr(1)–N(4)	109.9(4)
O(1)–Si(1)–N(1)	107.4(7)	O(2)–Si(3)–N(3)	104.8(6)
Si(1)–O(1)–Si(2)	140.5(11)	Cr(1)–N(1)–Si(1)	125.7(5)

Mononuclear tetrahedral Cr(IV) complexes have e^2 electron configurations and generally display temperature-independent magnetic moments close to spin-only μ_{eff} of 2.83 B.M. due to the presence of two unpaired *d* electrons.[211] The temperature dependence of the magnetic susceptibility χ_m of **11** was measured from 2 to 300 K. The plot of μ_{eff} vs. T for **11** is shown in Figure 3.10. The μ_{eff} of 3.06 B.M. at 298 K for **11** is almost independent of temperature and is indeed close to the expected spin-only value for tetrahedral Cr(IV) (μ_{so} = 2.83 B.M.; 2 unpaired electrons). At temperatures below 20 K, the Cr(IV) centre shows zero-field splitting effects[106,107] which cause a sudden drop in μ_{eff} to 2.12 B.M. at 2 K. This result, coupled with the crystal structure, is good confirmation of a Cr(IV) oxidation state present in **11**.

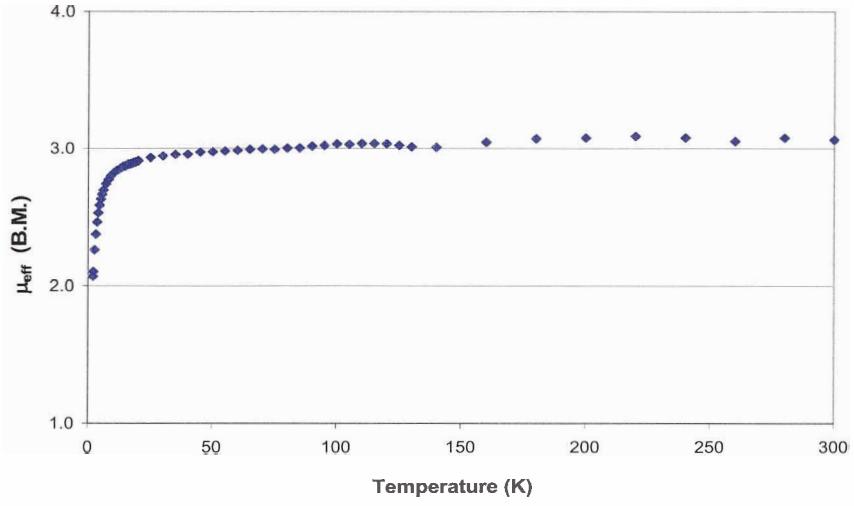

Figure 3.10 Plot of the magnetic moment vs. temperature for $\{Cr[(PrNSiMe_2)_2O]_2\}$ (**11**).

3.6.2 Oxidative-addition of I_2 to $\{Cr[^{R}NN'O]\}_2$

Computational studies by Ziegler, Schmid, and Firman have been predicted that cationic Cr(IV) bis(amido) alkyl complexes should be highly active catalysts toward olefin polymerization.[212-214] In this context, we were encouraged to synthesize high-valent Cr(IV) complexes from the synthesized Cr(II) complexes reported in the previous sections. The reaction of $\{Cr[N(SiMe_3)_2]_2 \bullet THF_2\}$ with I_2 was recently reported to yield the Cr(IV) product $\{CrI_2[N(SiMe_3)_2]_2\}$.[215] Thus using this procedure, oxidative-addition of *two* equivalent of the I_2 with *one* equivalent of $\{Cr^{II}[^{Me_3Ph}NN'O]\}_2$ (**8**) and $\{Cr^{II}[^{iPr_2Ph}NN'O]\}_2$ (**9**) at −30 °C resulted in the isolation of brown powders of $\{Cr^{IV}I_2[^{Me_3Ph}NN'O]\}$ (**13**) and $\{Cr^{IV}I_2[^{iPr_2Ph}NN'O]\}$ (**14**) in high yield, respectively. However, attempts to completely purify (e.g. remove unreacted iodine) and obtain single crystals suitable for X-ray analysis were unsuccessful. The combustion analyses of the products are close to calculated value but still not within the acceptable range. However, magnetic susceptibility measurements support the proposed Cr(IV) complex compositions. Nevertheless, these are preliminary results that require a significant in-depth study that is beyond the scope of this thesis; other oxidizing agent should also be explored.

The temperature dependence of the magnetic susceptibility χ_m of **13** and **14** were measured from 2 to 300 K. The plot of μ_{eff} vs. T for **13** is shown in Figure 3.11. The μ_{eff} of 2.76 B.M. for **13** is close to the expected spin-only value for tetrahedral Cr(IV) (μ_{so} = 2.83 B.M.; 2 unpaired electrons). The gradual decrease in μ_{eff} with temperature is consistent with antiferromagnetic interactions between the Cr centres. At temperature below 20 K, the Cr(IV) centre also shows zero-field splitting effects[106,107] which cause a

sudden drop in μ_{eff} to 1.29 B.M at 2 K. The plot of μ_{eff} vs. T for **14** is shown in Figure 3.11. The μ_{eff} of 2.97 B.M. for **14** is also close to the expected spin-only value for tetrahedral Cr(IV) (μ_{so} = 2.83 B.M.; 2 unpaired electrons). Similarly, the plot shows an antiferromagnetic interaction between Cr centres, which is indicative of a dimeric structure in the solid state.

With this in mind, Figure 3.12 shows two tentative proposed structures for **13** and **14**. A comparison with similar Cr(IV) halide-containing N-donor ligands suggests that a mononuclear structure with a distorted tetrahedral geometry around the Cr(IV) centre is resonable.[215-217] As an example, the aforementioned Cr(IV) bis(trimethylsilyl)amido complex $\{[CrI_2[N(SiMe_3)_2]_2\}$ adopts a mononuclear distorted tetrahedral structure. However, the magnetic moments of **13** and **14** are temperature-dependent, which suggests a dinuclear structure in the solid state, in which the unpaired electrons show coupling through iodide bridges.[218]

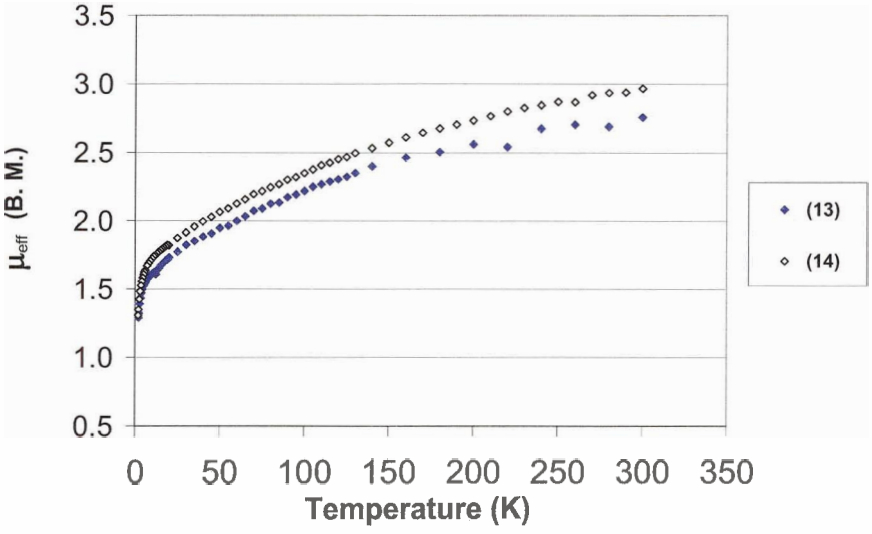

Figure 3.11 Plot of the magnetic moment vs. temperature for $\{CrI_2[^{Me_3Ph}NN'O]\}$ (**13**) and $\{CrI_2[^{iPr_2Ph}NN'O]\}$ (**14**).

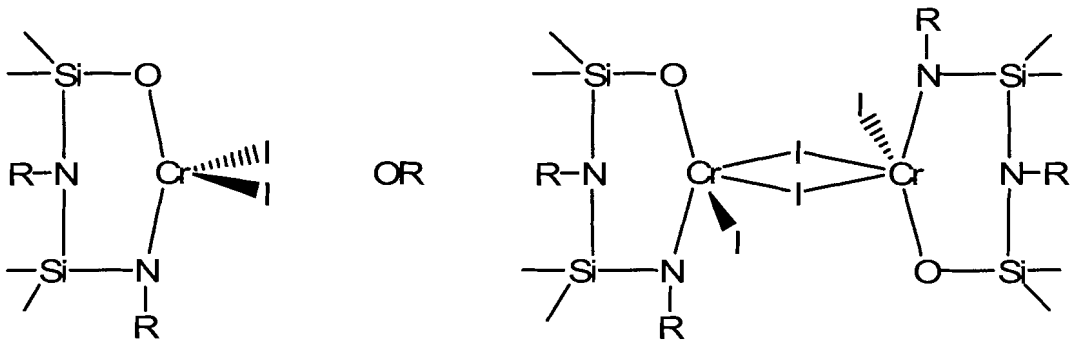

Figure 3.12 Proposed structures of $\{Cr^{IV}I_2[^{R}NN'O]\}$ (R = 2,4,6-Me_3Ph, **13**; 2,6-$^{i}Pr_2Ph$, **14**).

3.6.3 Catalytic reactivity of Cr(IV) complexes toward the polymerization of ethylene

As mentioned earlier in this chapter, mid- and high-valent chromium complexes containing O- and N-donor-based chelates have proven to be highly active catalysts for olefin polymerization.[17] Thus, it was encouraging to explore the catalytic activities of the chromium complexes bearing mixed-donor amido-amino-siloxo $[^{R}NN'O]^{2-}$ chelating ligands to demonstrate how changes within the ligand system affect the reactivity of these complexes. In this context, toluene solutions of **13** or **14** mixed with cocatalyst MAO were exposed to 1 atm of ethylene, resulting in the formation of white residues in different yields depending on the reaction conditions (Figure 3.13).

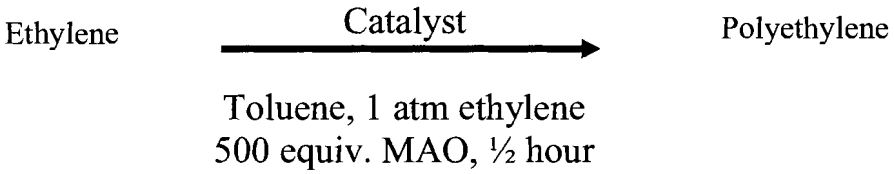

Figure 3.13 General reaction scheme of ethylene polymerization tests.

For comparison, the catalytic reactivity of Leznoff's previously reported diamagnetic $\{TiCl_2[^{Me_3Ph}NON]\}$[164] and $\{ZrCl_2[^{Me_3Ph}NON]\}$[164] complexes were also tested under similar conditions. None of these compounds showed any activity for ethylene polymerization without the presence of cocatalyst methylaluminoxane (MAO). However, addition of 500 equivalent of MAO per mole of catalyst was found to activate these complexes and initiate the polymerization process. The results are summarized in Table 3.6.

Table 3.6 Preliminary result of polymerization of ethylene catalyzed by Cr(IV), Ti(IV), and Zr(IV)/MAO systems (in 50 mL toluene, at 25 °C, 1 atm of ethylene, and 500 equiv. of MAO/mole of catalyst).

Catalyst	Catalyst (mmol)	Product (mg & mmol*)	mp (°C)	Activity (kg/mol.h)
$\{CrI_2[^{Me_3Ph}NN'O]\}$ (13)	**0.0142**	**37 mg 1.32 mmol**	**120-130**	**5.2**
$\{CrI_2[^{iPr_2Ph}NN'O]\}$ (14)	**0.0190**	**275 9.82**	**140-190**	**28.9**
$\{TiCl_2[^{Me_3Ph}NON]\}$	**0.0193**	**3 0.11**	**140-210**	**0.3**
$\{ZrCl_2[^{Me_3Ph}NON]\}$	**0.0178**	**20 0.71**	**130-209**	**2.2**

*The value of millimoles of product assuming a MW of 28 g/mol.

These results are preliminary and only serve as a general guideline for future references. The problem with the purification of compounds **13** and **14** adds great uncertainty to the polymerization results since the highest activity of 28.9 kg/mol.h was observed for the **14**/MAO system (and compound **14** is the least pure!). It is possible that

an impurity in the crude compounds seriously affects the outcome of the reactions, although the principal impurity likely to be I_2. In any case, future work should concentrate on preparing pure Cr(IV) complexes for further testing. Nevertheless, in general, it is expected that the more sterically encumbered $^{i}Pr_2Ph$ group offers higher steric protection to the chromium centre, which should increase the number of catalytic cycles.

If one assumes that the Cr(IV) complexes are acting as catalyst precursors (i.e. the primary impurity is I_2 and it does not impact the catalytic cycle), then analyzing the data in Table 3.6 shows that the Cr complexes **13** and **14** bearing mixed-donor $[^{R}NN'O]^{2-}$ ligand show higher catalytic activity than the Ti(IV) and Zr(IV) complexes with the symmetrical $[^{R}NON]^{2-}$ system. Furthermore, the melting point of the polyethylene produced from the Cr/MAO systems are in a narrower range compare to that of the Zr/MAO and Ti/MAO systems. This indicates that the polyethylene synthesized by the Cr/MAO system has a narrower molecular weight distribution. In general, a narrow molecular weight distribution suggests the presence of a uniformly active catalyst species.[17]

Comparing these very preliminary results with those in the literature, Ikeda *et al.* reported that Cr(II/III) complexes stabilized with the N,N-bidentate diamidosilyl ether ligand $[(^{t}BuNSiMe_2)_2O]^{2-}$ also showed catalytic activity toward ethylene polymerization upon activation with diethylaluminium chloride.[153] $\{Cr_2[(^{t}BuNSiMe_2)_2O]_3\}$, upon activation with 100 equiv. of MMAO, showed an activity of 1.8 kg/mol.h for polymerization of ethylene. In another example, Smith *et al.* reported that $\{CrI_2[N(SiMe_3)_2]_2\}$/180 equiv. MAO is active for ethylene polymerization with an

activity of 48.6 kg/mol.h.atm.[215] A comparison of the activity of the Cr(IV) **13** and **14**/MAO systems with Ikeda's Cr(III) and Smith's Cr(IV) systems indicates that the Cr(IV) mixed-donor $[^{R}NN'O]^{2-}$ ligand systems offer moderate catalytic activities. Although the **14**/MAO system showed the largest catalytic activity, this activity is small compared to other reported Cr complexes. For instance, at 40 °C, non-Cp MAO-activated complexes of the form $[CrCl_3(C_3H_6N_3R_3)]$ (R = Me, ^{n}Pentyl, ^{n}Octyl, ^{n}Dodecyl) are highly active ethylene polymerization catalysts with activities ranging from 455 to 717 kg/mol.h depending on the R groups.[219]

Indeed, more study is needed to fully explore the catalytic behaviour of these Cr complexes for tuning the activity and selectivity by altering the steric and electronic properties of the ligands. It is also important to experiment with different conditions under which the catalyst reacts for maximum optimization. It has been shown that the activity of the catalysts significantly depends on the type and the concentration of the cocatalyst.[220,221] Thus, the chromium compounds in this thesis should also be tested to see if can be activated by the addition of other cocatalysts such as MMAO, and DEAC at different concentrations. Other factors such as temperature, pressure of ethylene, and type of solvent are worthy to be considered to find the most effective condition for catalysis.

3.7 Summary

Like their symmetrical diamidosilyl ether analogous, the mixed-donor $[^{R}NN'O]^{2-}$ are also good ligands for the synthesis of transition metal complexes. Mononuclear, dinuclear, and pentanuclear chromium complexes with $[^{R}NN'O]^{2-}$ were synthesized, which indicated the sensitivity of the product to the stoichiometry of the reaction.

Differences in the Cr coordination chemistry of $[^{R}NN'O]^{2-}$ and $[^{R}NON]^{2-}$ ligands were readily reflected in the structural and magnetic features of $\{Cr[^{Me_3Ph}NN'O]\cdot THF\}_2$ (**7**) and the analogous compound $\{Cr[^{Me_3Ph}NON]\}_2$.[65,164] For instance, the potentially tridentate ligand $[^{Me_3Ph}NN'O]^{2-}$ acts as a bidentate amido-siloxo donor with Cr(II) as compared with the tridentate $[^{Me_3Ph}NON]$ chromium(II) complex.

Unlike **7**, dinuclear $\{Cr[^{iPr_2Ph}NN'O]\}_2$ (**8**) is a THF-free adduct and the highly coordinately unsaturated Cr(II) centres generate an unusual binding motif in the form of a metal-ipso-carbon bond. Similar $Cr–C_{ipso}$ bond was also observed for the terminal Cr centres of pentanuclear $\{(Cr_2[^{Me_3Ph}NN'O]_2)_2CrCl_2\}$ (**10**). These $Cr–C_{ipso}$ interactions are by far the shortest in the literature. Such interactions may help to stabilize the resting state of non-metallocene supported metal complexes that are active in olefin polymerization.[2,14]

Preliminary results suggest that mixed-hard-donor bidentate amido-amino-alkoxo ligand frameworks $[^{R}NN'O]^{2-}$ can also form stable Cr(IV) iodo complexes, which, once activated with MAO, may act as catalysts for polymerization of ethylene in relatively moderate activity. General features of the mixed-donor $[^{R}NN'O]^{2-}$ ligands are the presence of bulky aryl substituents and additional N-donor group in the ligand frame, which is a strategy that has proved to be successful for the stabilization of new N,O-chelate catalysts of early and late transition metals. Due to the hardness of the donor atoms of the mixed N,O-donor framework, these complexes may serve as model systems for hard donor environments present in the Phillips catalyst.

3.8 Experimental Section

3.8.1 General procedures, materials and instrumentation

General experimental details, materials, and instrumentation are similar to those reported in the previous chapter. The variable magnetic susceptibility of microcrystalline samples were measured over the range 2 – 300 K and at a field of 10 000 G using a Quantum Design (MPMS-XL-7S) SQUID magnetometer. Data were collected and interpreted by Julie Lefebvre (SFU). The airtight sample holder, made of PVC, was specifically designed to possess a constant cross-sectional area. All magnetic measurements were conducted in the solid state using a SQUID magnetometer. X-ray crystallographic experimental details can be found in the Appendix.

3.8.2 Synthesis of {Cr[2,4,6-Me_3PhNSiMe_2N(2,4,6-Me_3Ph)SiMe_2O]}$_2$, {Cr[^{Me_3Ph}NN'O]}$_2$ (7)

A white solid of Li_2[^{Me_3Ph}NN'O] (**3c**) (250 mg, 0.606 mmol) was dissolved in 15 mL of Et_2O and added dropwise to anhydrous $CrCl_2$ (74 mg, 0.606 mmol) in 20 mL of Et_2O at –30 °C, yielding a brown/green coloured solution. After being stirred for 24 hours at room temperature, the solvent was removed *in vacuo*, the residue was extracted in toluene and filtered through Celite. Removal of the hexanes *in vacuo* resulted in a dark green powder of **7**. Yield: 227 mg (83%). Recrystallization from THF solution gave single crystals of the purple THF-adduct. Anal. Calcd. (%) for $C_{26}H_{42}N_2CrO_2Si_2$: C: 59.73, H: 8.10, N: 5.36. Found: C: 59.50, H: 8.24, N: 5.10. μ_{eff}: 2.88 B.M. (298 K).

3.8.3 Synthesis of {Cr[2,6-^{i}Pr$_2$PhNSiMe$_2$N(2,6-^{i}Pr$_2$Ph)SiMe$_2$O]}$_2$, {Cr[^{iPr_2Ph}NN'O]}$_2$ (8)

A white solid of Li$_2$[^{iPr_2Ph}NN'O] (**4c**) (250 mg, 0.503 mmol) was dissolved in 15 mL of Et$_2$O and added dropwise to anhydrous CrCl$_2$ (61 mg, 0.503 mmol) in 20 mL of Et$_2$O at –30 °C, yielding a brown/green coloured solution. After being stirred for 24 hours at room temperature, the solvent was removed *in vacuo*, the residue was extracted in hexanes and filtered through Celite. Removal of the hexanes *in vacuo* resulted in a dark green powder of **8**. Yield: 251 mg (93%). Anal. Calcd. (%) for C$_{28}$H$_{46}$N$_2$CrOSi$_2$: C: 62.88, H: 8.67, N: 5.24. Found: C: 62.49, H: 8.41, N: 5.41. μ_{eff} = 3.80 B.M. (298 K). Single crystals were obtained from the slow evaporation of a saturated hexanes solution.

3.8.4 Synthesis of {Cr([2,4,6-Me$_3$PhNSiMe$_2$N(2,4,6-Me$_3$Ph)SiMe$_2$O]–μ–Li)$_2$• THF}, {Cr[^{Me_3Ph}NN'O]$_2$Li$_2$•THF} (9)

A white solid of Li$_2$[^{Me_3Ph}NN'O] (**3c**) (250 mg, 0.606 mmol) was dissolved in 20 mL of THF and added dropwise to anhydrous CrCl$_2$ (37 mg, 0.301 mmol) in 20 mL of THF at –30 °C. The reaction was warmed to room temperature, stirred for 24 hours, and solvent was removed *in vacuo*. The resulting residue was extracted with hexanes and filtered through Celite. Removal of the hexanes *in vacuo* resulted in a dark green powder of **9**. Yield: 195 mg (75 %). Recrystallization from THF/pentane solution gave single crystals of the purple THF-adduct. Anal. Calcd. for C$_{44}$H$_{68}$N$_4$CrLi$_2$O$_2$Si$_4$: C, 61.22; H, 7.94; N, 6.49. Found: C, 61.35; H, 8.33; N, 6.19.

3.8.5 Synthesis of $\{(Cr_2[2,4,6\text{-}Me_3PhNSiMe_2N(2,4,6\text{-}Me_3Ph)SiMe_2O]_2)_2CrCl_2\}$, $\{(Cr_2[^{Me_3Ph}NN'O]_2)_2CrCl_2\}$ (10)

A white solid of $Li_2[^{Me_3Ph}NN'O]$ (**3c**) (250 mg, 0.606 mmol) was dissolved in 20 mL of Et_2O and added dropwise to anhydrous $CrCl_2$ (93 mg, 0.757 mmol) in Et_2O at 0 °C. The reaction was warmed to room temperature, stirred for 72 hours, and the solvent was removed *in vacuo*. The resulting residue was extracted in hexanes and filtered through Celite. Removal of the hexanes *in vacuo* resulted in a grey/green powder of **10**. Yield: 276 mg (95 %). Anal. Calcd. for $C_{88}H_{136}N_8Cl_2Cr_5O_4Si_8$: C, 54.89; H, 7.11; N, 5.82. Found: C, 54.75; H, 7.31; N, 5.54. Single crystals were obtained from the slow evaporation of a saturated hexanes solution.

3.8.6 Synthesis of $\{Cr^{IV}[(PrNSiMe_2)_2O]_2\}$ (11) and $\{Cr^{II}[(PrNSiMe_2)_2O]_2Li_2\}$ (12)

A white solid of $Li_2[^{Pr}NON]$ (**1b**) (250 mg, 0.96 mmol) was dissolved in 25 mL of Et_2O and added dropwise to a slurry of anhydrous $CrCl_3$•3THF (180 mg, 0.48 mmol) in THF at –30 °C, yielding a dark green coloured solution. The reaction was warmed to room temperature, stirred for 24 hours, and the solvent was removed *in vacuo*. The resulting dark green residue was extracted in toluene and filtered through Celite. Removal of toluene *in vacuo* resulted in 0.237 g (89 %) of dark green powder. This powder was sublimed under vacuum at 70 °C for 12 hours to afford a volatile dark green powder of **11** on the cold-finger and a non-volatile dark green residue of **12**. Compound **11** was extracted from the cold-finger with hexanes and dried *in vacuo*. Compound **12** was washed with a minimum amount of cold pentane and dried *in vacuo*. For **11**: Yield: 0.076 g (64 %). Anal. Calcd. for $C_{20}H_{52}N_4CrO_2Si_4$: C, 44.08; H, 9.62; N, 10.28. Found: C, 43.39; H, 9.90; N, 9.28. μ_{eff}: 3.06 B.M. (298 K). Single crystals were obtained from

the slow evaporation of a pentane/toluene solution. For **12**: Yield: 0.098 g (83 %). Anal. Calcd. for $C_{20}H_{52}N_4CrLi_2O_2Si_4$: C, 42.98; H, 9.38; N, 10.02. Found: C, 42.42; H, 9.42; N, 9.88.

3.8.7 Synthesis of $\{CrI_2[^{Me_3Ph}NN'O]\}_2$ (13)

A dark red/purple solid of I_2 (73 mg, 0.288 mmol) was dissolved in 20 mL of Et_2O and added dropwise to a green solution of $\{Cr[^{Me_3Ph}NN'O]\}_2$ (**7**) (130 mg, 0.144 mmol) in 20 mL of Et_2O at –30 °C. After 24 hours of being stirred at room temperature, the solvent was removed *in vacuo*. The resulting dark brown residue was extracted in toluene, filtered through Celite, and dried *in vacuo*. The final brown powder of **13** was washed several times with a minimum amount of hexanes and dried *in vacuo*. Yield: 165 mg (81 %). Anal. Calcd. for $C_{22}H_{34}N_2CrI_2OSi_2$: C, 37.51; H, 4.86; N, 3.98. Found: C, 36.80; H, 4.88; N, 3.46. μ_{eff}: 2.76 B.M. (298 K). Attempts to completely purify and obtain single crystals for X-ray analysis were unsuccessful. The elemental analysis of **13** has been repeated twice (with the addition of oxidant) on two different batches. However, the observed percentages were consistently low, perhaps due to the presence of unreacted iodine.

3.8.8 Synthesis of $\{CrI_2[^{iPr_2Ph}NN'O]\}_2$ (14)

A dark red/purple solid of I_2 (133 mg, 0.523 mmol) was dissolved in 20 mL of Et_2O and added dropwise to a purple solution of $\{Cr[^{iPr_2Ph}NN'O]\}_2$ (**8**) (280 mg, 0.262 mmol) in 20 mL of Et_2O at –30 °C. An immediate colour change to dark brown occurred. After 48 hours of being stirred at room temperature, the solvent was removed *in vacuo*. The resulting dark brown residue was extracted in toluene, filtered through Celite, and

dried *in vacuo*. The final brown powder of **14** was washed several times with a minimum amount of hexanes and dried *in vacuo*. Yield: 346 mg (84 %). Anal. Calcd. for $C_{28}H_{46}N_2CrI_2OSi_2$: C, 42.64; H, 5.88; N, 3.55. Found: C, 37.59; H, 5.67; N, 2.33. μ_{eff}: 2.97 B.M. (298 K). Attempts to completely purify (e.g. remove unreacted iodine) and obtain single crystals for X-ray analysis were unsuccessful.

3.8.9 Polymerization reaction of ethylene

In a typical reaction, MAO was added slowly with stirring to a mixture of the selected metal complex and freshly distilled toluene (30 mL). The mixture was degassed via a freeze-pump-thaw cycle and the polymerization started by introducing ethylene at 1 atm to the solution at room temperature. The reaction was quenched after 30 minutes by venting of excess ethylene and addition of 50 mL of acidified methanol (10% concentrated hydrochloric acid in methanol). The white precipitates were collected on a frit filter, washed with methanol, and dried *in vacuo*.

APPENDIX:

SUMMARY OF CRYSTALLOGRAPHIC DATA

This appendix contains the details regarding the methods of crystallographic data collection and structure solution. It also contains summary tables of the crystallographic data and the list of fractional atomic coordinates and equivalent isotropic thermal parameters (U(iso) in $Å^2$) for the structures reported in this thesis. Data for **3a**, **1c**, **7**, **8**, **9**, and **11** were collected on suitable single crystals mounted in sealed glass capillaries under a nitrogen atmosphere. Data for **3c**, **4c**, and **10** were collected on suitable single crystals coated with oil (Paratone 8277, Exxon) on top of the nylon fiber of a mounted CryoLoop™, which were quickly transferred to the cold stream of the X-ray diffractometer. All diagrams were made using ORTEP-3.[222]

For **11**, data was collected using the diffractometer control program DIFRAC[223] on an Enraf Nonius CAD4F diffractometer with graphite monochromated Mo–Kα radiation (λ = 0.71073 Å). Data for crystals of **3a**, **1c**, and **9** were obtained on a Rigaku RAXIS RAPID imaging plate area detector with graphite monochromated Cu–Kα radiation (λ = 1.54180 Å) by Mr. Michael J. Katz (SFU). For these crystals, the programs used for all absorption corrections, data reduction and structure solutions were from the NRCVAX Crystal Structure System.[224] The structures were refined using CRYSTALS.[225] Unless otherwise indicated, all non-hydrogen atoms were refined using anisotropic thermal parameters.

Crystals of **7** and **8** were analyzed on a P4 Bruker diffractometer by Prof. James F. Britten (McMaster University) equipped with a Bruker SMART 1K CCD area detector (employing the program SMART)[226] and a rotating anode utilizing graphite-monochromated Mo–Kα radiation (λ = 0.71073 Å). Data processing was carried out by use of the SAINT program,[226] while the program SADABS[226] was utilized for the scaling of diffraction data, the application of a decay correction and an empirical absorption correction based on redundant reflections. The structures were solved by using the direct-methods procedure in the Bruker SHELXTL program library[227] and refined by full-matrix least-squares methods on F^2. All non-hydrogen atoms were refined using anisotropic thermal parameters.

Crystals of **3c**, **4c**, and **10** were analyzed by Dr. Gabriele Schatte (University of Saskatchewan) on a Nonius KappaCCD 4-Circle FR540C diffractometer using monochromated Mo–K_α radiation (λ = 0.71073 Å). Cell parameters were initially retrieved using the COLLECT[228] software, and refined with the HKL DENZO and SCALEPACK software.[229] The structures were solved using direct methods in the specific space groups (SIR-97)[230] and refined by full-matrix least-squares method on F^2 with SHELXL97-2.[231] The non-hydrogen atoms were refined anisotropically. Hydrogen atoms were included at geometrically idealized positions and were not refined. Neutral atom scattering factors for non-hydrogen atoms and anomalous dispersion coefficients were contained in the SHELXTL-NT 6.14[232] program library.

For **3a**, a minimum F_o = 20 cut-off was used to exclude image-plate background noise. Crystals of **1c** did not diffract very well and thus a limited amount of data was collected. Furthermore, disordered propyl groups were modelled with partial occupancies

(three restraints). For **3c**, in one of the two dimers the coordinating THF molecule (labelled as O(41), C(41), C(42), C(43), C(44) and O(41)*, C(41)*, C(42)*, C(43)*, C(44)*) was disordered over two positions. The disordered THF molecule was modelled using the split-atom model and partial occupancies. In addition, the atoms in one of the $SiMe_2$ groups (labelled as Si(2A), C(3A), C(4A) and Si(2B), C(3B), C(4B)) in the same dimer were also disordered.

For **4c**, all three ether molecules coordinating to the lithium atoms showed severe disorder, a series of restraints and partial occupancies were used to model these molecules. The isotropic atomic displacement parameters for equivalent atoms (e.g. O(61A) and O(61B)) in the two parts of each ether molecule were the same. Crystals of **9** were poorly diffracted and a limited amount of data was collected. Only the Cr and Si atoms were refined anisotropically and all other atoms were kept isotropic to maintain a reasonable data/parameter ratio. For **10**, the solvent molecule toluene showed severe disorder, which was modelled using a series of restraints and partial occupancies.

Table A.1 Summary of crystallographic data for compounds **3a** and **1c**.

	$H_2[^{Me_3Ph}NON]$ (**3a**)	$\{Li_2[^{Pr}NN'O]\}_4$ (**1c**)
Empirical Formula	$C_{22}H_{36}N_2OSi_2$	$C_{40}H_{104}Li_8N_8O_4Si_8$
Formula Weight	400.71	1041.52
Temperature (K)	293	293
Crystal Size	0.37 × 0.37 × 0.15	0.51 × 0.42 × 0.23
Crystal System	Monoclinic	Triclinic
Space Group	$P\,2_1/a$	$P\bar{1}$
a (Å)	8.4461(2)	12.3384(1)
b (Å)	16.0622(3)	16.27790(10)
c (Å)	18.6263(4)	19.6075(1)
α (°)	90	77.898(5)
β (°)	93.364(1)	78.038(5)
γ (°)	90	66.527(4)
V (Å^3)	2522.54(9)	3498.10(13)
Z	4	2
ρ_{calcd} (g cm^{-3})	1.055	1.013
θ range (deg)	2.38 – 56.20	2.33 – 72.37
Reflections Collected	3168	38536
Indep. Reflections	2966	11421
Data/Parameters	1923/248	3623/481
R_F, R_{WF} (I> Xσ(I))	0.0624, 0.0605 (X = 2.5)	0.0730, 0.0840 (X = 2.0)

Table A.2 Summary of crystallographic data for compounds **3c** and **4c**.

	$\{Li_2[^{Me_3Ph}NN'O]\bullet THF\}_2$ (**3c**)	$\{Li_2[^{iPr_2Ph}NN'O]\bullet(Et_2O)_3\}$ (**4c**)
Empirical Formula	$C_{52}H_{84}Li_4N_4O_4Si_4$	$C_{40}H_{76}Li_2N_2O_4Si_2$
Formula Weight	969.35	719.09
Temperature (K)	173	173
Crystal Size (mm)	0.20 × 0.20 × 0.18	0.20 × 0.20 × 0.18
Crystal System	Triclinic	Orthorhombic
Space Group	$P\bar{1}$	$Pna2_1$
a (Å)	12.8660(4)	19.4130(2)
b (Å)	13.9530(3)	12.3350(4)
c (Å)	16.9200(5)	19.0520(5)
α (°)	70.5380(18)	90
β (°)	88.7260(12)	90
γ (°)	89.5600(13)	90
V (Å^3)	2863.21(14)	4562.2(2)
Z	2	4
ρ_{calcd} (g cm^{-3})	1.124	1.047
θ range (deg)	2.05 – 23.26	1.96 – 23.26
Reflections Collected	7989	3391
Indep. Reflections	5518	2921
Data/Parameters	5518/709	2921/422
R_F, R_{WF} (I> 2.0σ(I))	0.0630, 0.1565	0.0745, 0.2067

Table A.3 Summary of crystallographic data for compounds **7** and **8**.

	$\{Cr[^{Me_3Ph}NN'O]\bullet THF\}_2$ (**7**)	$\{Cr[^{iPr_2Ph}NN'O]\}_2$ (**8**)
Empirical Formula	$C_{60}H_{100}Cr_2N_4O_6Si_4$	$C_{56}H_{92}Cr_2N_4O_2Si_4$
Formula Weight	1189.79	1069.69
Temperature (K)	173	173
Crystal Size (mm^3)	0.60 × 0.24 × 0.14	0.36 × 0.25 × 0.05
Crystal System	Monoclinic	Monoclinic
Space Group	*C2/c*	$P2_1/n$
a (Å)	11.146(3)	9.727(4)
b (Å)	27.506(7)	15.844(6)
c (Å)	22.192(5)	19.010(7)
α (°)	90	90
β (°)	99.630(4)	100.599(6)
γ (°)	90	90
V ($Å^3$)	6708(3)	2879.7(18)
Z	4	2
ρ_{calcd} (g cm^{-3})	1.178	1.234
θ range (deg)	1.48 – 27.48	1.69 – 25.00
Reflections Collected	23870	15641
Indep. Reflections	7682	4955
Data/Parameters	5187/310	3155/308
R_F, R_{WF} (I> 2.0σ(I))	0.0451, 0.1226	0.0508, 0.1113

Table A.4 Summary of crystallographic data for compounds **9** and **10**.

	$\{Cr[^{Me_3Ph}NN'O]_2Li_2 \cdot THF\}$ **(9)**	$\{(Cr_2[^{Me_3Ph}NN'O]_2)_2CrCl_2\}$ **(10)**
Empirical Formula	$C_{48}H_{76}CrLi_2N_4O_3Si_4$	$C_{102}H_{152}Cl_2Cr_5N_8O_4Si_8$
Formula Weight	935.36	2109.94
Temperature (K)	293	173
Crystal Size (mm^3)	0.30 × 0.25 × 0. 20	0.12 × 0.12 × 0.12
Crystal System	Monoclinic	Triclinic
Space Group	$P\,2_1/n$	$P\bar{1}$
a (Å)	19.6768(19)	14.3348(3)
b (Å)	11.7274(8)	14.3995(3)
c (Å)	23.586(3)	16.8012(3)
α (°)	90	94.042(1)
β (°)	95.890(4)	111.229(1)
γ (°)	90	111.478(1)
V ($Å^3$)	5413.8(9)	2934.74(10)
Z	4	1
ρ_{calcd} ($g\ cm^{-3}$)	1.38	1.194
θ range (deg)	2.25 – 72.38	2.53 – 24.81
Reflections Collected	36279	19456
Indep. Reflections	8248	9984
Data/Parameters	1669/278	7832/639
R_F, R_{WF} (I> 2.0σ(I))	0.0730, 0.0814	0.0472, 0.1357

Table A.5 Summary of crystallographic data for compound **11**.

	{Cr[^{Pr}NON]$_2$} (**11**)
Empirical Formula	$C_{20}H_{52}CrN_4O_2Si_4$
Formula Weight	544.99
Temperature (K)	293
Crystal Size (mm^3)	0.35 × 0.26 × 0.13
Crystal System	Monoclinic
Space Group	*C 2/c*
a (Å)	17.3734(9)
b (Å)	16.6595(6)
c (Å)	23.5317(10)
α (°)	90
β (°)	99.504(2)
γ (°)	90
V (Å^3)	6717.3(5)
Z	8
ρ_{calcd} (g cm^{-3})	0.974
θ range (deg)	1.70 – 18.85
Reflections Collected	2625
Indep. Reflections	2535
Data/Parameters	1463/200
R_F, R_{WF} (I> 2.5σ(I))	0.0692, 0.0777

Table A.6 Fractional atomic coordinates and equivalent isotropic thermal parameters [U(iso) ($Å^2$)] for **3a**.

Atom	x	y	z	[U(iso) ($Å^2$)]	Occ
Si1	0.7998(2)	0.47732(11)	0.29859(10)	0.0879	1
Si2	0.9960(2)	0.38580(11)	0.18575(10)	0.083	1
O1	0.8642(5)	0.4112(3)	0.2428(2)	0.0956	1
N1	0.8963(6)	0.4739(3)	0.3817(2)	0.0849	1
N2	0.9672(6)	0.4345(3)	0.1043(3)	0.0816	1
C1	0.5893(7)	0.4525(6)	0.3080(4)	0.1496	1
C2	0.8363(11)	0.5837(4)	0.2631(4)	0.1502	1
C3	1.1936(8)	0.4186(4)	0.2228(4)	0.1176	1
C4	0.9787(8)	0.2725(4)	0.1718(4)	0.1093	1
C5	0.8498(7)	0.4273(4)	0.4429(3)	0.0823	1
C6	0.8746(9)	0.3430(4)	0.4498(4)	0.0998	1
C7	0.8280(10)	0.3020(5)	0.5112(4)	0.1293	1
C8	0.7583(10)	0.3444(6)	0.5654(4)	0.123	1
C9	0.7325(8)	0.4284(5)	0.5569(4)	0.1075	1
C10	0.7756(8)	0.4711(4)	0.4961(4)	0.0909	1
C11	0.9527(10)	0.2932(4)	0.3920(4)	0.1383	1
C12	0.7085(12)	0.2959(6)	0.6317(4)	0.1803	1
C13	0.7391(8)	0.5639(4)	0.4911(4)	0.1146	1
C14	0.8826(8)	0.4053(3)	0.0400(3)	0.0762	1
C15	0.7165(8)	0.4044(4)	0.0336(4)	0.0834	1
C16	0.6440(9)	0.3784(4)	-0.0310(4)	0.1068	1
C17	0.7276(12)	0.3540(4)	-0.0884(4)	0.1105	1
C18	0.8913(11)	0.3536(4)	-0.0800(4)	0.1082	1
C19	0.9714(9)	0.3767(4)	-0.0167(4)	0.0881	1
C20	0.6188(7)	0.4365(4)	0.0933(3)	0.1027	1
C21	0.6449(11)	0.3303(5)	-0.1603(4)	0.1606	1
C22	1.1530(8)	0.3712(4)	-0.0079(4)	0.1155	1
H11	0.5359	0.5041	0.3181	0.245(9)	1

Atom	x	y	z	[U(iso) (Å^2)]	Occ
H12	0.5839	0.4137	0.3476	0.245(9)	1
H13	0.5449	0.4283	0.2644	0.245(9)	1
H14	0.9007	0.529	0.3969	0.12(2)	0.5
H15	0.9979	0.4555	0.3732	0.12(2)	0.5
H21	0.9496	0.5913	0.2597	0.136(9)	1
H22	0.7967	0.6247	0.2959	0.136(9)	1
H23	0.783	0.5907	0.2159	0.136(9)	1
H24	1.069	0.4455	0.0902	0.12(2)	0.5
H25	0.9175	0.4843	0.1149	0.12(2)	0.5
H31	1.2683	0.4052	0.1869	0.182(9)	1
H32	1.193	0.4784	0.2326	0.182(9)	1
H33	1.2179	0.3883	0.2671	0.182(9)	1
H41	1.0673	0.2542	0.1452	0.174(9)	1
H42	0.9824	0.2448	0.2179	0.174(9)	1
H43	0.8802	0.2599	0.1454	0.174(9)	1
H71	0.8482	0.2452	0.5169	0.136(13)	1
H91	0.6882	0.4577	0.5942	0.111(13)	1
H111	0.9593	0.2368	0.4092	0.201(9)	1
H112	1.0576	0.3163	0.3867	0.201(9)	1
H113	0.8894	0.2974	0.3474	0.201(9)	1
H121	0.5986	0.3112	0.6403	0.284(9)	1
H122	0.7803	0.3103	0.6735	0.284(9)	1
H123	0.7179	0.2368	0.6203	0.284(9)	1
H131	0.7013	0.5849	0.536	0.163(9)	1
H132	0.8371	0.5909	0.4805	0.163(9)	1
H133	0.659	0.5734	0.4519	0.163(9)	1
H161	0.5317	0.3785	-0.0363	0.122(13)	1
H181	0.9521	0.3413	-0.1188	0.108(13)	1
H201	0.5085	0.4292	0.0786	0.146(9)	1
H202	0.6464	0.4945	0.1005	0.146(9)	1

Atom	x	y	z	[U(iso) (Å^2)]	Occ
H203	0.6475	0.4047	0.1361	0.146(9)	1
H211	0.7268	0.3225	-0.1941	0.232(9)	1
H212	0.5746	0.3756	-0.1769	0.232(9)	1
H213	0.583	0.2797	-0.1569	0.232(9)	1
H221	1.1898	0.3412	-0.0493	0.179(9)	1
H222	1.1963	0.4271	-0.0051	0.179(9)	1
H223	1.1784	0.341	0.0359	0.179(9)	1

Table A.7 Fractional atomic coordinates and equivalent isotropic thermal parameters [U(iso) (Å^2)] for **1c**.

Atom	x	y	z	[U(iso) (Å^2)]	Occ
Si1	-0.1257(3)	0.1068(2)	0.33460(16)	0.0639	1
Si2	0.0888(3)	-0.0560(2)	0.27825(17)	0.0706	1
Si3	-0.2114(3)	0.4408(2)	0.22853(17)	0.068	1
Si4	-0.2424(3)	0.4368(2)	0.39047(17)	0.0731	1
Si5	0.2503(3)	0.1675(2)	0.34791(16)	0.0664	1
Si6	0.2717(3)	0.3563(2)	0.29757(17)	0.0739	1
Si7	0.1833(3)	0.2485(2)	0.08613(16)	0.0722	1
Si8	-0.0198(3)	0.2249(2)	0.03051(16)	0.0755	1
O1	-0.0690(5)	0.1716(4)	0.2782(3)	0.0542	1
O2	-0.0817(5)	0.3611(4)	0.2365(3)	0.053	1
O3	0.1228(5)	0.2100(4)	0.3185(3)	0.0531	1
O4	0.1249(5)	0.2198(4)	0.1645(3)	0.0546	1
N1	-0.0640(7)	0.0017(5)	0.3039(4)	0.0625	1
N2	0.1310(6)	0.0176(5)	0.2138(4)	0.0613	1
N3	-0.2473(7)	0.4933(5)	0.3033(4)	0.071	1
N4	-0.0986(7)	0.3622(5)	0.3921(4)	0.0631	1
N5	0.2789(7)	0.2601(6)	0.3605(4)	0.0736	1
N6	0.1323(7)	0.3977(5)	0.2746(4)	0.063	1

Atom	x	y	z	[U(iso) (Å^2)]	Occ
N7	0.1315(7)	0.2048(6)	0.0311(4)	0.0783	1
N8	-0.0678(6)	0.1855(5)	0.1138(4)	0.0603	1
C1	-0.2893(8)	0.1485(7)	0.3392(6)	0.0867	1
C2	-0.0965(9)	0.0983(7)	0.4256(5)	0.0928	1
C3	0.1705(9)	-0.0917(7)	0.3560(5)	0.0932	1
C4	0.1095(9)	-0.1638(7)	0.2474(6)	0.1	1
C5	-0.2072(9)	0.5259(7)	0.1487(5)	0.0942	1
C6	-0.3233(9)	0.3941(7)	0.2204(6)	0.0929	1
C7	-0.2920(9)	0.5220(7)	0.4531(6)	0.1006	1
C8	-0.3535(9)	0.3786(8)	0.4162(6)	0.1069	1
C9	0.2433(9)	0.0936(7)	0.4337(5)	0.0908	1
C10	0.3703(9)	0.0966(7)	0.2859(6)	0.0962	1
C11	0.3054(9)	0.4375(7)	0.3385(6)	0.1024	1
C12	0.3931(9)	0.3257(8)	0.2214(6)	0.1045	1
C13	0.1441(11)	0.3733(7)	0.0649(5)	0.1078	1
C14	0.3496(8)	0.1969(8)	0.0744(5)	0.1015	1
C15	-0.1042(10)	0.3479(7)	0.0041(6)	0.1127	1
C16	-0.0308(10)	0.1653(8)	-0.0386(5)	0.1132	1
C17	-0.1311(9)	-0.0581(7)	0.3390(6)	0.085(4)	1
C18	-0.2085(10)	-0.0658(8)	0.2937(6)	0.106(4)	1
C19	-0.2864(10)	-0.1211(8)	0.3338(6)	0.123(5)	1
C20	0.2541(9)	-0.0250(7)	0.1768(5)	0.079(4)	1
C21	0.2541(10)	-0.0541(8)	0.1071(6)	0.109(4)	1
C22	0.3816(11)	-0.0997(9)	0.0724(7)	0.151(6)	1
C23	-0.3263(11)	0.5951(8)	0.2959(7)	0.123(5)	1
C24	-0.4500(14)	0.6074(11)	0.2991(9)	0.181(7)	1
C25	-0.5201(16)	0.7153(12)	0.2946(9)	0.237(9)	1
C26	-0.0730(9)	0.3208(7)	0.4648(5)	0.072(3)	1
C27	-0.0099(10)	0.3712(8)	0.4957(6)	0.104(4)	1
C28	0.0113(12)	0.3266(9)	0.5696(7)	0.146(6)	1

Atom	x	y	z	[U(iso) (Å^2)]	Occ
C29	0.3856(11)	0.2284(8)	0.4021(6)	0.112(4)	1
C30	0.3397(11)	0.2523(8)	0.4717(6)	0.116(5)	1
C31	0.4568(10)	0.2173(8)	0.5118(6)	0.112(4)	1
C32	0.1018(9)	0.4866(7)	0.2283(5)	0.078(3)	1
C33	0.0309(10)	0.5679(7)	0.2691(6)	0.096(4)	1
C34	0.0034(11)	0.6545(9)	0.2202(7)	0.141(5)	1
C35	0.1882(17)	0.2200(13)	-0.0453(11)	0.102(8)	0.69(3)
C36	0.2702(18)	0.1314(13)	-0.0640(11)	0.109(9)	0.69(3)
C37	0.3215(12)	0.1538(9)	-0.1482(7)	0.147(6)	1
C38	-0.1924(9)	0.1876(7)	0.1234(5)	0.075(3)	1
C39	-0.2027(9)	0.1016(7)	0.1143(6)	0.085(4)	1
C40	-0.3362(10)	0.1121(8)	0.1260(6)	0.118(5)	1
C41	0.431(2)	0.6119(19)	0.0781(15)	0.1962	0.587(12)
C42	0.493(3)	0.587(2)	0.0223(16)	0.1992	0.587(12)
C43	0.479(3)	0.510(2)	0.0287(13)	0.185	0.587(12)
C44	0.221(3)	0.152(2)	-0.0253(16)	0.062(14)	0.31(3)
C45	0.239(3)	0.220(2)	-0.0892(17)	0.077(16)	0.31(3)
Li1	-0.0452(16)	0.0915(12)	0.2013(9)	0.075(6)	1
Li2	0.1113(15)	0.1354(11)	0.2542(9)	0.063(5)	1
Li3	0.1089(15)	0.1153(11)	0.1283(9)	0.062(5)	1
Li4	0.0800(17)	0.3240(13)	0.3650(10)	0.079(6)	1
Li5	-0.0542(16)	0.2570(12)	0.1887(9)	0.072(6)	1
Li6	0.0996(15)	0.3030(12)	0.2296(9)	0.068(5)	1
Li7	-0.0560(16)	0.2648(12)	0.3238(9)	0.070(5)	1
Li8	-0.0476(16)	0.4298(12)	0.2991(9)	0.076(6)	1
H11	-0.3087	0.1542	0.2935	0.102(6)	1
H12	-0.3229	0.2061	0.3548	0.102(6)	1
H13	-0.3206	0.108	0.3709	0.102(6)	1
H21	-0.0126	0.0756	0.4255	0.111(6)	1
H22	-0.1313	0.1562	0.4406	0.111(6)	1

Atom	x	y	z	[U(iso) (Å^2)]	Occ
H23	-0.129	0.0581	0.4568	0.111(6)	1
H31	0.1649	-0.0401	0.3739	0.104(6)	1
H32	0.1353	-0.127	0.3912	0.104(6)	1
H33	0.252	-0.127	0.3429	0.104(6)	1
H41	0.0702	-0.1491	0.2071	0.117(6)	1
H42	0.0751	-0.1982	0.2839	0.117(6)	1
H43	0.1918	-0.1982	0.2356	0.117(6)	1
H51	-0.151	0.551	0.1514	0.108(6)	1
H52	-0.2838	0.5726	0.1468	0.108(6)	1
H53	-0.184	0.4975	0.1076	0.108(6)	1
H61	-0.3274	0.3504	0.2605	0.113(6)	1
H62	-0.3995	0.4412	0.2182	0.113(6)	1
H63	-0.2996	0.3661	0.179	0.113(6)	1
H71	-0.2386	0.553	0.4451	0.114(6)	1
H72	-0.2954	0.493	0.5004	0.114(6)	1
H73	-0.3693	0.564	0.4446	0.114(6)	1
H81	-0.3329	0.3331	0.3872	0.123(6)	1
H82	-0.3558	0.3522	0.4642	0.123(6)	1
H83	-0.4297	0.4232	0.4085	0.123(6)	1
H91	0.1843	0.1274	0.4674	0.111(6)	1
H92	0.3187	0.0695	0.4501	0.111(6)	1
H93	0.2231	0.0456	0.4269	0.111(6)	1
H101	0.3782	0.1316	0.2412	0.115(6)	1
H102	0.444	0.0724	0.3042	0.115(6)	1
H103	0.3485	0.0486	0.281	0.115(6)	1
H111	0.2472	0.4566	0.3779	0.133(6)	1
H112	0.382	0.4075	0.3534	0.133(6)	1
H113	0.3052	0.4887	0.3046	0.133(6)	1
H121	0.3832	0.285	0.197	0.127(6)	1
H122	0.4677	0.2981	0.2388	0.127(6)	1

Atom	x	y	z	[U(iso) (Å^2)]	Occ
H123	0.3909	0.3793	0.1901	0.127(6)	1
H131	0.0598	0.4025	0.0692	0.140(6)	1
H132	0.1739	0.3933	0.0966	0.140(6)	1
H133	0.178	0.3877	0.0181	0.140(6)	1
H141	0.3752	0.1329	0.0848	0.125(6)	1
H142	0.377	0.2189	0.106	0.125(6)	1
H143	0.3811	0.2132	0.0274	0.125(6)	1
H151	-0.1016	0.3827	0.0367	0.132(6)	1
H152	-0.0671	0.365	-0.0411	0.132(6)	1
H153	-0.1848	0.3584	0.0017	0.132(6)	1
H161	0.0091	0.1021	-0.026	0.150(6)	1
H162	0.0054	0.1845	-0.0834	0.150(6)	1
H163	-0.1123	0.1779	-0.0405	0.150(6)	1
H171	-0.1849	-0.0309	0.3774	0.083(6)	1
H172	-0.0765	-0.1156	0.3561	0.083(6)	1
H181	-0.2539	-0.0083	0.2707	0.107(6)	1
H182	-0.1546	-0.1017	0.2596	0.107(6)	1
H191	-0.3295	-0.1285	0.3021	0.120(6)	1
H192	-0.3407	-0.0853	0.3679	0.120(6)	1
H193	-0.2413	-0.1788	0.3568	0.120(6)	1
H201	0.2967	-0.0763	0.2072	0.027(6)	1
H202	0.2919	0.0177	0.167	0.027(6)	1
H211	0.2261	-0.1025	0.1164	0.061(6)	1
H212	0.205	-0.0051	0.0777	0.061(6)	1
H221	0.3854	-0.119	0.0291	0.133(6)	1
H222	0.4303	-0.1486	0.102	0.133(6)	1
H223	0.4091	-0.0511	0.0634	0.133(6)	1
H231	-0.3136	0.6233	0.3297	0.119(6)	1
H232	-0.3006	0.6194	0.2499	0.119(6)	1
H241	-0.4769	0.5822	0.3445	0.193(6)	1

Atom	x	y	z	[U(iso) (Å^2)]	Occ
H242	-0.4648	0.5822	0.2642	0.193(6)	1
H251	-0.6033	0.7285	0.2987	0.266(6)	1
H252	-0.5054	0.7406	0.3296	0.266(6)	1
H253	-0.4933	0.7406	0.2493	0.266(6)	1
H261	-0.142	0.3162	0.4948	0.134(6)	1
H262	-0.0149	0.2619	0.4602	0.134(6)	1
H271	-0.0642	0.4321	0.4956	0.175(6)	1
H272	0.0638	0.3699	0.4684	0.175(6)	1
H281	0.0434	0.361	0.5871	0.298(6)	1
H282	-0.0616	0.328	0.598	0.298(6)	1
H283	0.0663	0.2658	0.5708	0.298(6)	1
H291	0.4433	0.2538	0.3793	0.172(6)	1
H292	0.4208	0.1644	0.4053	0.172(6)	1
H301	0.2975	0.3158	0.4687	0.179(6)	1
H302	0.2884	0.222	0.4967	0.179(6)	1
H311	0.4332	0.2326	0.5582	0.158(6)	1
H312	0.5075	0.2476	0.4858	0.158(6)	1
H313	0.4984	0.1537	0.5139	0.158(6)	1
H321	0.1757	0.4916	0.2068	0.126(6)	1
H322	0.0592	0.4867	0.1931	0.126(6)	1
H331	0.075	0.5687	0.3031	0.146(6)	1
H332	-0.0417	0.5615	0.292	0.146(6)	1
H341	-0.042	0.7013	0.2481	0.196(6)	1
H342	0.0746	0.6631	0.1972	0.196(6)	1
H343	-0.0421	0.656	0.186	0.196(6)	1
H351	0.2368	0.2546	-0.0511	0.191(6)	0.69(3)
H352	0.1333	0.2457	-0.0786	0.191(6)	0.69(3)
H361	0.329	0.1062	-0.0331	0.199(6)	0.69(3)
H362	0.2222	0.096	-0.0557	0.199(6)	0.69(3)
H371	0.3732	0.0978	-0.1636	0.183(6)	0.69(3)

Atom	x	y	z	[U(iso) (Å^2)]	Occ
H372	0.3648	0.1922	-0.1532	0.183(6)	0.69(3)
H373	0.258	0.182	-0.1758	0.183(6)	0.69(3)
H374	0.347	0.1846	-0.1913	0.183(6)	0.31(3)
H375	0.389	0.1081	-0.1294	0.183(6)	0.31(3)
H376	0.2704	0.127	-0.1563	0.183(6)	0.31(3)
H381	-0.226	0.1972	0.1706	0.070(6)	1
H382	-0.2386	0.2356	0.092	0.070(6)	1
H391	-0.1602	0.0524	0.1464	0.082(6)	1
H392	-0.17	0.0899	0.0675	0.082(6)	1
H401	-0.3443	0.0588	0.1194	0.100(6)	1
H402	-0.3683	0.1241	0.1729	0.100(6)	1
H403	-0.378	0.1617	0.094	0.100(6)	1
H411	0.4358	0.6685	0.0795	0.237(6)	0.587(12)
H412	0.4615	0.5704	0.1179	0.237(6)	0.587(12)
H413	0.3507	0.6197	0.0788	0.237(6)	0.587(12)
H421	0.574	0.5768	0.0221	0.287(6)	0.587(12)
H422	0.4647	0.6279	-0.0182	0.287(6)	0.587(12)
H431	0.5247	0.4697	0.0638	0.195(6)	0.587(12)
H432	0.3971	0.5185	0.0432	0.195(6)	0.587(12)
H441	0.2907	0.1146	-0.0045	0.061(6)	0.31(3)
H442	0.1871	0.1149	-0.038	0.061(6)	0.31(3)
H451	0.2898	0.2469	-0.0805	0.061(6)	0.31(3)
H452	0.1712	0.2658	-0.1074	0.061(6)	0.31(3)

Table A.8 Fractional atomic coordinates and equivalent isotropic thermal parameters [U(iso) (Å^2)] for **3c**.

Atom	x	y	z	[U(iso) (Å^2)]	Occ
Si1	0.47003(11)	0.46007(9)	0.34754(7)	0.0639(4)	1
Si2A	0.2751(6)	0.6112(2)	0.34578(18)	0.0598(13)	0.682(13)

Atom	x	y	z	[U(iso) (Å^2)]	Occ
Si2B	0.3321(9)	0.6314(5)	0.3313(4)	0.0501(18)	0.318(13)
Si3	0.04435(8)	-0.04404(8)	0.85039(6)	0.0465(3)	1
Si4	0.22683(10)	0.10564(8)	0.84808(7)	0.0593(3)	1
O1	0.5314(2)	0.47506(19)	0.42522(15)	0.0603(7)	1
O2	-0.02440(18)	-0.02594(17)	0.92549(14)	0.0422(6)	1
O41	0.7662(8)	0.4270(8)	0.3647(11)	0.079(3)	0.733(8)
O41'	0.765(2)	0.435(2)	0.350(3)	0.078(6)	0.267(8)
O71	-0.2552(2)	-0.0716(2)	0.85721(19)	0.0649(8)	1
N21	0.3339(3)	0.6471(2)	0.4246(2)	0.0608(9)	1
N31	0.3377(3)	0.4954(3)	0.3485(2)	0.0709(11)	1
N51	0.1760(2)	-0.0145(2)	0.85543(19)	0.0486(8)	1
N61	0.1727(2)	0.1419(2)	0.92688(19)	0.0463(7)	1
C1	0.4743(4)	0.3240(3)	0.3545(3)	0.0723(13)	1
C2	0.5360(6)	0.5390(5)	0.2486(3)	0.119(2)	1
C20	0.3274(3)	0.7476(3)	0.4284(2)	0.0556(10)	1
C21	0.4176(3)	0.8067(3)	0.4191(3)	0.0614(11)	1
C22	0.4136(4)	0.9012(3)	0.4309(3)	0.0749(13)	1
C23	0.3238(4)	0.9410(3)	0.4509(3)	0.0718(13)	1
C24	0.2344(4)	0.8843(3)	0.4581(3)	0.0689(12)	1
C25	0.2338(3)	0.7896(3)	0.4473(3)	0.0595(11)	1
C26	0.5219(4)	0.7688(4)	0.3987(4)	0.0935(17)	1
C27	0.3213(5)	1.0438(4)	0.4652(4)	0.112(2)	1
C28	0.1310(4)	0.7343(4)	0.4587(4)	0.0836(15)	1
C30	0.2621(4)	0.4153(4)	0.3575(3)	0.0710(14)	1
C31	0.2198(4)	0.3608(4)	0.4357(3)	0.0673(12)	1
C32	0.1528(4)	0.2802(4)	0.4433(4)	0.0842(16)	1
C33	0.1254(4)	0.2518(5)	0.3764(5)	0.101(2)	1
C34	0.1627(5)	0.3102(6)	0.2983(5)	0.104(2)	1
C35	0.2310(4)	0.3918(5)	0.2865(3)	0.0888(17)	1
C36	0.2438(4)	0.3896(3)	0.5112(3)	0.0670(12)	1

Atom	x	y	z	[U(iso) (Å^2)]	Occ
C37	0.0569(5)	0.1606(6)	0.3859(6)	0.144(3)	1
C38	0.2712(6)	0.4519(5)	0.1998(4)	0.123(3)	1
C3A	0.1317(8)	0.5963(7)	0.3400(6)	0.086(3)	0.682(13)
C3B	0.4155(19)	0.7184(12)	0.2435(10)	0.081(6)	0.318(13)
C41	0.7674(8)	0.3468(6)	0.3259(6)	0.101(3)	0.733(8)
C41'	0.841(2)	0.3607(18)	0.338(2)	0.123(6)	0.267(8)
C42	0.8526(8)	0.3597(7)	0.2720(7)	0.125(3)	0.733(8)
C42'	0.930(2)	0.3997(18)	0.376(3)	0.184(10)	0.267(8)
C43	0.9193(7)	0.4492(8)	0.2872(6)	0.124(3)	0.733(8)
C43'	0.9232(14)	0.5285(15)	0.3386(13)	0.094(5)	0.267(8)
C44	0.8384(9)	0.5066(8)	0.3172(10)	0.108(4)	0.733(8)
C44'	0.8130(17)	0.5358(17)	0.315(2)	0.080(6)	0.267(8)
C4A	0.3119(11)	0.7116(6)	0.2420(4)	0.101(5)	0.682(13)
C4B	0.1967(15)	0.6541(17)	0.2899(14)	0.089(8)	0.318(13)
C5	-0.0108(4)	0.0374(4)	0.7486(3)	0.0714(13)	1
C50	0.2493(3)	-0.0972(3)	0.8689(3)	0.0519(10)	1
C51	0.2836(3)	-0.1505(3)	0.9498(2)	0.0495(9)	1
C52	0.3480(3)	-0.2353(3)	0.9626(3)	0.0618(11)	1
C53	0.3808(3)	-0.2677(3)	0.8981(3)	0.0665(12)	1
C54	0.3509(3)	-0.2118(4)	0.8180(3)	0.0678(13)	1
C55	0.2864(3)	-0.1269(3)	0.8013(3)	0.0623(11)	1
C56	0.2547(3)	-0.1151(3)	1.0223(3)	0.0577(10)	1
C57	0.4469(4)	-0.3626(4)	0.9133(4)	0.0917(17)	1
C58	0.2563(4)	-0.0684(4)	0.7128(3)	0.0870(16)	1
C6	0.0366(3)	-0.1809(3)	0.8589(3)	0.0614(11)	1
C60	0.1763(3)	0.2428(3)	0.9286(2)	0.0469(9)	1
C61	0.0848(3)	0.3030(3)	0.9142(3)	0.0533(10)	1
C62	0.0839(3)	0.3981(3)	0.9244(3)	0.0629(11)	1
C63	0.1705(4)	0.4389(3)	0.9474(3)	0.0648(12)	1
C64	0.2594(3)	0.3809(3)	0.9596(3)	0.0629(11)	1

Atom	x	y	z	[U(iso) (Å^2)]	Occ
C65	0.2647(3)	0.2853(3)	0.9513(3)	0.0522(10)	1
C66	-0.0152(3)	0.2642(3)	0.8903(3)	0.0669(12)	1
C67	0.1670(4)	0.5425(4)	0.9596(4)	0.0906(16)	1
C68	0.3676(3)	0.2306(3)	0.9663(3)	0.0684(12)	1
C7	0.1991(5)	0.2032(4)	0.7442(3)	0.0989(18)	1
C71	-0.2555(4)	-0.1521(4)	0.8222(3)	0.0756(13)	1
C72	-0.3518(4)	-0.1484(5)	0.7788(4)	0.111(2)	1
C73	-0.4107(5)	-0.0596(6)	0.7886(5)	0.126(2)	1
C74	-0.3321(6)	0.0030(4)	0.8130(4)	0.118(2)	1
C8	0.3713(4)	0.0894(4)	0.8429(4)	0.0885(17)	1
Li1	0.4738(6)	0.5831(5)	0.4553(4)	0.0650(19)	1
Li2	0.6696(7)	0.4278(6)	0.4488(5)	0.075(2)	1
Li3	-0.1662(5)	-0.0694(5)	0.9462(4)	0.0542(16)	1
Li4	0.0306(5)	0.0806(5)	0.9553(4)	0.0480(14)	1
H1A	0.5466	0.3005	0.359	0.087	1
H1B	0.4441	0.3167	0.3041	0.087	1
H1C	0.4343	0.2831	0.4041	0.087	1
H22	0.476	0.9392	0.4248	0.09	1
H24	0.1706	0.9111	0.4709	0.083	1
H26A	0.5692	0.8265	0.3753	0.112	1
H26B	0.5129	0.7339	0.3577	0.112	1
H26C	0.5512	0.7213	0.45	0.112	1
H27A	0.3915	1.0729	0.4569	0.134	1
H27B	0.2967	1.0343	0.5226	0.134	1
H27C	0.2743	1.0901	0.4253	0.134	1
H28A	0.0879	0.7517	0.5005	0.1	1
H28B	0.1433	0.6608	0.4779	0.1	1
H28C	0.095	0.7546	0.4052	0.1	1
H2A	0.5514	0.6063	0.2519	0.142	1
H2B	0.4905	0.5464	0.2013	0.142	1

Atom	x	y	z	[U(iso) (Å^2)]	Occ
H2C	0.601	0.506	0.2405	0.142	1
H32	0.1249	0.2432	0.4972	0.101	1
H34	0.1413	0.2945	0.2507	0.124	1
H36A	0.3186	0.4023	0.5119	0.08	1
H36B	0.2235	0.334	0.5622	0.08	1
H36C	0.2052	0.4512	0.509	0.08	1
H37A	0.026	0.1363	0.4426	0.173	1
H37B	0.0988	0.1062	0.3765	0.173	1
H37C	0.0015	0.1802	0.3447	0.173	1
H38A	0.2335	0.4319	0.1581	0.148	1
H38B	0.3455	0.4382	0.1953	0.148	1
H38C	0.2608	0.5246	0.1898	0.148	1
H3A1	0.1047	0.5516	0.3942	0.103	0.682(13)
H3A2	0.117	0.5664	0.2965	0.103	0.682(13)
H3A3	0.0982	0.663	0.3261	0.103	0.682(13)
H3B1	0.3991	0.7893	0.2368	0.097	0.318(13)
H3B2	0.4015	0.7056	0.1911	0.097	0.318(13)
H3B3	0.489	0.7053	0.257	0.097	0.318(13)
H41A	0.7708	0.2792	0.37	0.121	0.733(8)
H41B	0.7027	0.3501	0.2945	0.121	0.733(8)
H41C	0.854	0.3692	0.2777	0.148	0.267(8)
H41D	0.8221	0.2894	0.3694	0.148	0.267(8)
H42A	0.8305	0.3795	0.2131	0.15	0.733(8)
H42B	0.8938	0.2962	0.2854	0.15	0.733(8)
H42C	0.9974	0.3761	0.3602	0.221	0.267(8)
H42D	0.9227	0.3747	0.438	0.221	0.267(8)
H43A	0.9729	0.4212	0.3299	0.148	0.733(8)
H43B	0.9534	0.4926	0.2345	0.148	0.733(8)
H43C	0.9363	0.5594	0.3823	0.113	0.267(8)
H43D	0.9707	0.5584	0.2898	0.113	0.267(8)

Atom	x	y	z	[U(iso) (Å^2)]	Occ
H44A	0.8688	0.5417	0.3534	0.13	0.733(8)
H44B	0.8037	0.5573	0.2697	0.13	0.733(8)
H44C	0.7762	0.585	0.3361	0.096	0.267(8)
H44D	0.808	0.5599	0.2528	0.096	0.267(8)
H4A1	0.269	0.7723	0.2341	0.121	0.682(13)
H4A2	0.3002	0.685	0.1961	0.121	0.682(13)
H4A3	0.3854	0.7294	0.2421	0.121	0.682(13)
H4B1	0.1487	0.6064	0.3294	0.107	0.318(13)
H4B2	0.1949	0.6438	0.2354	0.107	0.318(13)
H4B3	0.1757	0.724	0.2834	0.107	0.318(13)
H52	0.3698	-0.2716	1.0178	0.074	1
H54	0.3754	-0.2319	0.7725	0.081	1
H56A	0.2981	-0.0569	1.0202	0.069	1
H56B	0.2658	-0.1705	1.0751	0.069	1
H56C	0.1813	-0.095	1.0187	0.069	1
H57A	0.4116	-0.4103	0.8915	0.11	1
H57B	0.4572	-0.3947	0.9736	0.11	1
H57C	0.5145	-0.344	0.8845	0.11	1
H58A	0.2994	-0.0906	0.6736	0.104	1
H58B	0.2671	0.0044	0.7019	0.104	1
H58C	0.1829	-0.0809	0.7054	0.104	1
H5A	-0.0807	0.0134	0.7428	0.086	1
H5B	0.034	0.0334	0.7022	0.086	1
H5C	-0.0145	0.108	0.7474	0.086	1
H62	0.0211	0.4361	0.9152	0.076	1
H64	0.3207	0.4078	0.9746	0.075	1
H66A	-0.049	0.2169	0.9405	0.08	1
H66B	0.0004	0.2291	0.85	0.08	1
H66C	-0.0618	0.3216	0.8648	0.08	1
H67A	0.1993	0.5375	1.0128	0.109	1

Atom	x	y	z	[U(iso) (Å^2)]	Occ
H67B	0.0945	0.5643	0.9606	0.109	1
H67C	0.2049	0.5923	0.9133	0.109	1
H68A	0.4079	0.2485	0.9135	0.082	1
H68B	0.3556	0.157	0.9876	0.082	1
H68C	0.4063	0.2506	1.0075	0.082	1
H6A	0.0735	-0.2225	0.9087	0.074	1
H6B	0.0687	-0.1901	0.8088	0.074	1
H6C	-0.0364	-0.2019	0.8636	0.074	1
H71A	-0.249	-0.2186	0.8674	0.091	1
H71B	-0.1958	-0.1443	0.7826	0.091	1
H72A	-0.3916	-0.2122	0.8041	0.133	1
H72B	-0.338	-0.1386	0.7188	0.133	1
H73A	-0.4432	-0.0196	0.7352	0.151	1
H73B	-0.4658	-0.083	0.8325	0.151	1
H74A	-0.3007	0.0545	0.763	0.141	1
H74B	-0.3637	0.0376	0.8501	0.141	1
H7A	0.125	0.2206	0.7416	0.119	1
H7B	0.2173	0.1758	0.6993	0.119	1
H7C	0.2405	0.2643	0.7371	0.119	1
H8A	0.405	0.1561	0.8274	0.106	1
H8B	0.3888	0.0576	0.8007	0.106	1
H8C	0.3956	0.0462	0.8977	0.106	1

Table A.9 Fractional atomic coordinates and equivalent isotropic thermal parameters [U(iso) (Å^2)] for **4c**.

Atom	x	y	z	[U(iso) (Å^2)]	Occ
Si21	0.35984(9)	0.54692(13)	0.29952(11)	0.0468(5)	1
Si41	0.36410(8)	0.75564(13)	0.20932(12)	0.0478(5)	1
O11	0.3626(2)	0.6998(3)	0.1333(3)	0.0552(12)	1

Atom	x	y	z	[U(iso) (Å^2)]	Occ
O51A	0.3620(7)	0.4709(12)	0.0528(8)	0.091(2)	0.5
O51B	0.3768(7)	0.4601(13)	0.0474(8)	0.091(2)	0.5
O61A	0.2771(9)	0.7203(16)	-0.0221(10)	0.115(3)	0.5
O61B	0.3009(9)	0.7218(16)	-0.0257(10)	0.115(3)	0.5
O71A	0.3892(7)	0.8898(11)	0.0083(8)	0.107(3)	0.5
O71B	0.3618(7)	0.9236(12)	0.0322(8)	0.107(3)	0.5
N11	0.3414(3)	0.4789(4)	0.2256(3)	0.0488(12)	1
N31	0.3975(2)	0.6705(3)	0.2745(3)	0.0401(11)	1
C11	0.3074(3)	0.3795(5)	0.2212(4)	0.0540(15)	1
C110	0.1910(4)	0.4735(7)	0.2059(5)	0.081(2)	1
C111	0.1687(8)	0.5006(14)	0.1308(9)	0.158(6)	1
C112	0.1273(5)	0.4687(9)	0.2523(7)	0.111(4)	1
C12	0.3451(4)	0.2802(5)	0.2227(5)	0.072(2)	1
C13	0.3093(5)	0.1826(6)	0.2127(7)	0.100(3)	1
C14	0.2412(6)	0.1782(7)	0.1991(7)	0.119(4)	1
C15	0.2048(5)	0.2709(7)	0.1995(6)	0.097(3)	1
C16	0.2348(3)	0.3719(6)	0.2096(5)	0.0672(19)	1
C17	0.4225(5)	0.2790(6)	0.2300(5)	0.081(2)	1
C18	0.4475(7)	0.2060(8)	0.2914(8)	0.120(4)	1
C19	0.4575(6)	0.2449(9)	0.1629(7)	0.102(3)	1
C21	0.2818(4)	0.5691(6)	0.3571(5)	0.077(2)	1
C22	0.4204(5)	0.4810(6)	0.3625(4)	0.070(2)	1
C31	0.4599(3)	0.7060(4)	0.3095(4)	0.0485(15)	1
C310	0.3888(6)	0.7975(7)	0.4062(5)	0.085(3)	1
C311	0.3752(8)	0.9206(8)	0.4079(8)	0.129(5)	1
C312	0.3864(8)	0.7519(11)	0.4816(5)	0.125(5)	1
C32	0.5243(3)	0.6803(6)	0.2820(4)	0.0604(18)	1
C33	0.5831(5)	0.7242(9)	0.3140(6)	0.099(3)	1
C34	0.5788(7)	0.7870(12)	0.3725(9)	0.131(5)	1
C35	0.5167(7)	0.8095(8)	0.4015(6)	0.098(3)	1

Atom	x	y	z	[U(iso) (Å^2)]	Occ
C36	0.4561(4)	0.7715(6)	0.3714(4)	0.0661(19)	1
C37	0.5332(4)	0.6115(8)	0.2182(5)	0.085(2)	1
C38	0.5669(8)	0.6777(11)	0.1599(7)	0.135(5)	1
C39	0.5789(5)	0.5116(9)	0.2321(7)	0.114(4)	1
C41	0.2744(4)	0.7962(7)	0.2343(5)	0.082(2)	1
C42	0.4172(4)	0.8819(5)	0.2083(5)	0.0695(19)	1
C51A	0.4157(8)	0.4888(15)	0.0012(8)	0.086(4)	0.5
C51B	0.4404(7)	0.4548(16)	0.0071(9)	0.086(4)	0.5
C52A	0.4769(10)	0.548(3)	0.0334(15)	0.161(8)	0.5
C52B	0.5005(9)	0.498(3)	0.0507(16)	0.161(8)	0.5
C53A	0.3283(10)	0.3670(13)	0.0389(9)	0.109(5)	0.5
C53B	0.3197(7)	0.4205(15)	0.0040(10)	0.109(5)	0.5
C54A	0.2963(17)	0.370(2)	-0.0349(12)	0.163(9)	0.5
C54B	0.3098(16)	0.2989(15)	0.0163(18)	0.163(9)	0.5
C61A	0.2048(12)	0.710(2)	-0.0012(17)	0.183(11)	0.5
C61B	0.2362(13)	0.663(3)	-0.021(2)	0.183(11)	0.5
C62A	0.1698(18)	0.821(3)	-0.0064(14)	0.29(2)	0.5
C62B	0.1816(15)	0.717(4)	-0.068(3)	0.29(2)	0.5
C63A	0.2808(14)	0.713(3)	-0.0989(10)	0.158(9)	0.5
C63B	0.3106(15)	0.766(2)	-0.0958(13)	0.158(9)	0.5
C64A	0.352(2)	0.671(5)	-0.121(2)	0.255(18)	0.5
C64B	0.3739(19)	0.714(4)	-0.1306(17)	0.255(18)	0.5
C71A	0.3558(11)	0.9960(15)	0.0023(15)	0.142(8)	0.5
C71B	0.3159(9)	1.0168(14)	0.038(2)	0.142(8)	0.5
C72A	0.2899(12)	1.0001(18)	0.0460(14)	0.107(5)	0.5
C72B	0.2422(8)	0.9741(18)	0.0533(13)	0.107(5)	0.5
C73A	0.4636(7)	0.9037(19)	0.004(2)	0.139(7)	0.5
C73B	0.4318(8)	0.9606(18)	0.0182(18)	0.139(7)	0.5
C74A	0.4972(13)	0.796(3)	-0.017(3)	0.232(15)	0.5
C74B	0.4791(11)	0.863(3)	0.006(3)	0.232(15)	0.5

Atom	x	y	z	[U(iso) (Å^2)]	Occ
Li1	0.3603(7)	0.5493(9)	0.1382(7)	0.065(3)	1
Li2	0.3457(9)	0.7641(12)	0.0506(8)	0.086(4)	1
H110	0.22	0.5351	0.223	0.098	1
H11A	0.2093	0.5039	0.1004	0.19	1
H11B	0.1451	0.5709	0.1304	0.19	1
H11C	0.1372	0.4443	0.1136	0.19	1
H11D	0.1013	0.5363	0.2475	0.133	1
H11E	0.1413	0.4591	0.3013	0.133	1
H11F	0.0984	0.4075	0.2379	0.133	1
H13	0.3342	0.1165	0.2156	0.12	1
H14	0.2194	0.1109	0.1895	0.143	1
H15	0.1564	0.2671	0.1927	0.116	1
H17	0.4375	0.3548	0.2406	0.097	1
H18A	0.4979	0.2082	0.294	0.144	1
H18B	0.4323	0.1312	0.2833	0.144	1
H18C	0.4279	0.2324	0.3357	0.144	1
H19A	0.5076	0.245	0.1699	0.122	1
H19B	0.4455	0.2957	0.1254	0.122	1
H19C	0.4423	0.1718	0.15	0.122	1
H21A	0.2954	0.6089	0.3994	0.092	1
H21B	0.2623	0.4988	0.3705	0.092	1
H21C	0.2473	0.6111	0.3313	0.092	1
H22A	0.4271	0.5283	0.4033	0.084	1
H22B	0.4648	0.4686	0.3394	0.084	1
H22C	0.4012	0.4115	0.3779	0.084	1
H310	0.3511	0.7624	0.3786	0.101	1
H31A	0.3308	0.9346	0.4307	0.154	1
H31B	0.3742	0.9488	0.3598	0.154	1
H31C	0.4119	0.9567	0.4343	0.154	1
H31D	0.342	0.7697	0.5031	0.15	1

Atom	x	y	z	[U(iso) (Å^2)]	Occ
H31E	0.4237	0.7841	0.5094	0.15	1
H31F	0.3921	0.673	0.4802	0.15	1
H33	0.6271	0.7096	0.2943	0.118	1
H34	0.6196	0.8154	0.3931	0.157	1
H35	0.5146	0.8518	0.4431	0.118	1
H37	0.4869	0.5864	0.202	0.102	1
H38A	0.5725	0.6323	0.1181	0.162	1
H38B	0.6121	0.7033	0.1756	0.162	1
H38C	0.5377	0.7401	0.1485	0.162	1
H39A	0.583	0.4688	0.189	0.136	1
H39B	0.5581	0.4671	0.2691	0.136	1
H39C	0.6248	0.5355	0.2471	0.136	1
H41A	0.275	0.8303	0.2808	0.098	1
H41B	0.2449	0.7317	0.2356	0.098	1
H41C	0.2564	0.8476	0.1997	0.098	1
H42A	0.4174	0.9145	0.2552	0.083	1
H42B	0.3976	0.9335	0.1746	0.083	1
H42C	0.4645	0.8642	0.1945	0.083	1
H51A	0.3969	0.5321	-0.0382	0.103	0.5
H51B	0.4311	0.4182	-0.0178	0.103	0.5
H51C	0.4356	0.4985	-0.0362	0.103	0.5
H51D	0.4495	0.3788	-0.0067	0.103	0.5
H52A	0.5127	0.5581	-0.0023	0.193	0.5
H52B	0.4955	0.5052	0.0724	0.193	0.5
H52C	0.4619	0.619	0.0509	0.193	0.5
H52D	0.5421	0.5008	0.0216	0.193	0.5
H52E	0.5085	0.4495	0.0908	0.193	0.5
H52F	0.4896	0.5707	0.0679	0.193	0.5
H53A	0.292	0.3536	0.0744	0.131	0.5
H53B	0.3624	0.3075	0.0418	0.131	0.5

Atom	x	y	z	[U(iso) (Å^2)]	Occ
H53C	0.3298	0.434	-0.0462	0.131	0.5
H53D	0.2769	0.4597	0.0163	0.131	0.5
H54A	0.2688	0.3044	-0.0424	0.196	0.5
H54B	0.333	0.3738	-0.0701	0.196	0.5
H54C	0.2666	0.434	-0.0391	0.196	0.5
H54D	0.2768	0.2703	-0.0179	0.196	0.5
H54E	0.2923	0.2869	0.0639	0.196	0.5
H54F	0.3541	0.2617	0.0108	0.196	0.5
H61A	0.2019	0.6822	0.0476	0.219	0.5
H61B	0.1811	0.6572	-0.0323	0.219	0.5
H61C	0.2202	0.6616	0.0281	0.219	0.5
H61D	0.2432	0.5871	-0.0368	0.219	0.5
H62A	0.1203	0.8134	0.0021	0.349	0.5
H62B	0.1773	0.8514	-0.0534	0.349	0.5
H62C	0.1896	0.8701	0.0288	0.349	0.5
H62D	0.1408	0.6707	-0.0705	0.349	0.5
H62E	0.2004	0.7288	-0.1148	0.349	0.5
H62F	0.1687	0.7874	-0.0472	0.349	0.5
H63A	0.2728	0.7853	-0.1198	0.19	0.5
H63B	0.2446	0.6632	-0.1163	0.19	0.5
H63C	0.317	0.8456	-0.0928	0.19	0.5
H63D	0.2691	0.7517	-0.1246	0.19	0.5
H64A	0.3533	0.6614	-0.1719	0.306	0.5
H64B	0.3607	0.6008	-0.098	0.306	0.5
H64C	0.3874	0.7229	-0.1066	0.306	0.5
H64D	0.3809	0.7463	-0.1771	0.306	0.5
H64E	0.3665	0.636	-0.1354	0.306	0.5
H64F	0.4147	0.7273	-0.1015	0.306	0.5
H71A	0.3447	1.0105	-0.0476	0.17	0.5
H71B	0.3879	1.0531	0.0185	0.17	0.5

Atom	x	y	z	[U(iso) (Å^2)]	Occ
H71C	0.3161	1.0582	-0.0069	0.17	0.5
H71D	0.3314	1.0654	0.0758	0.17	0.5
H72A	0.2715	1.0742	0.0458	0.128	0.5
H72B	0.3001	0.9782	0.0943	0.128	0.5
H72C	0.2557	0.9506	0.0259	0.128	0.5
H72D	0.2103	1.0354	0.0566	0.128	0.5
H72E	0.2424	0.9342	0.0978	0.128	0.5
H72F	0.2275	0.9256	0.0154	0.128	0.5
H73A	0.4817	0.927	0.0504	0.167	0.5
H73B	0.475	0.9605	-0.0306	0.167	0.5
H73C	0.4489	1.0032	0.0587	0.167	0.5
H73D	0.432	1.0081	-0.0237	0.167	0.5
H74A	0.547	0.8059	-0.0225	0.278	0.5
H74B	0.4777	0.7715	-0.0622	0.278	0.5
H74C	0.4882	0.7409	0.0187	0.278	0.5
H74D	0.5258	0.8878	-0.0046	0.278	0.5
H74E	0.4617	0.8202	-0.0341	0.278	0.5
H74F	0.4798	0.8169	0.0478	0.278	0.5

Table A.10 Fractional atomic coordinates and equivalent isotropic thermal parameters [U(iso) (Å^2)] for **7**.

Atom	x	y	z	[U(iso) (Å^2)]	Occ
Cr1	0.49335(3)	0.082592(13)	0.317387(15)	0.02804(12)	1
Si1	0.72852(6)	0.05414(2)	0.42268(3)	0.03382(17)	1
Si2	0.74961(5)	0.04440(3)	0.28754(3)	0.03520(17)	1
O1	0.61741(13)	0.06943(6)	0.26297(7)	0.0324(4)	1
O2	0.34307(14)	0.10713(6)	0.35461(7)	0.0383(4)	1
N1	0.61107(17)	0.09322(7)	0.39770(8)	0.0332(4)	1
N2	0.74878(16)	0.01878(7)	0.35923(8)	0.0326(4)	1

Atom	x	y	z	[U(iso) (Å^2)]	Occ
C1	0.7128(3)	0.00773(10)	0.48322(11)	0.0502(7)	1
C2	0.8674(2)	0.09040(10)	0.45564(14)	0.0532(7)	1
C3	0.7816(3)	-0.00448(11)	0.23450(12)	0.0533(7)	1
C4	0.8720(2)	0.09128(11)	0.29287(14)	0.0549(8)	1
C5	0.2974(3)	0.08468(11)	0.40513(14)	0.0622(8)	1
C6	0.2338(4)	0.12437(15)	0.43415(18)	0.0841(11)	0.77(2)
C6A	0.2338(4)	0.12437(15)	0.43415(18)	0.0841(11)	0.23(2)
C7	0.1964(7)	0.1600(3)	0.3839(3)	0.0629(17)	0.77(2)
C7A	0.258(4)	0.1693(8)	0.4028(18)	0.091(10)	0.23(2)
C8	0.3018(2)	0.15695(10)	0.34730(13)	0.0496(7)	0.77(2)
C8A	0.3018(2)	0.15695(10)	0.34730(13)	0.0496(7)	0.23(2)
C11	0.5995(2)	0.13886(9)	0.42714(11)	0.0382(6)	1
C12	0.5741(3)	0.14236(10)	0.48707(12)	0.0496(7)	1
C13	0.5626(3)	0.18794(12)	0.51311(14)	0.0629(9)	1
C14	0.5761(3)	0.23100(11)	0.48379(15)	0.0587(8)	1
C15	0.5991(2)	0.22752(10)	0.42486(15)	0.0552(8)	1
C16	0.6103(2)	0.18327(9)	0.39612(13)	0.0451(6)	1
C21	0.7593(2)	-0.03346(8)	0.36593(10)	0.0333(5)	1
C22	0.8739(2)	-0.05538(9)	0.38310(12)	0.0420(6)	1
C23	0.8798(2)	-0.10553(10)	0.39254(13)	0.0500(7)	1
C24	0.7762(3)	-0.13530(9)	0.38409(13)	0.0480(7)	1
C25	0.6656(2)	-0.11274(9)	0.36573(12)	0.0431(6)	1
C26	0.6546(2)	-0.06263(9)	0.35702(10)	0.0341(5)	1
C121	0.5566(4)	0.09809(13)	0.52447(15)	0.0813(11)	1
C141	0.5675(3)	0.27983(12)	0.51450(19)	0.0877(13)	1
C161	0.6352(4)	0.18335(11)	0.33082(16)	0.0725(10)	1
C221	0.9891(2)	-0.02561(11)	0.39187(14)	0.0564(8)	1
C241	0.7846(3)	-0.18952(11)	0.39550(18)	0.0737(10)	1
C261	0.5303(2)	-0.04031(9)	0.33879(12)	0.0405(6)	1
H12A	0.5393	0.1082	0.5645	0.122	1

Atom	x	y	z	[U(iso) (Å^2)]	Occ
H12B	0.6308	0.0783	0.53	0.122	1
H12C	0.4883	0.0789	0.5033	0.122	1
H13A	0.5443	0.1892	0.5534	0.075	1
H14A	0.551	0.2748	0.5561	0.132	1
H14B	0.5014	0.2989	0.491	0.132	1
H14C	0.6445	0.2974	0.5163	0.132	1
H15A	0.6077	0.2566	0.4029	0.066	1
H16A	0.64	0.217	0.3168	0.109	1
H16B	0.5692	0.1664	0.3043	0.109	1
H16C	0.7125	0.1668	0.3293	0.109	1
H1A	0.6419	-0.0129	0.4693	0.075	1
H1B	0.7023	0.0244	0.521	0.075	1
H1C	0.7862	-0.0125	0.4908	0.075	1
H22A	1.0594	-0.047	0.4037	0.085	1
H22B	0.9864	-0.0015	0.4241	0.085	1
H22C	0.9964	-0.009	0.3536	0.085	1
H23A	0.9571	-0.1201	0.4052	0.06	1
H24A	0.7029	-0.2038	0.3872	0.111	1
H24B	0.8209	-0.1956	0.4382	0.111	1
H24C	0.8354	-0.2043	0.3685	0.111	1
H25A	0.5941	-0.1321	0.3587	0.052	1
H26A	0.4684	-0.0659	0.3347	0.061	1
H26B	0.5264	-0.0234	0.2997	0.061	1
H26C	0.5152	-0.0171	0.3702	0.061	1
H2A	0.8818	0.1156	0.4265	0.08	1
H2B	0.9381	0.0688	0.4637	0.08	1
H2C	0.8544	0.1057	0.4939	0.08	1
H3A	0.7179	-0.0293	0.2315	0.08	1
H3B	0.8607	-0.0193	0.2501	0.08	1
H3C	0.7832	0.0094	0.194	0.08	1

Atom	x	y	z	[U(iso) (Å^2)]	Occ
H4A	0.8559	0.1172	0.3207	0.082	1
H4B	0.8736	0.105	0.2523	0.082	1
H4C	0.9508	0.0762	0.3084	0.082	1
H5A	0.3652	0.0711	0.4349	0.075	1
H5B	0.24	0.0581	0.3904	0.075	1
H6A	0.1619	0.1115	0.4498	0.101	0.77(2)
H6AA	0.1452	0.1179	0.4288	0.101	0.23(2)
H6AB	0.2662	0.1267	0.4784	0.101	0.23(2)
H6B	0.2894	0.1397	0.4684	0.101	0.77(2)
H7A	0.1886	0.1931	0.4001	0.076	0.77(2)
H7AA	0.182	0.1887	0.3931	0.109	0.23(2)
H7AB	0.3191	0.1891	0.4295	0.109	0.23(2)
H7B	0.1182	0.1505	0.3585	0.076	0.77(2)
H8A	0.2733	0.1646	0.3037	0.059	0.77(2)
H8AA	0.3696	0.1787	0.3413	0.059	0.23(2)
H8AB	0.2359	0.16	0.3116	0.059	0.23(2)
H8B	0.3678	0.1798	0.3639	0.059	0.77(2)

Table A.11 Fractional atomic coordinates and equivalent isotropic thermal parameters [U(iso) (Å^2)] for **8**. The occupancies (Occ) for all atoms are 1.0.

Atom	x	y	z	[U(iso) (Å^2)]
Cr1	0.48671(7)	0.03071(4)	0.92637(3)	0.01633(19)
Si1	0.61747(12)	0.21462(6)	0.88307(6)	0.0163(3)
Si2	0.70897(12)	0.13695(6)	1.02917(6)	0.0165(3)
O1	0.5947(3)	0.05946(15)	1.02096(14)	0.0171(6)
N1	0.5595(3)	0.11440(18)	0.86646(17)	0.0157(7)
N2	0.6423(3)	0.22159(18)	0.97596(16)	0.0147(7)
C1	0.7825(4)	0.2347(2)	0.8495(2)	0.0247(10)
C2	0.4960(5)	0.2998(2)	0.8425(2)	0.0268(10)

Atom	x	y	z	[U(iso) ($Å^2$)]
C3	0.8700(4)	0.0968(3)	1.0021(2)	0.0288(11)
C4	0.7482(5)	0.1699(3)	1.1233(2)	0.0279(11)
C11	0.4986(4)	0.0628(2)	0.8103(2)	0.0169(9)
C12	0.5787(5)	0.0074(2)	0.7747(2)	0.0221(10)
C13	0.5128(5)	-0.0540(3)	0.7301(2)	0.0283(11)
C14	0.3683(5)	-0.0630(3)	0.7181(2)	0.0311(11)
C15	0.2901(5)	-0.0099(3)	0.7496(2)	0.0290(11)
C16	0.3502(4)	0.0539(2)	0.7959(2)	0.0216(10)
C21	0.6011(4)	0.2964(2)	1.0106(2)	0.0190(9)
C22	0.6968(4)	0.3609(2)	1.0317(2)	0.0195(9)
C23	0.6546(5)	0.4318(3)	1.0656(2)	0.0287(11)
C24	0.5223(5)	0.4386(3)	1.0791(3)	0.0350(12)
C25	0.4275(5)	0.3752(3)	1.0585(2)	0.0328(11)
C26	0.4636(5)	0.3033(2)	1.0238(2)	0.0233(10)
C121	0.7351(4)	0.0188(2)	0.7838(2)	0.0244(10)
C122	0.7699(5)	0.0644(3)	0.7185(3)	0.0418(13)
C123	0.8143(5)	-0.0640(3)	0.7942(3)	0.0487(15)
C161	0.2546(4)	0.1181(2)	0.8210(2)	0.0239(10)
C162	0.1467(5)	0.0778(3)	0.8600(3)	0.0368(12)
C163	0.1830(6)	0.1712(3)	0.7578(3)	0.0443(14)
C221	0.8443(4)	0.3587(2)	1.0173(2)	0.0247(10)
C222	0.8613(5)	0.4241(3)	0.9613(2)	0.0342(12)
C223	0.9524(5)	0.3724(3)	1.0851(3)	0.0351(12)
C261	0.3546(5)	0.2364(3)	1.0031(2)	0.0299(11)
C262	0.3301(6)	0.1863(3)	1.0684(3)	0.0484(14)
C263	0.2152(5)	0.2725(3)	0.9625(3)	0.0477(14)
H12A	0.7668	0.0549	0.8269	0.029
H12B	0.7186	0.1179	0.7117	0.063
H12C	0.7429	0.029	0.676	0.063
H12D	0.8706	0.0757	0.726	0.063

Atom	x	y	z	[U(iso) (Å^2)]
H12E	0.7919	-0.0934	0.8361	0.073
H12F	0.9151	-0.0528	0.8017	0.073
H12G	0.7873	-0.0994	0.7516	0.073
H13A	0.5669	-0.0912	0.707	0.034
H14A	0.3246	-0.1067	0.6876	0.037
H15A	0.1912	-0.0159	0.74	0.035
H16A	0.3141	0.1567	0.8555	0.029
H16B	0.1948	0.0437	0.9001	0.055
H16C	0.0837	0.0417	0.8267	0.055
H16D	0.0924	0.1222	0.8782	0.055
H16E	0.254	0.1962	0.7336	0.067
H16F	0.1286	0.2162	0.7751	0.067
H16G	0.1206	0.1353	0.724	0.067
H1A	0.8521	0.1919	0.8688	0.037
H1B	0.8183	0.2908	0.8649	0.037
H1C	0.7642	0.2319	0.7971	0.037
H22A	0.8608	0.3017	0.9978	0.03
H22B	0.7911	0.4143	0.918	0.051
H22C	0.9551	0.4195	0.9497	0.051
H22D	0.8485	0.4806	0.9799	0.051
H22E	0.9399	0.3299	1.1208	0.053
H22F	0.9404	0.4289	1.1042	0.053
H22G	1.0466	0.3674	1.074	0.053
H23A	0.7195	0.4762	1.0797	0.034
H24A	0.4957	0.4871	1.1028	0.042
H25A	0.3354	0.3804	1.0681	0.039
H26A	0.3907	0.1962	0.9702	0.036
H26B	0.2901	0.2235	1.1006	0.073
H26C	0.2321	0.3046	0.9208	0.072
H26D	0.4192	0.1635	1.0937	0.073

Atom	x	y	z	[U(iso) (Å^2)]
H26E	0.2652	0.1398	1.0528	0.073
H26F	0.1503	0.2261	0.9465	0.072
H26H	0.1744	0.3099	0.9943	0.072
H2A	0.406	0.2934	0.8581	0.04
H2B	0.4819	0.2959	0.7902	0.04
H2C	0.5364	0.355	0.8579	0.04
H3A	0.8489	0.0793	0.9518	0.043
H3B	0.9055	0.0484	1.0321	0.043
H3C	0.9408	0.1415	1.008	0.043
H4A	0.6628	0.1912	1.1376	0.042
H4B	0.8191	0.2145	1.1293	0.042
H4C	0.7837	0.1215	1.1534	0.042

Table A.12 Fractional atomic coordinates and equivalent isotropic thermal parameters [U(iso) (Å^2)] for **9**. The occupancies (Occ) for all atoms are 1.0.

Atom	x	y	z	[U(iso) (Å^2)]
Cr1	0.26096(15)	0.0369(2)	0.44697(13)	0.0584
Si1	0.3917(3)	0.0255(5)	0.3647(3)	0.099
Si2	0.3109(3)	-0.1916(4)	0.3848(2)	0.0588
Si3	0.2422(3)	0.2924(4)	0.5144(3)	0.0707
Si4	0.1401(3)	0.1021(4)	0.5232(2)	0.0645
O1	0.3434(6)	0.0762(8)	0.4079(5)	0.0835
O2	0.2676(5)	0.2017(8)	0.4714(5)	0.0637
O3	0.4085(9)	0.3384(11)	0.4282(8)	0.1235
N1	0.3689(7)	-0.1147(9)	0.3483(5)	0.0547
N2	0.2407(6)	-0.1161(9)	0.3988(5)	0.0432
N3	0.1806(6)	0.2277(10)	0.5518(6)	0.0569
N4	0.1958(7)	-0.0080(10)	0.5098(5)	0.0556
C1	0.4782(12)	0.0429(18)	0.3901(10)	0.177(11)

Atom	x	y	z	[U(iso) (Å^2)]
C2	0.3853(11)	0.1188(16)	0.2943(8)	0.144(9)
C3	0.2908(8)	-0.3199(12)	0.3396(7)	0.081(6)
C4	0.3514(9)	-0.2382(13)	0.4568(7)	0.095(7)
C5	0.2115(10)	0.4228(14)	0.4742(8)	0.112(8)
C6	0.3132(9)	0.3473(13)	0.5641(7)	0.094(7)
C7	0.0939(9)	0.1351(13)	0.4520(7)	0.090(7)
C8	0.0770(9)	0.0670(13)	0.5735(7)	0.090(7)
C9	0.4082(10)	-0.1666(13)	0.3040(8)	0.059(5)
C10	0.4701(10)	-0.2186(14)	0.3234(9)	0.076(6)
C11	0.5105(10)	-0.2578(13)	0.2800(9)	0.086(7)
C12	0.4864(10)	-0.2440(14)	0.2253(10)	0.079(6)
C13	0.4246(10)	-0.1974(14)	0.2068(9)	0.087(6)
C14	0.3836(9)	-0.1579(13)	0.2479(9)	0.065(6)
C15	0.5000(10)	-0.2376(15)	0.3819(8)	0.119(8)
C16	0.5343(10)	-0.2823(15)	0.1783(8)	0.130(8)
C17	0.3143(9)	-0.1131(14)	0.2283(8)	0.100(7)
C18	0.1776(9)	-0.1228(14)	0.3637(7)	0.053(5)
C19	0.1308(9)	-0.2156(13)	0.3673(7)	0.062(5)
C20	0.0664(10)	-0.2147(15)	0.3401(7)	0.075(6)
C21	0.0437(10)	-0.1301(15)	0.3035(8)	0.079(6)
C22	0.0879(9)	-0.0377(14)	0.2977(7)	0.070(6)
C23	0.1506(9)	-0.0329(14)	0.3270(7)	0.060(5)
C24	0.1493(8)	-0.3212(12)	0.4038(7)	0.082(6)
C25	-0.0273(10)	-0.1289(16)	0.2736(8)	0.132(9)
C26	0.1974(8)	0.0674(12)	0.3182(7)	0.074(6)
C27	0.1586(9)	0.2881(13)	0.6003(8)	0.051(5)
C28	0.1914(9)	0.2667(14)	0.6530(9)	0.072(6)
C29	0.1753(9)	0.3305(14)	0.7013(8)	0.080(6)
C30	0.1252(10)	0.4126(15)	0.6941(9)	0.076(6)
C31	0.0898(9)	0.4297(13)	0.6428(8)	0.069(6)

Atom	x	y	z	[U(iso) (Å^2)]
C32	0.1068(10)	0.3701(15)	0.5927(9)	0.076(6)
C33	0.2434(8)	0.1715(13)	0.6659(7)	0.089(6)
C34	0.1086(10)	0.4817(15)	0.7464(8)	0.117(8)
C35	0.0615(9)	0.3882(14)	0.5384(8)	0.095(7)
C36	0.2179(9)	-0.0928(14)	0.5519(8)	0.056(5)
C37	0.1751(9)	-0.1900(14)	0.5593(7)	0.065(5)
C38	0.2001(10)	-0.2771(14)	0.5959(7)	0.072(6)
C39	0.2642(10)	-0.2762(14)	0.6215(8)	0.073(6)
C40	0.3059(9)	-0.1842(13)	0.6146(7)	0.072(6)
C41	0.2843(9)	-0.0955(13)	0.5793(8)	0.056(5)
C42	0.1011(8)	-0.1996(13)	0.5318(7)	0.082(6)
C43	0.2906(10)	-0.3744(15)	0.6606(8)	0.121(8)
C44	0.3334(8)	0.0027(11)	0.5716(7)	0.067(6)
C45	0.4762(16)	0.345(2)	0.4582(13)	0.175(13)
C46	0.5160(13)	0.402(2)	0.4175(13)	0.173(12)
C47	0.4684(17)	0.432(2)	0.3719(13)	0.195(13)
C48	0.3980(15)	0.416(2)	0.3808(13)	0.171(12)
Li1	0.340(2)	0.216(3)	0.4381(17)	0.112(14)
Li2	0.1809(16)	-0.138(2)	0.4561(14)	0.074(10)
H11	0.5046	0.0212	0.3558	0.176(15)
H12	0.487	0.0123	0.4183	0.176(15)
H13	0.4865	0.1302	0.3884	0.176(15)
H21	0.4227	0.0845	0.2694	0.191(15)
H22	0.4056	0.191	0.3043	0.191(15)
H23	0.3473	0.1128	0.2776	0.191(15)
H31	0.257	-0.367	0.3568	0.117(15)
H32	0.3289	-0.3609	0.3354	0.117(15)
H33	0.268	-0.2968	0.3027	0.117(15)
H41	0.3178	-0.2746	0.4731	0.126(15)
H42	0.365	-0.1683	0.476	0.126(15)

Atom	x	y	z	[U(iso) (Å^2)]
H43	0.3876	-0.2798	0.448	0.126(15)
H51	0.1911	0.4717	0.4985	0.158(15)
H52	0.243	0.4487	0.4547	0.158(15)
H53	0.1706	0.3954	0.4458	0.158(15)
H61	0.2963	0.395	0.5911	0.135(15)
H62	0.3334	0.2789	0.5874	0.135(15)
H63	0.3455	0.3755	0.5446	0.135(15)
H71	0.0701	0.0654	0.4406	0.117(15)
H72	0.0583	0.1898	0.4597	0.117(15)
H73	0.124	0.1586	0.4319	0.117(15)
H81	0.0589	-0.0076	0.5627	0.118(15)
H82	0.1066	0.0493	0.611	0.118(15)
H83	0.0509	0.121	0.5759	0.118(15)
H111	0.5541	-0.2916	0.2964	0.10(2)
H131	0.4138	-0.1886	0.1672	0.11(2)
H151	0.5389	-0.282	0.3811	0.148(12)
H152	0.5023	-0.1722	0.3985	0.148(12)
H153	0.465	-0.2887	0.3983	0.148(12)
H161	0.5082	-0.267	0.1453	0.165(12)
H162	0.5744	-0.2398	0.1845	0.165(12)
H163	0.5433	-0.3614	0.184	0.165(12)
H171	0.3121	-0.1133	0.188	0.143(12)
H172	0.3142	-0.0384	0.2423	0.143(12)
H173	0.2852	-0.1613	0.2427	0.143(12)
H201	0.0379	-0.2744	0.3459	0.09(2)
H221	0.0721	0.0177	0.271	0.09(2)
H241	0.1106	-0.3698	0.398	0.113(12)
H242	0.1566	-0.2949	0.4404	0.113(12)
H243	0.1874	-0.3542	0.3901	0.113(12)
H251	-0.033	-0.0607	0.2511	0.168(12)

Atom	x	y	z	[U(iso) (Å^2)]
H252	-0.0595	-0.13	0.3003	0.168(12)
H253	-0.0323	-0.193	0.2494	0.168(12)
H261	0.1741	0.1194	0.2901	0.117(12)
H262	0.2079	0.0996	0.3517	0.117(12)
H263	0.2363	0.0382	0.3009	0.117(12)
H291	0.1987	0.319	0.7382	0.10(2)
H311	0.0521	0.4841	0.6427	0.08(2)
H331	0.2637	0.1799	0.7044	0.130(12)
H332	0.2828	0.1936	0.6426	0.130(12)
H333	0.226	0.1085	0.6555	0.130(12)
H341	0.0658	0.5334	0.7334	0.172(12)
H342	0.1411	0.5265	0.7601	0.172(12)
H343	0.0892	0.4334	0.7738	0.172(12)
H351	0.0301	0.4445	0.5442	0.122(12)
H352	0.0384	0.3173	0.5281	0.122(12)
H353	0.0903	0.4073	0.5108	0.122(12)
H381	0.1705	-0.3389	0.5994	0.09(2)
H401	0.3513	-0.1859	0.6316	0.07(2)
H421	0.0835	-0.2684	0.5427	0.115(12)
H422	0.0772	-0.1365	0.5418	0.115(12)
H423	0.1033	-0.2	0.4905	0.115(12)
H431	0.3389	-0.3578	0.6767	0.150(12)
H432	0.2649	-0.3813	0.6907	0.150(12)
H433	0.2924	-0.4407	0.639	0.150(12)
H441	0.3718	-0.006	0.5946	0.103(12)
H442	0.3103	0.0757	0.5808	0.103(12)
H443	0.338	0.0053	0.5324	0.103(12)
H451	0.4759	0.3894	0.4918	0.28(6)
H452	0.4936	0.2711	0.4678	0.28(6)
H461	0.5402	0.465	0.4349	0.29(6)

Atom	x	y	z	[U(iso) (Å^2)]
H462	0.5475	0.3493	0.4042	0.29(6)
H471	0.4761	0.5114	0.3672	0.31(6)
H472	0.479	0.3924	0.3388	0.31(6)
H481	0.3793	0.4882	0.3798	0.31(6)
H482	0.3786	0.3854	0.3383	0.31(6)

Table A.13 Fractional atomic coordinates and equivalent isotropic thermal parameters [U(iso) (Å^2)] for **10**.

Atom	x	y	z	[U(iso) (Å^2)]	Occ
Cr1	0.5	0.5	0	0.03820(19)	1
Cr2	0.64594(4)	0.44008(4)	0.16146(3)	0.03382(15)	1
Cr3	0.68179(4)	0.33941(4)	0.30526(3)	0.03396(14)	1
Cl1	0.56167(9)	0.36988(7)	0.00441(5)	0.0571(3)	1
Si1	0.71204(8)	0.67416(7)	0.17395(6)	0.0427(2)	1
Si2	0.81178(7)	0.60546(6)	0.34285(5)	0.0355(2)	1
Si3	0.68749(8)	0.11277(7)	0.28840(7)	0.0457(2)	1
Si4	0.68154(7)	0.22190(6)	0.13716(6)	0.0386(2)	1
O1	0.61797(18)	0.55828(16)	0.12059(13)	0.0384(5)	1
O2	0.68256(17)	0.32334(15)	0.18908(13)	0.0368(5)	1
N11	0.8218(2)	0.66034(18)	0.25452(16)	0.0366(6)	1
N21	0.6930(2)	0.48891(18)	0.29883(15)	0.0334(5)	1
N31	0.6573(2)	0.2029(2)	0.33151(19)	0.0413(6)	1
N41	0.7408(2)	0.16392(19)	0.21477(18)	0.0393(6)	1
C1	0.7607(4)	0.7406(3)	0.0964(3)	0.0663(11)	1
C11	0.9276(3)	0.7084(2)	0.2513(2)	0.0418(8)	1
C12	0.9975(3)	0.8125(3)	0.2897(2)	0.0485(8)	1
C13	1.0962(3)	0.8558(3)	0.2808(3)	0.0566(10)	1
C14	1.1296(3)	0.8004(3)	0.2357(3)	0.0610(10)	1
C15	1.0612(3)	0.6980(3)	0.1991(3)	0.0552(9)	1

Atom	x	y	z	[U(iso) (Å^2)]	Occ
C16	0.9615(3)	0.6510(3)	0.2052(2)	0.0473(8)	1
C17	0.9679(4)	0.8785(3)	0.3418(3)	0.0655(11)	1
C18	1.2377(4)	0.8493(4)	0.2263(4)	0.0861(15)	1
C19	0.8904(3)	0.5398(3)	0.1621(3)	0.0534(9)	1
C2	0.6496(4)	0.7423(3)	0.2213(3)	0.0689(12)	1
C21	0.6183(3)	0.4575(2)	0.3404(2)	0.0359(7)	1
C22	0.6536(3)	0.4344(2)	0.4241(2)	0.0412(7)	1
C23	0.5788(3)	0.3982(3)	0.4622(2)	0.0497(9)	1
C24	0.4715(3)	0.3844(3)	0.4221(2)	0.0497(9)	1
C25	0.4364(3)	0.4043(3)	0.3401(2)	0.0486(8)	1
C26	0.5044(3)	0.4380(2)	0.2971(2)	0.0427(8)	1
C27	0.7721(3)	0.4523(3)	0.4786(2)	0.0525(9)	1
C28	0.3942(4)	0.3476(3)	0.4673(3)	0.0636(11)	1
C29	0.4557(3)	0.4508(3)	0.2054(2)	0.0556(9)	1
C3	0.7976(3)	0.6882(3)	0.4248(2)	0.0558(9)	1
C31	0.5941(3)	0.1762(2)	0.3821(2)	0.0442(8)	1
C32	0.6445(3)	0.1810(3)	0.4727(3)	0.0548(9)	1
C33	0.5790(4)	0.1531(3)	0.5193(3)	0.0684(12)	1
C34	0.4651(4)	0.1215(3)	0.4793(4)	0.0703(13)	1
C35	0.4180(3)	0.1205(3)	0.3919(3)	0.0607(11)	1
C36	0.4788(3)	0.1477(2)	0.3427(3)	0.0505(9)	1
C37	0.7656(3)	0.2150(4)	0.5215(3)	0.0682(12)	1
C38	0.3991(5)	0.0938(4)	0.5352(4)	0.101(2)	1
C39	0.4212(3)	0.1466(3)	0.2478(3)	0.0575(10)	1
C4	0.9449(3)	0.5930(3)	0.3963(2)	0.0490(9)	1
C41	0.8435(2)	0.1610(2)	0.2226(2)	0.0361(7)	1
C42	0.9443(3)	0.2399(2)	0.2815(2)	0.0394(7)	1
C43	1.0417(3)	0.2323(3)	0.2914(2)	0.0465(8)	1
C44	1.0424(3)	0.1507(3)	0.2453(2)	0.0493(9)	1
C45	0.9427(3)	0.0749(3)	0.1870(2)	0.0499(9)	1

Atom	x	y	z	[U(iso) (Å^2)]	Occ
C46	0.8425(3)	0.0782(2)	0.1739(2)	0.0429(8)	1
C47	0.9468(3)	0.3306(3)	0.3316(2)	0.0506(9)	1
C48	1.1491(4)	0.1437(4)	0.2577(4)	0.0817(14)	1
C49	0.7360(3)	-0.0060(3)	0.1077(3)	0.0643(11)	1
C5	0.7923(3)	0.0771(3)	0.3671(3)	0.0639(11)	1
C51A	0.1266(6)	0.4562(5)	0.1114(4)	0.099(3)	0.673(11)
C51B	0.2970(11)	0.6039(10)	0.1986(11)	0.115(6)	0.327(11)
C52A	0.1369(7)	0.4481(6)	0.1963(5)	0.105(3)	0.673(11)
C52B	0.2569(14)	0.5676(14)	0.2625(8)	0.139(7)	0.327(11)
C53A	0.2251(8)	0.5228(7)	0.2689(4)	0.129(4)	0.673(11)
C53B	0.1584(16)	0.4753(14)	0.2363(10)	0.139(8)	0.327(11)
C54A	0.3030(7)	0.6057(6)	0.2566(5)	0.141(4)	0.673(11)
C54B	0.1001(11)	0.4192(12)	0.1462(12)	0.107(5)	0.327(11)
C55A	0.2928(7)	0.6138(6)	0.1718(6)	0.125(4)	0.673(11)
C55B	0.1402(13)	0.4554(14)	0.0824(8)	0.132(7)	0.327(11)
C56A	0.2045(7)	0.5391(7)	0.0992(5)	0.111(3)	0.673(11)
C56B	0.2386(14)	0.5478(14)	0.1086(9)	0.108(6)	0.327(11)
C57A	0.0522(8)	0.3862(8)	0.0429(6)	0.197(7)	0.673(11)
C57B	0.3803(14)	0.6942(12)	0.2365(17)	0.218(13)	0.327(11)
C6	0.5608(3)	-0.0118(3)	0.2337(4)	0.0701(12)	1
C7	0.5354(3)	0.1360(3)	0.0634(3)	0.0608(11)	1
C8	0.7645(3)	0.2601(3)	0.0721(2)	0.0523(9)	1
H13	1.1425	0.9263	0.3068	0.068	1
H15	1.0833	0.6582	0.1685	0.066	1
H17A	1.007	0.9505	0.3428	0.079	1
H17B	0.9895	0.8693	0.402	0.079	1
H17C	0.8882	0.8584	0.3141	0.079	1
H18A	1.2619	0.9236	0.2365	0.103	1
H18B	1.2268	0.8222	0.167	0.103	1
H18C	1.294	0.8337	0.2694	0.103	1

Atom	x	y	z	[U(iso) (Å^2)]	Occ
H19A	0.8239	0.5325	0.1121	0.064	1
H19B	0.8692	0.5041	0.2046	0.064	1
H19C	0.9314	0.5102	0.1416	0.064	1
H1A	0.7846	0.6989	0.0668	0.08	1
H1B	0.8227	0.8071	0.1288	0.08	1
H1C	0.7003	0.7509	0.0525	0.08	1
H23	0.6037	0.3827	0.518	0.06	1
H25	0.3617	0.3943	0.3115	0.058	1
H27A	0.8176	0.5257	0.5039	0.063	1
H27B	0.8004	0.4267	0.4411	0.063	1
H27C	0.7747	0.4161	0.526	0.063	1
H28A	0.3621	0.2728	0.4552	0.076	1
H28B	0.3351	0.3705	0.4449	0.076	1
H28C	0.4356	0.376	0.5308	0.076	1
H29A	0.4495	0.3954	0.1638	0.067	1
H29B	0.5034	0.5168	0.2004	0.067	1
H29C	0.3823	0.4484	0.1922	0.067	1
H2A	0.5936	0.7537	0.1737	0.083	1
H2B	0.7071	0.8083	0.26	0.083	1
H2C	0.6151	0.7008	0.2551	0.083	1
H33	0.6131	0.1557	0.58	0.082	1
H35	0.3406	0.1003	0.3641	0.073	1
H37A	0.7922	0.2633	0.5771	0.082	1
H37B	0.8031	0.2486	0.486	0.082	1
H37C	0.7812	0.1556	0.5335	0.082	1
H38A	0.412	0.1564	0.5725	0.122	1
H38B	0.4229	0.0501	0.5722	0.122	1
H38C	0.3203	0.057	0.4966	0.122	1
H39A	0.3419	0.1225	0.2315	0.069	1
H39B	0.4337	0.1008	0.2111	0.069	1

Atom	x	y	z	[U(iso) (Å^2)]	Occ
H39C	0.4506	0.2159	0.2389	0.069	1
H3A	0.8646	0.7524	0.4517	0.067	1
H3B	0.787	0.6524	0.4704	0.067	1
H3C	0.7339	0.7031	0.395	0.067	1
H43	1.11	0.2855	0.3314	0.056	1
H45	0.9421	0.0181	0.1543	0.06	1
H47A	1.0235	0.3774	0.3697	0.061	1
H47B	0.906	0.3083	0.3677	0.061	1
H47C	0.9127	0.3657	0.2905	0.061	1
H48A	1.1337	0.0844	0.2149	0.098	1
H48B	1.1845	0.1361	0.3173	0.098	1
H48C	1.1983	0.2061	0.249	0.098	1
H49A	0.6954	-0.0469	0.1384	0.077	1
H49B	0.7521	-0.0499	0.0724	0.077	1
H49C	0.6911	0.0239	0.0692	0.077	1
H4A	0.948	0.5426	0.3563	0.059	1
H4B	0.9494	0.5705	0.4507	0.059	1
H4C	1.0069	0.6594	0.4098	0.059	1
H52A	0.0838	0.3917	0.2046	0.126	0.673(11)
H52B	0.2956	0.6048	0.3221	0.166	0.327(11)
H53A	0.232	0.5172	0.3266	0.154	0.673(11)
H53B	0.1318	0.4513	0.2785	0.167	0.327(11)
H54A	0.3631	0.6566	0.306	0.169	0.673(11)
H54B	0.0348	0.358	0.1288	0.128	0.327(11)
H55A	0.3459	0.6703	0.1634	0.15	0.673(11)
H55B	0.1015	0.4182	0.0228	0.159	0.327(11)
H56A	0.1976	0.5447	0.0415	0.133	0.673(11)
H56B	0.2652	0.5718	0.0664	0.13	0.327(11)
H57A	0.0596	0.4072	-0.0096	0.237	0.673(11)
H57B	-0.0209	0.3756	0.0391	0.237	0.673(11)

Atom	x	y	z	[U(iso) (Å^2)]	Occ
H57C	0.0612	0.3224	0.0466	0.237	0.673(11)
H57D	0.4089	0.7203	0.1939	0.262	0.327(11)
H57E	0.4388	0.6882	0.2861	0.262	0.327(11)
H57F	0.3554	0.7415	0.2579	0.262	0.327(11)
H5A	0.8584	0.1393	0.4038	0.077	1
H5B	0.8119	0.0342	0.3342	0.077	1
H5C	0.7616	0.0392	0.4044	0.077	1
H6A	0.5226	-0.028	0.2723	0.084	1
H6B	0.5825	-0.0665	0.2222	0.084	1
H6C	0.5114	-0.0056	0.1781	0.084	1
H7A	0.4915	0.1209	0.0979	0.073	1
H7B	0.5316	0.0722	0.0353	0.073	1
H7C	0.5062	0.1698	0.0183	0.073	1
H8A	0.7333	0.2952	0.0292	0.063	1
H8B	0.7629	0.1991	0.0413	0.063	1
H8C	0.8409	0.3062	0.1115	0.063	1

Table A.14 Fractional atomic coordinates and equivalent isotropic thermal parameters [U(iso) (Å^2)] for **11**.

Atom	x	y	z	[U(iso) (Å^2)]	Occ
Cr1	0.74864(9)	0.52058(10)	0.62718(7)	0.0771	1
Si1	0.80890(19)	0.6767(2)	0.69679(17)	0.1053	1
Si2	0.65303(18)	0.6040(2)	0.71468(14)	0.0925	1
Si3	0.7180(2)	0.4641(2)	0.49740(13)	0.0932	1
Si4	0.7979(2)	0.3488(2)	0.58925(15)	0.1026	1
O11	0.7347(9)	0.6539(10)	0.7273(7)	0.100(6)	0.5
O12	0.7156(8)	0.6744(8)	0.7019(6)	0.071(4)	0.5
O21	0.7777(9)	0.3962(10)	0.5288(7)	0.091(5)	0.5
O22	0.7417(10)	0.3788(10)	0.5307(7)	0.095(6)	0.5

Atom	x	y	z	[U(iso) (Å^2)]	Occ
N1	0.8202(4)	0.6020(5)	0.6504(4)	0.0858	1
N2	0.6690(4)	0.5289(5)	0.6697(4)	0.0878	1
N3	0.7105(5)	0.5314(5)	0.5493(3)	0.0957	1
N4	0.7949(5)	0.4208(5)	0.6408(4)	0.0985	1
C1	0.8816(7)	0.6746(10)	0.7624(6)	0.2537	1
C2	0.8116(8)	0.7762(7)	0.6640(6)	0.2221	1
C3	0.6530(7)	0.5694(8)	0.7873(5)	0.1677	1
C4	0.5633(6)	0.6610(8)	0.6912(5)	0.1604	1
C5	0.7764(7)	0.4998(8)	0.4463(5)	0.1681	1
C6	0.6210(7)	0.4319(8)	0.4583(5)	0.1632	1
C7	0.8957(7)	0.3176(9)	0.5837(6)	0.2041	1
C8	0.7414(9)	0.2624(8)	0.6026(6)	0.1971	1
C11	0.907(2)	0.586(2)	0.6440(12)	0.122(2)	0.5
C12	0.8745(15)	0.6218(15)	0.6088(16)	0.116(2)	0.5
C13	0.912(3)	0.597(3)	0.5862(13)	0.204(2)	0.5
C14	0.944(2)	0.578(2)	0.620(2)	0.207(2)	0.5
C15	1.0020(7)	0.5873(8)	0.5785(5)	0.160(2)	1
C21	0.6238(16)	0.4506(19)	0.6787(13)	0.125(2)	0.5
C22	0.5886(19)	0.4867(16)	0.6458(15)	0.145(2)	0.5
C23	0.5617(16)	0.434(2)	0.6296(13)	0.147(2)	0.5
C24	0.587(2)	0.4152(19)	0.6792(18)	0.170(2)	0.5
C25	0.5226(17)	0.3544(17)	0.6272(12)	0.146(2)	0.5
C26	0.5025(16)	0.3761(18)	0.6539(11)	0.132(2)	0.5
C31	0.6353(19)	0.5884(16)	0.5361(13)	0.139(2)	0.5
C32	0.7025(14)	0.6183(17)	0.5265(11)	0.113(2)	0.5
C33	0.669(2)	0.6698(19)	0.5350(15)	0.160(2)	0.5
C34	0.6232(17)	0.6432(19)	0.5339(14)	0.136(2)	0.5
C35	0.5873(14)	0.7188(18)	0.5089(11)	0.128(2)	0.5
C36	0.6134(17)	0.7396(16)	0.5320(11)	0.134(2)	0.5
C41	0.861(2)	0.412(2)	0.6918(13)	0.154(2)	0.5

Atom	x	y	z	[U(iso) (Å^2)]	Occ
C42	0.8039(17)	0.3835(18)	0.7045(13)	0.132(2)	0.5
C43	0.822(2)	0.407(2)	0.7400(12)	0.148(2)	0.5
C44	0.8779(19)	0.4144(19)	0.7364(14)	0.148(2)	0.5
C45	0.8849(8)	0.3955(9)	0.8002(6)	0.191(2)	1
H11	0.8803	0.6244	0.7823	0.240(13)	1
H12	0.8707	0.7176	0.7871	0.240(13)	1
H13	0.9323	0.6822	0.7522	0.240(13)	1
H21	0.7735	0.7776	0.6294	0.205(13)	1
H22	0.8012	0.8187	0.6892	0.205(13)	1
H23	0.8627	0.7832	0.6544	0.205(13)	1
H31	0.6998	0.5395	0.8005	0.191(13)	1
H32	0.6496	0.6138	0.8128	0.191(13)	1
H33	0.6085	0.5352	0.7868	0.191(13)	1
H41	0.5629	0.6816	0.653	0.170(13)	1
H42	0.5604	0.7048	0.7173	0.170(13)	1
H43	0.5193	0.6262	0.6912	0.170(13)	1
H51	0.8275	0.5153	0.4653	0.208(13)	1
H52	0.7496	0.546	0.4284	0.208(13)	1
H53	0.7812	0.4602	0.4174	0.208(13)	1
H61	0.5901	0.4095	0.4847	0.180(13)	1
H62	0.5954	0.4787	0.4404	0.180(13)	1
H63	0.627	0.3929	0.4294	0.180(13)	1
H71	0.9275	0.3624	0.5768	0.221(13)	1
H72	0.9179	0.2919	0.6192	0.221(13)	1
H73	0.8932	0.2799	0.5526	0.221(13)	1
H81	0.6899	0.2815	0.6051	0.272(13)	1
H82	0.7632	0.2366	0.6381	0.272(13)	1
H83	0.7385	0.2246	0.5715	0.272(13)	1
H111	0.9246	0.6402	0.6513	0.141(11)	0.5
H112	0.9389	0.5506	0.6706	0.141(11)	0.5

Atom	x	y	z	[U(iso) (Å^2)]	Occ
H121	0.8944	0.6757	0.6121	0.141(11)	0.5
H122	0.8491	0.6123	0.57	0.141(11)	0.5
H131	0.8827	0.634	0.56	0.141(11)	0.5
H132	0.8926	0.5437	0.5784	0.141(11)	0.5
H141	0.9651	0.586	0.6599	0.141(11)	0.5
H142	0.9243	0.5246	0.6142	0.141(11)	0.5
H151	0.9754	0.581	0.5396	0.141(11)	0.5
H152	1.0163	0.6425	0.5853	0.141(11)	0.5
H153	1.0481	0.5546	0.5843	0.141(11)	0.5
H154	1.0026	0.5724	0.5391	0.141(11)	0.5
H155	1.0231	0.6403	0.5852	0.141(11)	0.5
H156	1.033	0.55	0.6036	0.141(11)	0.5
H211	0.5931	0.4694	0.7063	0.141(11)	0.5
H212	0.6525	0.4038	0.6935	0.141(11)	0.5
H221	0.5471	0.5119	0.6614	0.141(11)	0.5
H222	0.5755	0.485	0.6045	0.141(11)	0.5
H231	0.5259	0.4781	0.621	0.141(11)	0.5
H232	0.5955	0.4319	0.6012	0.141(11)	0.5
H241	0.6081	0.4196	0.7195	0.141(11)	0.5
H242	0.6243	0.3878	0.6599	0.141(11)	0.5
H251	0.4929	0.3492	0.5892	0.141(11)	0.5
H252	0.4877	0.3557	0.6549	0.141(11)	0.5
H253	0.5573	0.3094	0.6351	0.141(11)	0.5
H261	0.5052	0.3222	0.6686	0.141(11)	0.5
H262	0.4676	0.407	0.6728	0.141(11)	0.5
H263	0.4837	0.3752	0.6132	0.141(11)	0.5
H311	0.6015	0.5838	0.5644	0.141(11)	0.5
H312	0.6061	0.5776	0.4986	0.141(11)	0.5
H321	0.7407	0.6547	0.5462	0.141(11)	0.5
H322	0.7045	0.6194	0.486	0.141(11)	0.5

Atom	x	y	z	[U(iso) (Å^2)]	Occ
H331	0.6906	0.6855	0.5737	0.141(11)	0.5
H332	0.7096	0.6725	0.5115	0.141(11)	0.5
H341	0.6153	0.6255	0.5713	0.141(11)	0.5
H342	0.5822	0.6226	0.5052	0.141(11)	0.5
H351	0.6026	0.7741	0.5076	0.141(11)	0.5
H352	0.5479	0.7137	0.5329	0.141(11)	0.5
H353	0.5669	0.7007	0.4707	0.141(11)	0.5
H361	0.5672	0.7671	0.5387	0.141(11)	0.5
H362	0.6568	0.7557	0.5604	0.141(11)	0.5
H363	0.6237	0.7527	0.4942	0.141(11)	0.5
H411	0.8919	0.4603	0.6986	0.141(11)	0.5
H412	0.8948	0.3683	0.6851	0.141(11)	0.5
H421	0.7584	0.3978	0.7206	0.141(11)	0.5
H422	0.8116	0.3265	0.7073	0.141(11)	0.5
H431	0.7823	0.4469	0.7391	0.141(11)	0.5
H432	0.7989	0.3549	0.7343	0.141(11)	0.5
H441	0.8692	0.4713	0.7364	0.141(11)	0.5
H442	0.9229	0.4031	0.719	0.141(11)	0.5
H451	0.9249	0.3557	0.8	0.141(11)	0.5
H452	0.9083	0.4478	0.8048	0.141(11)	0.5
H453	0.8572	0.3851	0.8315	0.141(11)	0.5
H454	0.9291	0.4193	0.8241	0.141(11)	0.5
H455	0.8385	0.4067	0.816	0.141(11)	0.5
H456	0.8923	0.3385	0.7986	0.141(11)	0.5

REFERENCES

(1) Lappert, M. F.; Power, P. P.; Sanger, A. R.; Srivastava, R. C. *Metal and Metalloid Amides: Syntheses, Structures, and Physical and Chemical Properties*; E. Horwood; Halsted Press: Chichester, New York, 1980.

(2) Kempe, R. *Angew. Chem., Int. Ed. Engl.* **2000**, *39*, 468.

(3) Muragavel, R.; Voigt, A.; Walawalkar, M. G.; Roesky, H. W. *Chem. Rev.* **1996**, *96*, 2205.

(4) King, L.; Sullivan, A. C. *Coord. Chem. Rev.* **1999**, *189*, 19.

(5) Lorenz, V.; Fischer, A.; Giessmann, S.; Gilje, J. W.; Gun'ko, Y.; Jacob, K.; Edelmann, F. T. *Coord. Chem. Rev.* **2000**, *206-207*, 321.

(6) Bradley, D. C.; Mehrotra, R. C.; Rothwell, I. P.; Singh, A. *Alkoxo and Aryloxo Derivatives of Metals*; Academic Press: London, 2001.

(7) Chisholm, M. H. *Chemtracts: Inorg. Chem.* **1992**, *4(s)*, 273.

(8) Elias, A. J.; Roesky, H. W.; Robinson, W. T.; Sheldrick, G. M. *J. Chem. Soc. Dalton. Trans* **1993**, 495.

(9) Pearson, R. G. *J. Am. Chem. Soc.* **1963**, *85*, 3533.

(10) Pearson, R. G. *J. Chem. Educ.* **1968**, *45*, 581.

(11) Black, D. S. C.; Hartshorn, A. J. *Coord. Chem. Rev.* **1972**, *9*, 219.

(12) Bradley, D. C.; Chisholm, M. H. *Acc. Chem. Res.* **1976**, *9*, 273.

(13) Bourget-Merle, L.; Lappert, M. F.; Severn, J. R. *Chem. Rev.* **2002**, *102*, 3031.

(14) Gade, L. H. *Chem. Commun.* **2000**, 173.

(15) Gade, L. H.; Mountford, P. *Coord. Chem. Rev.* **2001**, *216-217*, 65.

(16) Britovsek, G. J. P.; Gibson, V. C.; Wass, D. F. *Angew. Chem., Int. Ed.* **1999**, *38*, 428.

(17) Gibson, V. C.; Spitzmesser, S. K. *Chem. Rev.* **2003**, *103*, 283.

(18) Lee, C. H.; La, Y.-H.; Park, J. W. *Organometallics* **2000**, *19*, 344.

(19) Lorber, C.; Donnadieu, B.; Choukroun, R. *Organometallics* **2000**, *19*, 1963.

(20) Schrock, R. R.; Casado, A. L.; Goodman, J. T.; Liang, L.-C.; Bonitatebus, P. J.; Davis, W. M. *Organometallics* **2000**, *19*, 5325.

(21) Cummins, C. C. *Chem. Commun.* **1998**, 1777.

(22) Clough, C. R.; Greco, J. B.; Figueroa, J. S.; Diaconescu, P. L.; Davis, M. W.; Cummins, C. C. *J. Am. Chem. Soc.* **2004**, *126*, 7742.

(23) Ritleng, V.; Yandulov, D. V.; Weare, W. W.; Schrock, R. R.; Hock, S. S.; Davis, W. M. *J. Am. Chem. Soc.* **2004**, *126*, 6150.

(24) van der Linden, A.; Schaverien, C. J.; Meijboom, N.; Ganter, C.; Orpen, A. G. *J. Am. Chem. Soc.* **1995**, *117*, 3008.

(25) Fokken, S.; Spaniol, T. P.; Kang, H.-C.; Massa, W.; Okuda, J. *Organometallics* **1996**, *15*, 5069.

(26) Fryzuk, M. D.; Johnson, S. A.; Patrick, B. O.; Albinati, A.; Mason, S. A.; Koetzle, T. F. *J. Am. Chem. Soc.* **2001**, *123*, 3960.

(27) Johnson, L. K.; Killian, C. M.; Brookhart, M. S. *J. Am. Chem. Soc.* **1995**, *117*, 6414.

(28) Scollard, J. D.; McConville, D. H.; Payne, N. C.; Vittal, J. J. *Macromolecules* **1996**, *29*, 5241.

(29) Scollard, J. D.; McConville, D. H. *J. Am. Chem. Soc.* **1996**, *118*, 10008.

(30) Horton, A. D.; de With, J.; van der Linden, A. J.; van de Weg, H. *Organometallics* **1996**, *15*, 2672.

(31) Mehrkhodavandi, P.; Bonitatebus, P. J.; Schrock, R. R. *J. Am. Chem. Soc.* **2000**, *122*, 7841.

(32) Mehrkhodavandi, P.; Schrock, R. R. *J. Am. Chem. Soc.* **2001**, *123*, 10746.

(33) Flores, M. A.; Manzoni, M. R.; Baumann, R.; Davis, W. M.; Schrock, R. R. *Organometallics* **1999**, *18*, 3220.

(34) Schrock, R. R.; Schattenmann, F.; Aizenberg, M.; Davis, W. M. *Chem. Commun.* **1998**, 199.

(35) Baumann, R.; Stumpf, R.; Davis, W. M.; Liang, L. C.; Schrock, R. R. *J. Am. Chem. Soc.* **1999**, *121*, 7822.

(36) Graf, D. D.; Schrock, R. R.; Davis, W. M.; Stumpf, R. *Organometallics* **1999**, *18*, 843.

(37) Clark, H. C. S.; Cloke, F. G. N.; Hitchcock, P. B.; Love, J. B.; Wainwright, A. P. J. *Organomet. Chem.* **1995**, *503*, 333.

(38) Guérin, F.; McConville, D. H.; Vittal, J. J. *Organometallics* **1996**, *15*, 5586.

(39) Guérin, F.; McConville, D. H.; Vittal, J. J.; Yap, G. A. P. *Organometallics* **1998**, *17*, 5172.

(40) Male, N. A. H.; Thornton-Pett, M.; Bochmann, M. *J. Chem. Soc. Dalton. Trans* **1997**, 2487.

(41) Gavrilova, A. L.; Bosnich, B. *Chem. Rev.* **2004**, *104*, 349.

(42) Liang, L.-C.; Schrock, R. R.; Davis, M. W. *Organometallics* **2000**, *19*, 2526.

(43) Sernetz, F. G.; Mülhaupt, R.; Fokken, S.; Okuda, J. *Macromolecules* **1997**, *30*, 1562.

(44) Fokken, S.; Spaniol, T. P.; Okuda, J.; Sernetz, F. G.; Mülhaupt, R. *Organometallics* **1997**, *16*, 4240.

(45) Miyatake, T.; Mizunuma, K.; Seki, Y.; Kakugo, M. *Macromol. Rapid Commun.* **1989**, *10*, 349.

(46) Repo, T.; Klinga, M.; Pietikäinen, P.; Leskelä, M.; Uusitalo, A.-M.; Pakkanen, T.; Hakala, K.; Aaltonen, P.; Löfgren, B. *Macromolecules* **1997**, *30*, 171.

(47) Theopold, K. H. *Eur. J. Inorg. Chem.* **1998**, 15.

(48) Leznoff, D. B.; Mund, G.; Jantunen, K. C.; Bhatia, P. H.; Gabert, A. J.; Batchelor, R. J. *J. Nuc. Sci. Technol.* **2002**, *Suppl. 3*, 406.

(49) Mund, G.; Gabert, A. J.; Batchelor, R. J.; Britten, J. F.; Leznoff, D. B. *Chem. Commun.* **2002**, 2990.

(50) Gauvin, R. M.; Lorber, C.; Choukroun, R.; Donnadieu, B.; Kress, J. *Eur. J. Inorg. Chem.* **2001**, 2337.

(51) Jeon, Y.-M.; Heo, J.; Lee, W. M.; Chang, T.; Kim, K. *Organometallics* **1999**, *18*, 4107.

(52) Makio, H.; Kashiwa, N.; Fujita, T. *Adv. Synth. Catal.* **2002**, *344*, 477.

(53) Li, X.-F.; Dai, K.; Ye, W.-P.; Pan, L.; Li, Y.-S. *Organometallics* **2004**, *23*, 1223.

(54) Eaborn, C.; Hill, M. S.; B., H. P.; Smith, J. D. *Chem. Commun.* **2000**, 691.

(55) Younkin, T. R.; Connor, E. F.; Henderson, J. I.; Friedrich, S. K.; Grubbs, R. H.; Bansleben, D. A. *Science* **2000**, *287*, 460.

(56) Wang, C.; Friedrich, S. K.; Younkin, T. R.; Li, R. T.; Grubbs, R. H.; Bansleben, D. A.; Day, M. W. *Organometallics* **1998**, *17*, 3149.

(57) Rhodes, B.; Chien, J. C. W.; Wood, J. S.; Chandrasekaran, A.; Rausch, M. D. *J. Organomet. Chem.* **2001**, *625*, 95.

(58) Tjaden, E. B.; Swenson, D. C.; Jordan, R. F.; Petersen, J. L. *Organometallics* **1995**, *14*, 371.

(59) Tjaden, E. B.; Jordan, R. F. *Macromol. Symp.* **1995**, *89*, 231.

(60) Brook, M. A. *Silicon in Organic, Organometallic, and Polymer Chemistry*; Wiley-interscience, 2000.

(61) Brook, A. G.; Bassindale, A. R. *Org. Chem.* **1980**, *42*, 149.

(62) Brook, A. G. *Acc. Chem. Res.* **1974**, *7*, 77.

(63) West, R.; Lowe, R.; Stewart, H. F.; Wright, A. *J. Am. Chem. Soc.* **1971**, *93*, 282.

(64) Katti, K. V.; Pinkerton, A. A.; Cavell, R. G. *Inorg. Chem.* **1991**, *30*, 2631.

(65) Haftbaradaran, F.; Mund, G.; Batchelor, R. J.; Britten, J. F.; Leznoff, D. B. *J. Chem. Soc. Dalton Trans.* **2005**, 2343.

(66) Brook, A. G.; LeGrow, G. E.; MacRae, D. M. *Can. J. Chem.* **1967**, *45*, 239.

(67) Colvin, E. W. *Silicon in Organic Synthesis*; Butterworths: London, 1981.

(68) Brook, A. G.; Bassindale, A. R. In *Rearrangements in Ground and Excited States*; de Mayo, P., Ed.; Academic Press: 1980; Vol. 42-2, p 149.

(69) Lepley, A. R.; Giumanini, A. G. In *Mechanisms of Molecular Migrations*; Thyagarajan, B. S., Ed.; Wiley-Interscience: New York, 1971; Vol. 3.

(70) Mergardt, B.; Weber, K.; Adiwidjaja, G.; Schaumann, E. *Angew. Chem., Int. Ed. Engl.* **1991**, *30*, 1687.

(71) Wright, A.; West, R. *J. Am. Chem. Soc.* **1974**, *96*, 3214.

(72) Brook, A. G. *J. Am. Chem. Soc.* **1958**, *80*, 1886.

(73) Brook, A. G.; Warner, C. M.; Limburg, W. W. *Can. J. Chem.* **1967**, *45*, 1231.

(74) Tietze, L. F.; Geissler, H.; Gewert, J. A.; Jakobi, U. *Synlett* **1994**, 511.

(75) Antoniotti, P.; C., C.; Tonachini, G. *J. Org. Chem.* **1994**, *59*, 3952.

(76) Duff, J. M.; Brook, A. G. *Can. J. Chem.* **1973**, *51*, 2869.

(77) West, R.; Bichlmeir, B. *J. Am. Chem. Soc.* **1972**, *94*, 1649.

(78) West, R.; Boudjouk, P. *J. Am. Chem. Soc.* **1973**, *95*, 3987.

(79) Duff, J. M.; Brook, A. G. *Can. J. Chem.* **1977**, *55*, 2589.

(80) Vedejs, E.; Mullins, M. *Tetrahedron Lett.* **1975**, *16*, 2017.

(81) Hudrlik, P. F.; Roberts, R. R.; Ma, D.; Hudrlik, A. M. *Tetrahedron Lett.* **1997**, *38*, 4029.

(82) Baudrillard, V.; Ple, G.; Davoust, D. *J. Org. Chem.* **1995**, *60*, 1473.

(83) Duhamel, L.; Gralak, J.; Ngono, B. *J. Organomet. Chem.* **1994**, *464*, C11.

(84) Brook, A. G.; MacRae, D. M.; Bassindale, A. R. *J. Organomet. Chem.* **1975**, *86*, 185.

(85) Evans, D. A.; Takacs, J. M.; Hurst, K. M. *J. Am. Chem. Soc.* **1979**, *101*, 371.

(86) Comanita, B. M.; Woo, S.; Fallis, A. G. *Tetrahedron Lett.* **1999**, *40*, 5283.

(87) Bailey, W. F.; Jiang, X.-L. *Organometallics* **1995**, *14*, 5704.

(88) He, H.-M.; Fanwick, P. E.; Wood, K.; Cushman, M. *J. Org. Chem.* **1995**, *60*, 5905.

(89) Lautens, M.; Delanghe, P. H. M.; Goh, J. B.; Zhang, C. H. *J. Org. Chem.* **1995**, *60*, 4213.

(90) Bush, R. P.; Lloyd, N. C.; Pearce, C. A. *Chem. Commun.* **1968**, *19*, 1191.

(91) Forbes, G. C.; Kennedy, A. R.; Mulvey, R. E.; Rodger, P. J. A.; Rowlings, R. B. *J. Chem. Soc. Dalton Trans.* **2001**, 1477.

(92) Mulvey, R. E. *Chem. Soc. Rev.* **1991**, *20*, 167.

(93) Armstrong, D. R.; Barr, D.; Clegg, W.; Hodgson, S. M.; Mulvey, R. E.; Reed, D.; Snaith, R.; Wright, D. S. *J. Am. Chem. Soc.* **1989**, *111*, 4719.

(94) Lappert, M. F.; Slade, M. J.; Singh, A.; Atwood, J. L.; Rogers, R. D.; Shakir, R. *J. Am. Chem. Soc.* **1983**, *105*, 302.

(95) Bezombes, J. P.; Hitchcock, P. B.; Lappert, M. F.; Merle, P. G. *J. Chem. Soc. Dalton Trans.* **2001**, 816.

(96) Grotjahn, D. B.; Sheridan, P. M.; Al Jihad, I.; Ziurys, L. M. *J. Am. Chem. Soc.* **2001**, *123*, 5489.

(97) Gregory, K.; Schleyer, P. v. R.; Snaith, R. *Adv. Inorg. Chem.* **1991**, *37*, 47.

(98) Collum, D. B. *Acc. Chem. Res.* **1993**, *26*, 227.

(99) Mulvey, R. E. *Chem. Soc. Rev.* **1998**, *27*, 339.

(100) Clegg, W.; Liddle, S. T.; Mulvey, R. E.; Robertson, A. *J. Chem. Soc., Chem. Commun.* **1999**, 511.

(101) Sapse, A.-M.; Schleyer, P. v. R. *Lithium Chemistry: A Theoretical and Experimental Overview*; Wiley-Interscience: New York, 1995.

(102) Kimura, B. Y.; Brown, T. L. *J. Organomet. Chem.* **1971**, *26*, 57.

(103) Setzer, W. N.; Schleyer, P. v. R. *Adv. Organommet. Chem.* **1985**, *24*, 353.

(104) Gorrell, I. B. *Annu. Rep. Prog. Chem., Sect. A* **2002**, *98*, 3.

(105) Beswick, M. A.; Wright, D. S. In *Comprehensive Organometallic Chemistry II*; Abel, E. W., Stone, F. G., Wilkinson, G., Eds.; Pergamon: New York, 1995; Vol. 1, p 1.

(106) Kahn, O. *Molecular Magnetism*; VCH: New York, NY, 1993.

(107) Carlin, R. L. *Magnetochemistry*; Springer-Verlag: Berlin, 1986.

(108) Drago, R. S. *Physical Methods for Chemists*; 3rd ed.; W. B. Saunders: USA, 1996.

(109) Cotton, F. A.; Wilkinson, G.; Murillo, C. A.; Bochmann, M. *Advanced Inorganic Chemistry*; 6th ed.; Wiley-Interscience: New York, 1999.

(110) Wiberg, E.; Wiberg, N.; Holleman, A. F. *Inorganic Chemistry*; 1st English ed.; Academic Press; De Gruyter: Berlin, New York, 2001.

(111) Janes, R.; Moore, E. *Metal-Ligand Bonding*; Royal Society of Chemistry: Cambridge, UK, 2004.

(112) Cotton, F. A.; Murillo, C. A.; Walton, R. A. *Multiple Bonds Between Metal Atoms*; 3rd ed.; Springer Science and Business Media: New York, NY, 2005.

(113) Mund, G.; Batchelor, R. J.; Sharma, R. D.; Jones, C. H. W.; Leznoff, D. B. *J. Chem. Soc. Dalton Trans.* **2002**, 136.

(114) Jantunen, K. C.; Batchelor, R. J.; Leznoff, D. B. *Organometallics* **2004**, *23*, 286.

(115) Mund, G.; Vidovic, D.; Batchelor, R. J.; Britten, J. F.; Sharma, R. D.; Jones, C. H. W.; Leznoff, D. B. *Chem. Eur. J.* **2003**, *9*, 4757.

(116) Elias, A. J.; Schmidt, H. G.; Noltemeyer, M.; Roesky, H. W. *Eur. J. Solid State Inorg. Chem.* **1992**, *29*, 23.

(117) Roesky, P. W. *Z. Anorg. Allg. Chem.* **2003**, *629*, 1881.

(118) Galindo, A. *C. R. Chimie* **2005**, *8*, 1353.

(119) Ward, B. D.; Dubberley, S. R.; Gade, L. H.; Mountford, P. *Inorg. Chem.* **2003**, *42*, 4961.

(120) Kempe, R.; Noss, H.; Irrgang, T. *J. Organomet. Chem.* **2002**, *647*, 12.

(121) Kempe, R.; Brenner, S.; Arndt, P. *Organometallics* **1996**, *15*, 1071.

(122) Aoyagi, K.; Gantzel, P. K.; Kalai, K.; Tilley, T. D. *Organometallics* **1996**, *15*, 923.

(123) Cloke, F. G. N.; Geldbach, T. J.; Hitchcock, P. B.; Love, J. B. *J. Organomet. Chem.* **1996**, *506*, 343.

(124) Horton, A. D.; de-With, J. *J. Chem. Commun.* **1996**, 1375.

(125) Tinker, S.; Deeth, R. J.; Duncalf, D. J.; McCamley, A. *Chem. Commun.* **1996**, 2623.

(126) Herrmann, W. A.; Denk, M.; Albach, R. W.; Behm, J.; Herdtweck, E. *Chem. Ber.* **1991**, *124*, 683.

(127) Wilkinson, G.; Gillard, R. D.; McCleverty, J. A. *Comprehensive Coordination Chemistry: The Synthesis, Reactions, Properties and Applications of Coordination Compounds*; 1st ed.; Pergamon Press: Oxford, 1987; Vol. 2.

(128) Krueger, C.; Rochow, E. G. *Angew. Chem.* **1962**, *74*, 491.

(129) Krueger, C.; Rochow, E. G. *Inorg. Chem.* **1963**, *2*, 1295.

(130) Murray, J. G.; Griffith, R. K. *J. Org. Chem.* **1964**, *29*, 1215.

(131) Bildstein, B.; Malaun, M.; Kopacka, H.; Wurst, K.; Mitterbock, M.; Ongania, K.-H.; Opromolla, G.; Zanello, P. *Organometallics* **1999**, *18*, 4325.

(132) Sato, M.; Ebine, S. *Synthesis* **1981**, 472.

(133) Wannagat, U. In *Advances in Inorganic Chemistry and Radiochemistry*; Emeleus, H. J., Sharpe, A. G., Eds.; Academic Press: New York, 1964; Vol. 6, p 225.

(134) Robiette, A. G.; Sheldrick, G. M.; Sheldrick, W. S.; Beagley, B.; Cruickshank, D. W. J.; Monaghan, J. J.; Aylett, B. J.; Ellis, I. A. *Chem. Commun.* **1968**, 909.

(135) Barrow, M. J.; Ebsworth, E. A. V.; Harding, M. M. *Acta Cryst.* **1979**, *B35*, 2093.

(136) Glidewell, C.; Liles, D. C. *Acta Cryst.* **1978**, *B34*, 124.

(137) Berenbaum, A.; Lough, A. J.; Manners, I. *Acta Cryst.* **2002**, *E58*, m562.

(138) Shambayati, S.; Schreiber, S. S. L.; Blake, J. F.; Wierschke, S. G.; Jorgensen, W. L. *J. Am. Chem. Soc.* **1990**, *112*, 697.

(139) Kaftory, M.; Kapon, M.; Botoshansky, M. In *The Chemistry of Organic Silicon Compounds*; Rappoport, Z., Apeloig, Y., Eds.; John Wiley & Sons, Ltd.: New York, 1998; Vol. 2, Part 1.

(140) Voronkov, M. G.; Mileshkevish, V. P.; Yuzhelevskii, Y. A. *The Siloxane Bond: Physical Properties and Chemical Transformations*; Consultants Bureau: New York, 1978.

(141) Gillespie, R. J.; Johnson, S. A. *Inorg. Chem.* **1997**, *36*, 3031.

(142) Marsch, M.; Harms, K.; Lochmann, L.; Boche, G. *Angew. Chem., Int. Ed. Engl.* **1990**, *29*, 308.

(143) Jones, C.; Junk, P. C.; Leary, S. G.; Smithies, N. A. *J. Chem. Soc. Dalton Trans.* **2000**, 3186.

(144) Danièle, S.; Drost, C.; Gehrhus, B.; Hawkins, S. M.; Hitchcock, P. B.; Lappert, M. F.; Merle, P. G.; Bott, S. G. *J. Chem. Soc. Dalton Trans.* **2001**, 3179.

(145) Geissler, M.; Kopf, J.; Schubart, B.; Weiss, E.; Neugebauer, W.; Schleyer, P. v. R. *Angew. Chem.* **1987**, *99*, 569.

(146) Hursthouse, M. B.; Hossain, M. A.; Motevalli, M.; Sanganee, M. *J. Organomet. Chem.* **1990**, *381*, 293.

(147) Chen, H.; Barlett, R. A.; Deas, H. V. R.; Olmstead, M. M.; Power, P. P. *Inorg. Chem.* **1991**, *30*, 2487.

(148) Armstrong, D. R.; Barr, D.; Clegg, W.; Mulvey, R. E.; Reed, D.; Snaith, R.; Wade, K. *J. Chem. Soc., Chem. Commun.* **1986**, 869.

(149) Armstrong, D. R.; Clegg, W.; Mulvey, R. E.; Barr, D.; Snaith, R. *J. Chem. Soc., Chem. Commun.* **1984**, 285.

(150) Armstrong, D. R.; Mulvey, R. E.; Walker, G. T.; Barr, D.; Snaith, R. *J. Chem. Soc. Dalton Trans.* **1988**, 617.

(151) Noggle, J. H. *Physical Chemistry*; 3rd ed.; HarperCollins College Publishers: New York, 1996.

(152) Veith, M.; Wieczorek, S.; Fries, K.; Huch, V. *Z. Anorg. Allg. Chem.* **2000**, *626*, 1237.

(153) Ikeda, H.; Monoi, T.; Nakayama, Y.; Yasuda, H. *J. Organomet. Chem.* **2002**, *642*, 156.

(154) Karol, F. J.; Karapinka, G. L.; Wu, C.; Dow, A. W.; Johnson, R. N.; Carrick, W. L. *J. Polym. Sci., Part A-1* **1972**, *10*, 2621.

(155) Hogan, J. P.; Banks, R. L. In *Chem. Abstr.* 1958; Vol. US patent 2825721, p 8621h.

(156) Gibson, V. C.; Maddox, P. J.; Newton, C.; Redshaw, C.; Solan, G. A.; White, A. J. P.; Williams, D. J. *J. Chem. Soc., Chem. Commun.* **1998**, *1651*.

(157) Kim, W.-K.; Fevola, M. J.; Liable-Sands, L. M.; Rheingold, A. L.; Theopold, K. H. *Organometallics* **1998**, *17*, 4541.

(158) Gibson, V. C.; Newton, C.; Redshaw, C.; Solan, G. A.; White, A. J. P.; Williams, D. J. *J. Chem. Soc. Dalton Trans.* **1999**, 827.

(159) Gibson, V. C.; Mastroianni, S.; Newton, C.; Redshaw, C.; Solan, G. A.; White, A. J. P.; Williams, D. J. *J. Chem. Soc. Dalton Trans.* **2000**, 1969.

(160) MacAdams, L. A.; Buffone, G. P.; Incarvito, C. D.; Rheingold, A. L.; Theopold, K. H. *J. Am. Chem. Soc.* **2005**, *127*, 1082.

(161) McDaniel, M. P. *Adv. Catal.* **1985**, *33*, 47.

(162) Groppo, E.; Lamberti, C.; Bordiga, S.; Spoto, G.; Zecchina, A. *Chem. Rev.* **2005**, *105*, 115.

(163) Terry, K. W.; Gantzel, P. K.; Tilley, T. D. *Inorg. Chem.* **1993**, *32*, 5402.

(164) Mund, G. Thesis Ph D, Simon Fraser University, 2004.

(165) Vahrenkamp, H. *Angew. Chem., Int. Ed.* **1978**, *17*, 379.

(166) Edema, J. J. H.; Gambarotta, S.; Meetsma, A.; Spek, A. L.; Smeets, W. J. J.; Chiang, M. Y. *J. Chem. Soc. Dalton Trans.* **1993**, 789.

(167) Edema, J. J. H.; Gambarotta, S.; Meetsma, A.; Smeets, W. J. J.; Spek, A. L. *Inorg. Chem.* **1991**, *30*, 1380.

(168) Edema, J. J. H.; Gambarotta, S.; Spek, A. L. *Inorg. Chem.* **1989**, *28*, 811.

(169) Murray, B. D.; Hope, H.; Power, P. P. *J. Am. Chem. Soc.* **1985**, *107*, 169.

(170) Fryzuk, M. D.; Leznoff, D. B.; Rettig, S. J. *Organometallics* **1995**, *14*, 5193.

(171) Jandciu, E. W.; Kuzelka, J.; Legzdins, P.; Rettig, S. J.; Smith, K. M. *Organometallics* **1999**, *18*, 1994.

(172) Harlan, J.; Bridgewater, B. M.; Hascall, T.; Norton, J. R. *Organometallics* **1999**, *18*, 3827.

(173) Gountchev, T. I.; Tilley, T. D. *Organometallics* **1999**, *18*, 2896.

(174) Odom, A. L.; Arnold, P. L.; Cummins, C. C. *J. Am. Chem. Soc.* **1998**, *120*, 5836.

(175) Deacon, G. B.; Fallon, G. D.; Forsyth, C. M.; Schumann, H.; Weimann, R. *Chem. Ber.* **1997**, *130*, 409.

(176) Blake, A. J.; Mountford, P.; Nikonov, G. I. *Acta Cryst.* **1996**, *C52*, 1911.

(177) Evans, W. J.; Ansari, M. A.; Ziller, J. W.; Khan, S. I. *Inorg. Chem.* **1996**, *35*, 5435.

(178) Arney, D. J.; Bruck, M. A.; Huber, S. R.; Wigley, D. E. *Inorg. Chem.* **1992**, *31*, 3749.

(179) Ruppa, K. B. P.; Desmangles, N.; Gambarotta, S.; Yap, G.; Rheingold, A. L. *Inorg. Chem.* **1997**, *36*, 1194.

(180) Johnson, A. R.; Davis, W. M.; Cummins, C. C. *Organometallics* **1996**, *15*, 3825.

(181) Roussel, P.; Alcock, N. W.; Scott, P. *Chem. Commun.* **1998**, 801.

(182) Edelmann, F. T.; Freckmann, D. M. M.; Schumann, H. *Chem. Rev.* **2002**, *102*, 1851.

(183) Schumann, H.; Meese-Marktscheffel, J. A.; Esser, L. *Chem. Rev.* **1995**, *95*, 865.

(184) Just, O.; Rees, W. S., Jr. *Inorg. Chem.* **2001**, *40*, 1751.

(185) Kirchbauer, F. G.; Pellny, P.-M.; Sun, H.; Burlakov, V. V.; Arndt, P.; Baumann, W.; Spannenberg, A.; Rosenthal, U. *Organometallics* **2001**, *20*, 5289.

(186) Hagadorn, J. R.; Arnold, J. *Organometallics* **1996**, *15*, 984.

(187) Sasai, H.; Arai, T.; Satow, Y.; Houk, K. N.; Shibasaki, M. *J. Am. Chem. Soc.* **1995**, *117*, 6194.

(188) Schiemenz, B.; Power, P. P. *Angew. Chem. Int. Ed.* **1996**, *35*, 2150.

(189) Kurz, S.; Hey-Hawkins, E. *Organometallics* **1992**, *11*, 2729.

(190) Hellmann, K. W.; Galka, C.; Gade, L. H.; Steiner, A.; Wright, D. S.; Kottke, T.; Stalke, D. *Chem. Commun.* **1998**, 549.

(191) Ruhlandt-Senge, K.; Ellison, J. J.; Wehmschulte, R. J.; Pauer, F.; Power, P. P. *J. Am. Chem. Soc.* **1993**, *115*, 11353.

(192) Motevalli, M.; Sanganee, M.; Savage, P. D.; Shah, S.; Sullivan, A. C. *J. Chem. Soc., Chem. Commun.* **1993**, 1132.

(193) Abrahams, I.; M., L.; Motevalli, M.; Simon, C. K.; Sullivan, A. C. *Chem. Heterocycl. Compd.* **1999**, *35*, 954.

(194) Motevalli, M.; Shah, D.; Sullivan, A. C. *J. Chem. Soc., Chem. Commun.* **1994**, 2427.

(195) Hursthouse, M. B.; Mazid, M. A.; Motevalli, M.; Sanganee, M.; Sullivan, A. C. *J. Organomet. Chem.* **1990**, *381*, 43.

(196) Abrahams, I.; Motevalli, M.; Shah, D.; Sullivan, A. C.; Thornton, P. *J. Chem. Soc., Chem. Commun.* **1993**, 1514.

(197) Motevalli, M.; Shah, D.; Sullivan, A. C. *J. Chem. Soc. Dalton Trans.* **1993**, 2849.

(198) Berry, J. F.; Cotton, F. A.; Fewox, C. S.; Lu, T.; Murillo, C. A.; Wang, X. *J. Chem. Soc. Dalton Trans.* **2004**, 2297.

(199) Cotton, F. A.; Daniels, L. M.; Lu, T.; Murillo, C. A.; Wang, X. *J. Chem. Soc. Dalton Trans.* **1999**, 517.

(200) Chang, H.-C.; Li, J.-T.; Wang, C.-C.; Lin, T.-W.; Lee, H.-C.; Lee, G.-H.; Peng, S.-M. *Eur. J. Inorg. Chem.* **1999**, 1243.

(201) Cotton, F. A.; Daniels, L. M.; Kibala, P. A. *Inorg. Chem.* **1991**, *31*, 1865.

(202) Clerac, R.; Cotton, F. A.; Daniels, L. M.; Dunbar, K. R. *Inorg. Chem.* **2000**, *39*, 3414.

(203) Cotton, F. A.; Wenning, W. *Inorg. Chem.* **1982**, *21*, 2675.

(204) Mowat, W.; Shortland, A. J.; Hill, N. J.; Wilkinson, G. *J. Chem. Soc. Dalton Trans.* **1973**, 770.

(205) Lay, P. A.; Levina, A. In *Comprehensive Coordination Chemistry II : from Biology to Nanotechnology*; McCleverty, J. A., Meyer, T. J., Eds.; Boston : Elsevier Pergamon: Amsterdam, 2004; Vol. 4, p 313.

(206) Alyea, E. C.; Basi, J. S.; Bradley, D. C.; Chisholm, M. H. *J. Chem. Soc. (A)* **1971**, 772.

(207) Clark, H. C.; Sadana, Y. N. *Can. J. Chem.* **1964**, *42*, 50.

(208) Bochmann, M.; Wilkinson, G.; Young, G. B. *J. Chem. Soc. Dalton Trans.* **1980**, 1863.

(209) Bradley, D. C.; Chisholm, M. H. *J. Chem. Soc. (A)* **1971**, 2741.

(210) Stavropoulos, P.; Savage, P. D.; Tooze, R. P.; Wilkinson, G.; Hussain, B.; Motevalli, M.; Hursthouse, M. B. *J. Chem. Soc. Dalton Trans.* **1987**, 557.

(211) Basi, J. S.; Bradley, D. C.; Chisholm, M. H. *J. Chem. Soc. (A)* **1971**, 1433.

(212) Schmid, R.; Ziegler, T. *Organometallics* **2000**, *19*, 2756.

(213) Schmid, R.; Ziegler, T. *Can. J. Chem.* **2000**, *78*, 265.

(214) Firman, T. K.; Ziegler, T. *J. Organomet. Chem.* **2001**, *635*, 153.

(215) Ballem, K. H. D.; Shetty, V.; Etkin, N.; Patrick Brian, O.; Smith, K. M. *J. Chem. Soc. Dalton Trans.* **2004**, 3431.

(216) Danopoulos, A. A.; Wilkinson, G.; Sweet, T. K. N.; Hursthouse, M. B. *J. Chem. Soc. Dalton Trans.* **1995**, 2111.

(217) Mindiola, D. J.; Cummins, C. C. *Angew. Chem., Int. Ed.* **1998**, *37*, 945.

(218) Ruppa, K. B. P.; Feghali, K.; Kovacs, I.; Aparna, K.; Gambarotta, S.; Yap, G. P. A.; Bensimon, C. *J. Chem. Soc. Dalton Trans.* **1998**, 1595.

(219) Kohn, R. D.; Haufe, M.; Mihan, S.; Lilge, D. *Chem. Commun.* **2000**, 1927.

(220) Speiser, F.; Braunstein, P. *Inorg. Chem.* **2004**, *43*, 4234.

(221) Darensbourg, D. J.; Mackiewicz, R. M.; Rodgers, J. L.; Phelps, A. P. *Inorg. Chem.* **2004**, *43*, 1831.

(222) Farrugia, L. J. *J. Appl. Cryst.* **1997**, *30*, 565.

(223) Gabe, E. J.; White, P. S.; Enright, G. D. *DIFRAC A Fortran 77 Control Routine for 4-Circle Diffractometers;* N. R. C.: Ottawa, 1995.

(224) Gabe, E. J.; LePage, Y.; Charland, J.-P.; Lee, F. L.; White, P. S. *J. Appl. Cryst.* **1989**, *22*, 384.

(225) Watkin, D. J.; Prout, C. K.; Carruthers, J. R.; Betteridge, P. W.; Cooper, R. I. *CRYSTALS* Issue 11, Chemical Crystallography Laboratory; University of Oxford: Oxford, England, **1999**.

(226) Sheldrick, G. M.; SMART, version 4.05, Siemens Energy and Automation Inc.: Madison, WI, 1996.

(227) Sheldrick, G. M.; SHELXTL, version 5.03, Siemens Crystallographic Research Systems: Madison, WI, 1994.

(228) COLLECT data collection software, Nonius B.V., 1998.

(229) Otwinowski, Z.; Minor, W.; HKL DENZO and SCALEPACK v1.96: San Diego, CA, 1997.

(230) Altomare, A.; Cascarano, G.; Giacovazzo, C.; Guagliardi, A.; Moliterni, A. G. G.; Burla, M. C.; Polidori, G.; Camalli, M.; Spagna, R. *SIR-97, A Package for Crystal Structure Solution by Direct Methods and Refinement; J. Appl. Crystallogr.* **1999**, *32*, 115.

(231) Sheldrick, G. M.; SHELXL97-2, Program for the Solution of Crystal Structures: University of Göttingen, Göttingen, Germany, 1997.

(232) Sheldrick, G. M.; SHELXTL-NT, version 6.14, XPREP, Program Library for Structure Solution and Molecular Graphics; Bruker AXS Inc.: Madison, WI, 2000-2003.